

Summer 8-4-2011

Subsurface controls on mainland marsh shoreline response during barrier island transgressive submergence

Mary Ellison
University of New Orleans, mellison@uno.edu

Follow this and additional works at: <https://scholarworks.uno.edu/td>



Part of the [Earth Sciences Commons](#), [Environmental Sciences Commons](#), and the [Fresh Water Studies Commons](#)

Recommended Citation

Ellison, Mary, "Subsurface controls on mainland marsh shoreline response during barrier island transgressive submergence" (2011). *University of New Orleans Theses and Dissertations*. 458.
<https://scholarworks.uno.edu/td/458>

This Thesis is protected by copyright and/or related rights. It has been brought to you by ScholarWorks@UNO with permission from the rights-holder(s). You are free to use this Thesis in any way that is permitted by the copyright and related rights legislation that applies to your use. For other uses you need to obtain permission from the rights-holder(s) directly, unless additional rights are indicated by a Creative Commons license in the record and/or on the work itself.

This Thesis has been accepted for inclusion in University of New Orleans Theses and Dissertations by an authorized administrator of ScholarWorks@UNO. For more information, please contact scholarworks@uno.edu.

Subsurface controls on mainland marsh shoreline response during barrier island transgressive
submergence

A Thesis

Submitted to the Graduate Faculty of the
University of New Orleans
in partial fulfillment of the
requirements for the degree of

Master of Science
in
Earth and Environmental Sciences
Coastal Geology

by

Mary S. Ellison

B.A. Boston University, 2008

August 2011

Copyright 2011, Mary Ellison

Acknowledgements

I would like to acknowledge the funding provided by the Gulf Coast Association of Geological Societies Student Research Grant and the U.S. Geological Survey Northern Gulf of Mexico (NGOM) Ecosystem Change and Hazard Susceptibility Project.

I would like to thank my advisor, Dr. Mark Kulp, for his guidance and assistance. Your willingness to set aside time in your hectic schedule and your dedication to science has been greatly appreciated. I would also like to thank Dr. Michael Miner for his input and help forming ideas and editing this thesis. Your insight and knowledge has expanded my understanding of not only Louisiana coastal geology, but geologic processes in general. Last but certainly not least, I would like to thank Dr. Ioannis Georgiou for miscellaneous advice. You have been incredibly helpful and compassionate throughout this process.

Thanks to Mike Brown and Phil McCarty for putting up with me during field work and showing me the way it is done down in Louisiana. Thanks to Dallan Weathers for helping me with any technical issues, and as always, providing some much needed laughter.

Finally, thanks to all my family and friends who have always been supportive of my goals.

Table of Contents

List of Figures	vi
List of Tables	ix
Abstract	x
Introduction	1
Key Questions	3
Research Goals and Hypothesis	5
Background.....	8
Delta Plain Development	8
St. Bernard Delta Complex	9
Marsh Platforms of the Mississippi River Delta Plain	11
Barrier Island Formation.....	12
Barrier Island Response to Sea Level Rise	14
Barrier Island Formation on the Mississippi River Delta Plain	16
Methods and Data	21
Historic Datasets and Regional Stratigraphic Relationships	21
Recent Data and Shallow Stratigraphy	23
Modern Marsh Surface Data	25
Coastwide Reference Monitoring System	26
Bathymetric Data of Chandeleur Sound	28
Results	30
Regional Stratigraphy	30
Shallow Stratigraphy	38
Modern Marsh Surface	43
Bathymetric Profiles of Chandeleur Sound and Seaward of the Chandeleur Islands	45
Discussion.....	47
Stratigraphic Models.....	47
Volumetric Calculations	47
Modern Marsh Surface	50
Conclusion.....	59
Regional Stratigraphic Relationships	59

Modern Marsh Surface	59
References	63
Appendix A - Vibracore Description Sheets	72
Appendix B - Cross-sections	99
Vita.....	133

List of Figures

Figure 1 - Area map showing the locations of major water bodies: Lake Pontchartrain, Lake Borgne, and Chandeleur Sound as well as the Mississippi River-Gulf Outlet (MR- GO) and the Mississippi River to the south. The study area is located to the northeast of the MR-GO in the red circle.	4
Figure 2 - Map showing the timing and spatial relationships between various delta complexes of the Mississippi River. The St. Bernard delta complex is located in the east (color tan here), and extends out past the arc of the Chandeleur Islands. Kulp et al. (2005) modified from Frazier (1967).	9
Figure 3 - Conceptual model of the delta cycle. The top half of the graph has two scales: Delta area and time. Notice that time also correlates to the shift between the regressive and transgressive phases. The lower half of the graph describes the sedimentary processes related to relative sea level rise and sediment supply. Reproduced from Roberts (1997).10	
Figure 4 - Formation and evolution of barrier islands on the Mississippi River delta plain. The first stage is initiated by fluvial abandonment, and further stages are driven by the combined forces sea-level rise and subsidence. The transition from Stage 2 to Stage 3 is the primary focus of this research, and the formation of the sandy shoreline shown in Stage 3. Modified from Penland et al. , 1988.....	18
Figure 5 - Locations of borings and cross-sections. Borings and cross-sections from Kolb and van Lopik (1958a) are shown as magenta dots and lines. Borings and cross-sections from Kolb and van Lopik (1958b) are shown as green dots and lines. Satellite image is a 2005 LANDSAT image accessed through Louisiana State University's Atlas website (atlas.lsu.edu)	22
Figure 6 - Locations of vibracores in the St. Bernard Marsh from 2001 to 2009. Satellite image was accessed through LSU's Atlas website (atlas.lsu.edu)	24
Figure 7 - Locations of CRMS sites in the St. Bernard marsh from coordinates obtained online at www.lacoast.gov/crms . CRMS data includes locations, accretion rates, vegetation types, as well as hydrologic data for a given site.	28
Figure 8 - Bathymetry of the north-central Gulf of Mexico (Schindler, 2010). Transects (pink) were extracted from this data to produce profiles of the marsh and Chandeleur island shoreline. Grid coordinates are in meters, Universal Transverse Mercator (UTM) Zone 15N.	29
Figure 9 - Locations of cross-sections A-A' and Q-Q'.....	30
Figure 10 - Cross-section based on over 60 borings, modified from Kolb and van Lopik (1958a), showing discrete locations of deltaic deposits, including locations of formerly active distributary channels.....	33
Figure 11 - Idealized cross-section of the St. Bernard delta complex showing the distribution and location of deltaic deposits. Modified from Kolb and van Lopik (1958a).	34
Figure 12 - Fence diagram of the St. Bernard delta complex showing the location and relationship between stratigraphic units based on the cross-sections provided by Kolb and	

van Lopik (1958a, b). This model contains spatial inaccuracies (i.e. the location of point bar deposits), but does provide a useful conceptual model for the St. Bernard delta. Vertical Exaggeration is 1000.	36
Figure 13 - Fence diagram of the lower St. Bernard delta complex showing a more detailed view of the lower-delta complex. Vertical Exaggeration is 600.	37
Figure 14 - Three dimensional block diagram of the St. Bernard delta complex based on cores and cross-sections provided by Kolb and van Lopik. Vertical Exaggeration is 1500.	38
Figure 15 - C-C' trending north to south along Bayou La Loutre for 5 kilometers. Notice the lack of sand-rich material in the cores and also in the cross-section in general. CL is clay, ST is silt, FS is fine sand, and MS is medium sand. The vertical scale is in meters.	42
Figure 16 - Cross-section Z-Z' that trends north-south across the study area for a distance of 6 km. This cross section indicates the high sand content and the range of lithologies that are present in this area. Lithofacies have been interpreted to show the depositional environments.	43
Figure 17 - Shoreface profiles, both from bathymetric data (Schindler, 2010) in red and blue, and an empirically derived equation (blue; Wilson and Allison, 2008; $y = -1.5e^{(-0.05x)}$), showing the window of ravinement between the blue and red profiles. The blue and green lines are considered the current shoreline profiles of the St. Bernard marsh. The red profile, which was extracted from the Gulf side of the Chandeleur Islands, is considered to be the profile to which the current marsh profiles will equilibrate as the Chandeleur Islands disintegrate and submerge.	46
Figure 18 - Locations of sand bodies in the St. Bernard delta complex located above the window of ravinement depth (12 m).	48
Figure 19 - Oblique aerial photograph near Isle Au Pitre in the northermost extent of the St. Bernard marshes, looking south. Notice the evidence of waves washing into the marsh and overwash platforms behind the shell shoreline.	53
Figure 20 - Oblique aerial photograph of Martin Island, located in Chandeleur Sound, looking west. Notice the marsh platform exposed seaward of the shell shoreline on the southern shoreline.	54
Figure 21 - Plan-view conceptual geomorphic model suggesting a progression of shell pocket beaches to submerged shell mounds, note the shell pocket beaches occur more inland than the shell-rimmed marsh islands and the subaqueous shell mounds. Relict distributary channels are preferentially preserved due to their lithology (compacted silts and clays more resistant to erosion). As these channels become isolated, shell-rimmed islands form, which eventually become shell islands due to the inability of the marsh to accrete vertically. Eventually, subsidence forces the entire mass to submerge as a shell mound.	55
Figure 22 - Conceptual model of marsh-edge processes contributing to the formation of shell pocket beaches. B is initiated when a marsh scarp is formed, producing sediment that can be placed on the marsh surface by wave action. Eventually, as this marsh scarp deepens, shells and shell material are eroded from the bay-bottom deposits and the fine sediment is	

winnowed, leaving behind a shell pocket beach. Eventually, this shells smother the marsh, but also serve to armor the shoreline and fundamentally change the equilibrium profile. S1, S2, and S3 are subsidence lines indicating the progression of subsidence in the marsh system.56

Figure 23 - Conceptual model showing the the influence of sandy material on the shoreline. C is initiated when the marsh scarp intersects a sand-rich body, and waves move the material to the surface of the marsh. Eventually, this deposit on the marsh thickens as more of the deposit at depth is eroded, and a sandy-shoreline is formed. S1, S2, and S3 are subsidence lines indicating the progression of subsidence in the marsh system.58

List of Tables

Table 1 - Table of the stratigraphic facies as identified and described by Kolb and van Lopik (1958a). The italicized facies are sand-rich. All text is from Kolb and van Lopik (1958a), but percentages are from Kolb and van Lopik (1966).....	31
Table 2 - This table shows volumetric calculations for various sand bodies located in the cross-sections A-A', C-C', F-F', and PC_B.	50

Abstract

Many recent studies have sought to understand the response of barrier islands and their attendant marshes to sea level rise. The Mississippi River delta plain, specifically the Chandeleur Islands and associated interior wetlands in eastern Louisiana, serves as an excellent natural laboratory for studying these responses. This region is presently undergoing the highest rates of shoreline erosion ($> 15 \text{ m yr}^{-1}$) in North America as wetlands are converted to open water in a regime of subsidence-driven rapid relative sea-level rise ($\sim 1 \text{ cm yr}^{-1}$). Three conceptual models were developed based on the geomorphic relationships observed in the marsh that describe and predict shoreline processes as the Chandeleur Islands continue to disintegrate and submerge. These models indicate that shells are the dominant shoreline-forming material in the marsh due to the lack of sand-rich strata in the subsurface of the marsh.

Keywords: marsh, barrier, island, shell, Louisiana, stratigraphy

Introduction

The Mississippi River delta plain is currently experiencing high rates of erosion as formerly active deltaic headlands and associated wetlands become inundated due to combined pressures of eustatic sea level rise and subsidence (Williams et al., 2006; Penland et al., 1990). An average of 5 mm yr⁻¹ of relative sea level rise for southeast Louisiana has been suggested by various authors using a variety of methods (Törnqvist et al., 2004; Penland and Ramsey, 1990; Kolb and van Lopik, 1958b) and is considered an accurate value for relative sea level rise in southeast Louisiana. While relative sea level rise across the modern delta plain is detrimental to the many coastal environments and ecosystems, it is also a fundamental component of the regional coastal system evolution through geologic timescales.

In a healthy deltaic system, sediment deposited by the river would allow for vertical accretion in the marshes and offset the impacts of relative sea level rise. Since the 1950s, the Mississippi River has been increasingly channelized and restricted by man-made levee systems so that the majority of the sediment from the river deposits in deep water off the modern Birdfoot delta (Blum and Roberts, 2009). Additionally, the amount of sediment carried by Mississippi River during construction of the Holocene delta was much higher than modern sediment loads in the river, mainly due to the abundance of upstream dams and irrigation (Meade et al., 1990). As a result, the Mississippi River delta is sediment-starved and unable to combat relative sea level rise as effectively as in the recent past (Blum and Roberts, 2009)

The Mississippi River delta plain is composed of active and inactive distributary networks separated by interdistributary bays and wetlands. The majority of the flow from the Mississippi River is concentrated to the modern "Birdfoot" delta and Atchafalaya River bayhead deltas. The wetlands have a general fresh to saline gradient in a seaward direction. This skeletal

structure is fronted by barrier islands, such as Grand Isle, associated with Holocene delta lobes. An existing three-stage, conceptual model for the formation and evolution of barrier islands from abandoned deltaic headlands within the Holocene Mississippi River delta plain invokes a high rate of relative sea level rise as a contributory mechanism by which Mississippi River delta barrier island systems form (Penland et al., 1988). The first stage of the evolutionary model commences when a delta lobe is abandoned by fluvial processes and attendant sediment load due to an upstream avulsion. In turn, a new deltaic depocenter is developed at a distant geographic location. As a consequence of the reduced sediment load the abandoned deltaic headland is subjected to transgression and reworking by marine processes, which leads to the generation of terminal spits and barrier islands flanking the deltaic headland (stage 1 of the conceptual model; Figure 4; Penland et al., 1988). Interior wetland submergence due to relative sea level rise, edge erosion by waves in bays, and scour due to tidal currents forces the transgressive shoreline to become detached from the mainland, forming a barrier island arc (stage 2; Penland et al., 1988). Continued loss of sandy sediment from the barrier shoreline and relative sea level rise leads to transgressive submergence, the conversion of barriers islands to subaqueous sand shoals (stage 3; Penland et al., 1988). There remains however temporal intervals of the conceptual model (100 to 1,000 yrs) for which the process controlling the overall evolution are not well understood. For example, the mainland detachment process as the stage 1 barrier forms a detached stage 2 barrier is not well understood and the timeframe of this evolution is not well defined. Moreover, it is widely recognized that a fundamental requirement of forming a sandy barrier shoreline is the presence of coarse-grained sediment that can be liberated from the deltaic headland through shoreface retreat. The source of sediment for the barriers in this conceptual model is sand-rich deposits including distributary channels, mouth bars, and antecedent coastal deposits (Penland et

al., 1988). The relative role and importance that the availability of subsurface sediment, relative sea level rise processes, and tidal prism evolution play in shoreline formation along the Mississippi River delta are prime examples where many questions yet remain.

Key Questions

The research presented herein focuses on the fate of the St Bernard marshes which are located to the east of New Orleans (Figure 1). During the last decade, the Chandeleur Islands, which front the marshes, have become progressively more fragmented due to lack of sediment supply and relative sea level rise. It has been suggested that the islands are crossing the transgressive submergence threshold and becoming a subaqueous shoal system (Fearnley et al., 2009; Miner et al., 2009; Rogers et al., 2009, and others). As the Chandeleur Islands have fragmented, the St. Bernard marshes have been exposed to progressively more open Gulf processes, and the complete disappearance of the islands would lead to fully open marine conditions impacting the St. Bernard marshes. On the basis of existing models for shoreline systems of the Mississippi River delta, submergence of the Chandeleur Islands could lead to the development of a sandy shoreline along the modern seaward periphery of the upper Chandeleur Sound marshes (Penland et al., 1988; Figure 1, circled area). This is possible if there is an adequate volume of sandy sediment in the subsurface to contribute to sandy shoreline development. Typical barrier shorelines in Louisiana are composed of fine-grained sand, and this is the coarse fraction of sediment found in the Mississippi River delta plain (Penland et al., 1988). If sand is absent from the eroding marsh, it is unlikely that a sand-rich shoreline will form, unless this sand originated from another source. Moreover, if an adequate amount of sandy sediment is present, then the marsh that backs the shoreline must be stable enough to support such a sandy shoreline. In this case, stability refers to both the persistence of the marsh and its

ability to remain in place during changing marine conditions and the ability of the marsh to remain above sea level when loaded with coarse-grained sediment. Thus a secondary focus of this thesis addresses the geomorphology and erosional processes within the marsh and their correlation to modern marsh accretionary processes. Marsh stability during periods of 100 to 1000 years relevant to this study is locally governed by types of erosion and rates of accretion (and thus stability; DeLaune et al., 1989). However, if there are no sand-rich strata in the subsurface to contribute to a sandy shoreline, but the marsh is stable enough to support a sandy beach shoreline, a "substitute" coarse-grained material, such as shells and shell hash, may contribute toward development of coarse-grained shorelines. A third point of this research focuses on the timing and nature of marine conditions that will likely impact the marsh shoreline if the Chandeleur Islands become submerged and fully converted to inner shelf shoals as predicted by Fearnley et al., (2009).

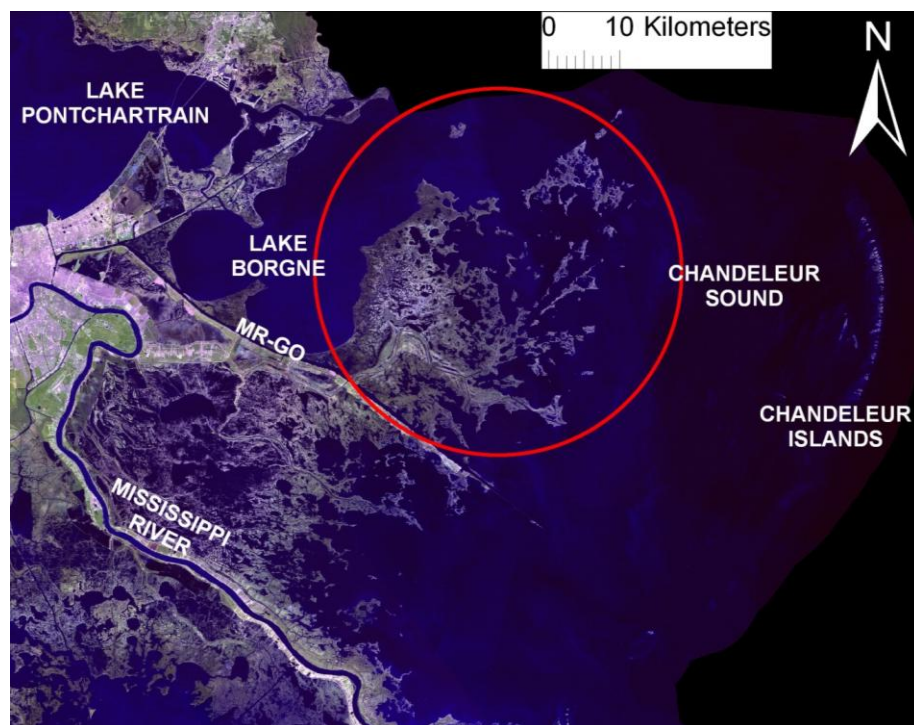


Figure 1 - Area map showing the locations of major water bodies: Lake Pontchartrain, Lake Borgne, and Chandeleur Sound as well as the Mississippi River-Gulf Outlet (MR- GO) and the Mississippi River to the south. The study area is located to the northeast of the MR-GO in the red circle.

Research Goals and Hypothesis

The research goals for this study are to: (1) identify and quantify the availability and amount of subsurface sediment that would be hydrodynamically suitable for barrier shoreline material, (2) describe and categorize the historic St. Bernard marsh response to relative sea level rise, and (3) quantify the relative contribution and nature of marine conditions that will impact the shoreline with the disappearance of the Chandeleur Islands. Examination of the underlying stratigraphy of the marsh will reveal the presence or absence of sandy facies, as well as identify stable, relatively compaction resistant strata such as distributary natural levees. Marsh accretion, in relation to localized subsidence, is important for determining marsh stability and soil content and to assess its potential long term sustainability as a subaerial substrate supporting sandy shoreline development. The geomorphic evolution of the marsh is important to understand because it may provide insight into underlying stratigraphic controls on marsh stability and response to hydrodynamic forcing. Additionally, geomorphic evolution of the Chandeleur Islands, and particularly the surrounding bathymetry, will elucidate on the nature of the potential marine conditions that will be affecting the future marsh shoreline.

The goal of this research is to establish whether sand-rich strata are present in the subsurface of the upper Chandeleur Sound marshes. A second goal is to estimate whether there is sufficient quantity of sand to generate a sandy shoreline as the periphery of the marsh platform becomes progressively more exposed to open marine conditions. A working hypothesis of this research is that *if sand-rich strata exist in the subsurface of the upper sound marshes, they will be localized to former distributary networks*. Distributary networks are typically composed of channel deposits, point bar and mouth bar deposits, and natural levees, all of which contain large fraction of sand (Coleman, 1980). Questions linked to this hypothesis include the following:

1) Is the sand located at a depth accessible by erosion? Specifically, will the equilibrium profile for marsh erosion (Wilson and Allison, 2008) in this area intersect sand layers at depth, or has relative sea level rise and marsh accretion led to the sands being too deep in the subsurface? A second hypothesis is: *If the sand-rich strata are available for liberation during marsh shoreface retreat, they will be located within the vertical ravinement envelope.* The ravinement envelope is defined by the space above the shoreline profile of the Chandeleur Islands but below the shoreline profile of the St. Bernard marsh.

2) Is the marsh stable enough to enable a shoreline to form against it if sandy sediments are liberated during shoreface ravinement in a regime of increasing wave energy?

Stability in marshes is achieved by balancing the magnitude of accretion with subsidence and eustatic sea level change as well as the ability to resist wave erosion along the marsh edge. Typically, in a marsh system where subsidence is high and clastic sediment accumulation is low, organic vertical accretion must be sufficiently high to historically keep pace with relative sea level changes. A fourth hypothesis is: *If the marsh is stable, then the accretion rates will be equal to or greater than relative sea level rates.*

3) What do historical to recent marsh fragmentation patterns and mode of marsh shoreline erosion tell us about response to increasing wave energy, tidal current and prism evolution, and zones of relative stability? It appears that most of the remaining marsh along the fringe overlies former distributary levees, which are fine-grained, highly compacted deposits overlying coarser-grained channels, point bars, and crevasse splays. Thus, the marsh that is resistant to erosion is likely underlain by sandy deposits. A fifth

hypothesis is that: *If historical patterns of erosion in the marsh continue into the future, then the preferential preservation of former distributary levees will continue.*

Background

Delta Plain Development

The Mississippi River constructed an 30,000 km² delta plain (Coleman et al., 1998) along the northern Gulf of Mexico during the Holocene. Early studies of the Mississippi River delta plain found different ages for the oldest deposits from 4250 years BP to 7250 years BP (Fisk, 1944; Kolb and van Lopik, 1958b; and Frazier, 1967). Additionally, multiple delta complexes and delta lobes within the delta plain were identified by each author. For the purposes of clarification, a hierarchy of delta terminology was established by Roberts (1997). Delta complexes are composed of multiple delta lobes fed by many distributary networks (Roberts 1997). Several studies (including those mentioned above and others) have sought to assign chronology to not only delta complexes but also delta lobes within those complexes. A more recent study by Törnqvist et al. (1996) revised ages for some of the delta complexes identified by Frazier (1967; Figure 2). Törnqvist et al. (1996) developed this revision by dating basal peats marking the initiation of fluvial occupation instead of the peats marking the end of activity, which were sampled by Frazier (1967).

For the sake of simplicity, the delta complex terminology established by Frazier and the chronology of deltaic development of Törnqvist et al. (1996) for each Holocene delta complex will be used. Frazier (1967) identified four delta complexes, the Teche, the St. Bernard, the Lafourche and the Modern-Plaquemines (also called the Balize). Törnqvist et al. (1996) assigned timeframes of fluvial occupation to each lobe on the basis of radiocarbon dated peat deposits. Each of these delta complexes represents a specific depo-center for the Mississippi River as it constructed the delta plain by delta switching events during the mid to late Holocene. The

overlap of these deltaic deposits produces complex subsurface stratigraphy, including multiple transgressive and regressive facies successions (Figure 3; Roberts, 1997).

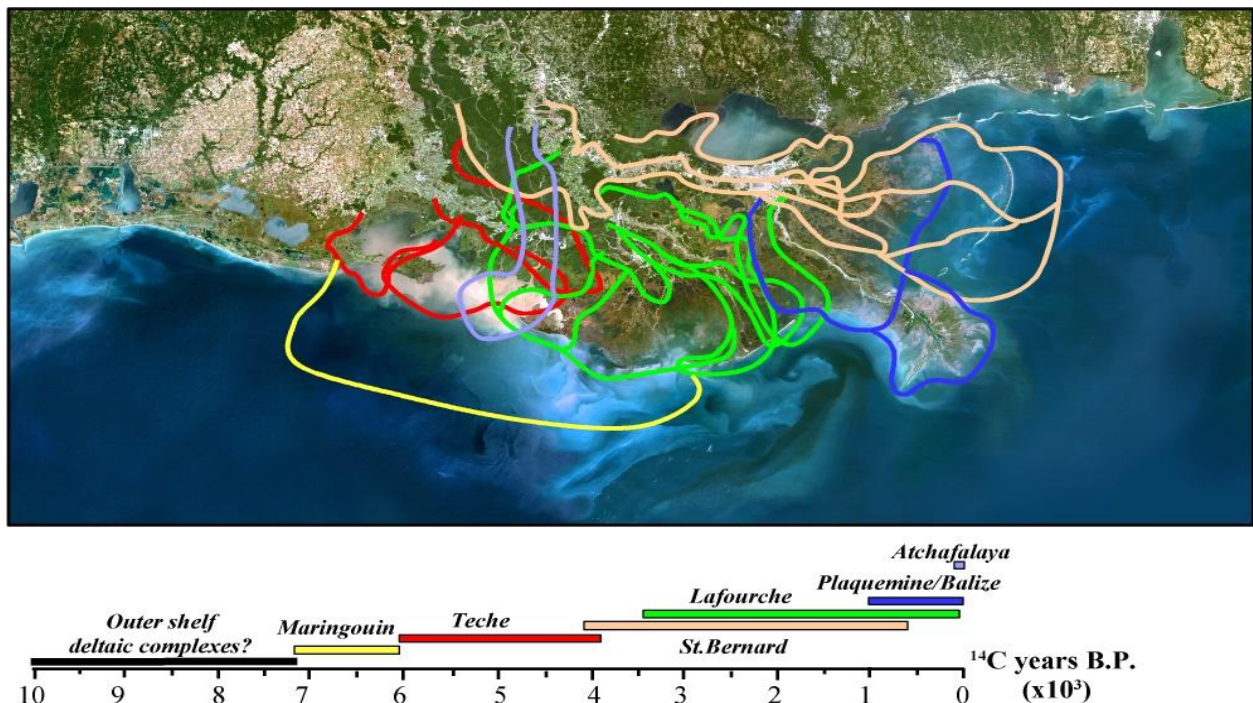


Figure 2 - Map showing the timing and spatial relationships between various delta complexes of the Mississippi River. The St. Bernard delta complex is located in the east (color tan here), and extends out past the arc of the Chandeleur Islands. Kulp et al. (2005) modified from Frazier (1967).

St. Bernard Delta Complex

The St. Bernard delta complex was initially active at approximately 3,500 years BP and abandoned approximately 1,500 years BP (Tornqvist et al., 1996). The delta complex extends east from Lake Pontchartrain to the Chandeleur Islands (Frazier, 1967; Rogers et al. 2009). Once the delta complex was abandoned, marine processes became dominant over fluvial processes and shoreline processes, such as longshore transport, began to rework the deltaic sediment leading to the formation of the Chandeleur Islands.

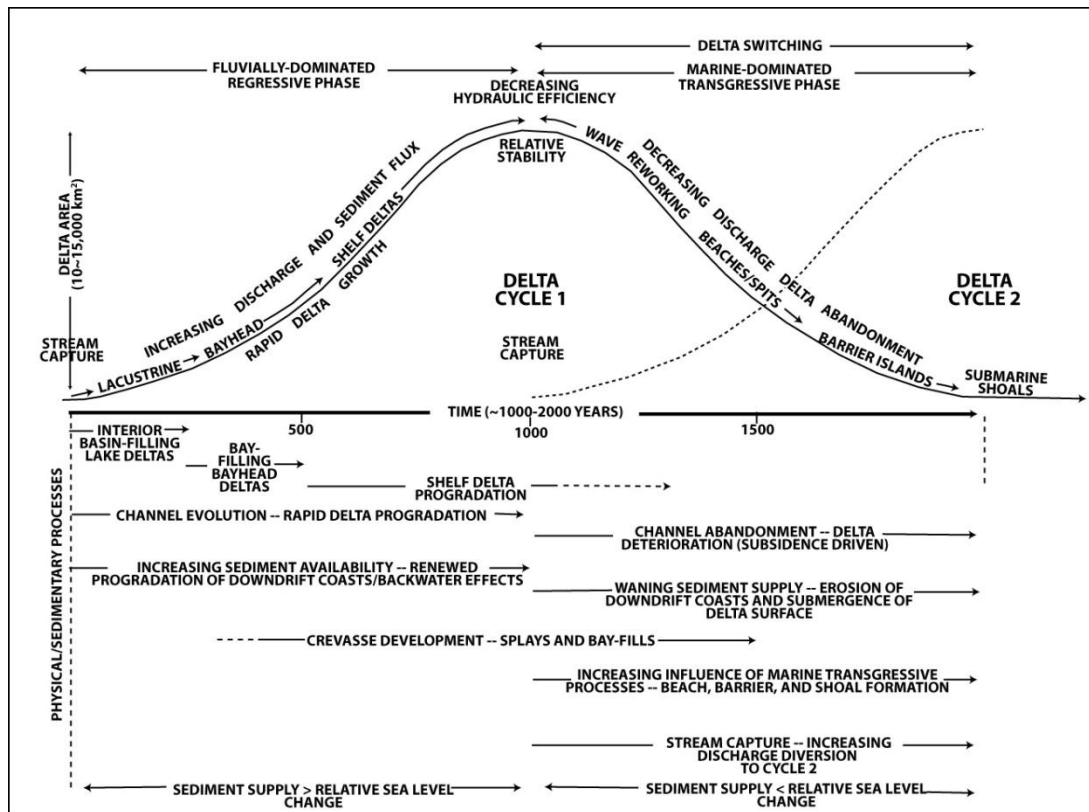


Figure 3 - Conceptual model of the delta cycle. The top half of the graph has two scales: Delta area and time. Notice that time also correlates to the shift between the regressive and transgressive phases. The lower half of the graph describes the sedimentary processes related to relative sea level rise and sediment supply. Reproduced from Roberts (1997).

Kolb and van Lopik (1958a) completed a report on the Mississippi River-Gulf Outlet (MRGO) channel as a pre-construction report on the sedimentary packages within the proposed construction area in the late '50s and '60s. This report includes 115 borings and seven transects along the proposed MRGO channel as well as within the St. Bernard marsh and Chandeleur Sound to develop a regional stratigraphic framework of the delta complex. The work completed by Kolb and van Lopik (1958a) classified the sedimentary units within these borings based on environment of deposition and correlated these units along transects.

Subsequent studies, such as Frazier (1967), used the borings and cross-sections produced by Kolb and van Lopik (1958a) to establish delta lobe and facies relationships in the St. Bernard delta complex. Delta lobe relationships include both numbers assigned to individual lobes as well as differentiating between aggradational, progradational, and transgressive facies within each

lobe. Facies relationships include more detail than the original cross-sections of Kolb and van Lopik (1958a); specifically, Frazier (1967) further divides the aforementioned facies (progradational) into specific environments of deposition and lithology (i.e. delta-front silty sand).

Marsh Platforms of the Mississippi River Delta Plain

Marshes form by vegetation colonizing low-lying muddy areas, such as tidal flats, subsiding natural levees, or interdistributary deposits. Once these areas are well established with vegetation, the marshes begin a cycle of accretion where they balance the magnitude of accretion with subsidence and absolute sea level change as well as the ability to resist wave erosion along the marsh edge (Delaune et al., 1989). Primarily, marshes maintain elevation in relation to sea level through the process of vertical accretion. Accretion is the balance of sediment accumulation and peat formation (DeLaune et al., 1989). Typically, in a marsh system where subsidence is high and mineral accumulation is low, organic vertical accretion must be sufficiently high to historically keep pace with regional subsidence-driven relative sea level changes. In Louisiana marshes, a variety of studies have concluded that modern mineral sedimentation rates are not adequate to offset rates of relative sea level rise (Cahoon and Reed, 1995; Rybczyk and Cahoon, 2002). These studies largely assumed that the mineral accretion was the primary source for accretion on the marsh surface. In a study by Nyman et al. (2006), results indicated that marshes were able to accrete organically through vegetative growth, even in marshes with considerably high mineral sedimentation rates. These studies focus on the marsh surface processes: that is, ponding of surface water, mineral sedimentation, organic accretion and vegetative growth. There are two erosion processes that occur in the St. Bernard marshes: interior and edge erosion. Interior erosion begins with ponding on the marsh surface, followed by marsh disintegration in

the same circular patterns formed by the ponding process. This process is obvious in land loss maps of the St. Bernard marshes (Couvillion et al., 2011). Marsh edge erosion is a separate topic that is the result of wave action and tidal scour on marsh shorelines. In a study by Wilson and Allison (2008), marsh shoreline morphology was analyzed and quantified in response to relative sea level rise and wave action. Their study proposed a quantitative model for shoreline erosion and retreat in marsh systems. The resulting conceptual model described not only the impacts of relative sea level rise on Louisiana marshes, but also the proposed impact on other marshes during eustatic sea level rise alone. Since the St. Bernard marsh has an historically low rate of land loss (Couvillion et al., 2011), the dominant marsh erosion process in this area is marsh edge erosion, as discussed by Wilson and Allison (2008).

Barrier Island Formation

Barrier islands are thin strips of land composed of unconsolidated material that trend parallel to the mainland shoreline and are separated from the mainland by a lagoon or wetland complex (Hoyt, 1967). Barrier island genesis has been the subject of much debate in the literature (deBeaumont, 1845; Gilbert, 1885; McGee, 1890; Johnson, 1919; Hoyt, 1967; Fischer, 1968; Otvos, 1979). deBeaumont (1845) proposed that offshore erosion at the shoreface and onshore movement of sediment allowed subaqueous bars to emerge and become subaerially exposed, eventually organizing into barrier islands. This process occurs frequently on shorelines as sediment is reworked onshore in the form of bars that become subaerial and adhere to the mainland shoreline. Gilbert's (1885) hypothesis posited that wave action and longshore transport formed spits from existing coastal features such as headlands. Eventually, the spit becomes detached from the mainland by a breach that stays open as a tidal inlet, thus forming a barrier island. This process occurs frequently on rocky coasts or coasts with large sediment supply, such

as glacial drumlins on glaciated coasts (*e.g.* Boston Harbor). McGee (1890) proposed that barrier islands were relict mainland beach ridges and dune fields that formed during lower sea level positions. During sea level rise, these ridges became isolated and the low-lying area behind the shoreline became a lagoon. Hoyt's (1967) hypothesis for barrier island formation rekindled the debate between the three previous hypotheses and agreed with McGee (1890) that sea level fluctuations are the key driver for development of barrier islands. Fisher (1968) responded to Hoyt's hypothesis, championing Gilbert's spit-building hypothesis. The debate completed the full circle when Otvos (1970) cited deBeaumont's model of barrier island formation from submerged sand shoals.

What is interesting about the shoal hypothesis and the spit hypothesis is that the processes driving these barrier island genesis mechanisms are known to alter existing barrier island geomorphology. Longshore transport does produce spits that prograde and can develop into a significant morphologic feature of a barrier island (Gilbert 1885; Fisher 1968). Wave action does create sand shoals (deBeaumont, 1845; Otvos, 1970), although the ability of those shoals to become subaerially exposed is questioned. However, the only hypothesis for island formation that invokes a larger-scale process, sea level rise, is that provided by McGee (1890) and later, Hoyt (1967). Once a beach ridge is drowned and converted into an island, longshore transport along the shoreface will likely produce a spit, as in the hypotheses of Gilbert (1885) and Fisher (1968). Additionally, offshore sand bars or shoals may move onshore and weld to the shoreface of a barrier island; a process similar to the processes driving barrier formation proposed by the hypotheses of deBeaumont (1845) and Otvos (1970). The widely recognized hypothesis of barrier island formation, following the work of McGee (1890) and Hoyt (1967), is that of Swift (1975). Additionally, Swift (1975) indicated that the debate regarding barrier island formation is

irrelevant because modern barrier islands have migrated to such an extent that any underlying stratigraphy indicating their origins has been removed. Thus, the questions surrounding barrier island migration and response to sea level rise became the focus of a variety of studies.

Barrier Island Response to Sea Level Rise

There has been extensive debate in the literature regarding barrier island response to sea level rise. Rampino and Sanders (1981) propose that during rapid sea-level rise, barrier islands drown in-place, becoming submerged as the surf zone abruptly jumps landward to the former mainland shoreline. Furthermore, the back barrier lagoon deepens and widens, preventing the barrier from retreating and forcing an abrupt jump in shoreline to the mainland. This proposed mode of barrier response to sea level rise contrasts with that of shoreface retreat; an equilibrium response to sea level rise where the barrier continually migrates landward and the lagoon is maintained during retreat (Fischer, 1961; Swift, 1975). A third hypothesis, transgressive submergence, that was developed based on geomorphic and stratigraphic relationships identified in Mississippi River delta plain barrier island systems, suggests that high rates of relative sea level rise submerge the island system while simultaneous transgression results in shoreface retreat (Penland et al., 1988). Unlike the backstepped barrier island in shoreface retreat and the new mainland shoreline resulting from in-place drowning, the end result of transgressive submergence is the formation of a subaqueous offshore retrograding sand shoal.

In a discussion by Swift and Moslow (1982), the authors disagree with the in-place drowning hypothesis posited by Rampino and Sanders (1981) for two specific reasons. The first is that lagoons are natural sediment traps with depths equal to the shallow wave base based on fetch for that lagoon. Therefore, the wide, deep lagoons discussed by Rampino and Sanders (1981) do not have an adequate mechanism for deepening and widening. The second issue

addressed by Swift and Moslow (1982) is the aforementioned equilibrium response to sea level rise. Barriers are highly dynamic features that change on small timescales and sea level rise occurs slowly over hundreds to thousands of years. Therefore, it is unlikely that the barriers would resist the affects of sea level rise and respond suddenly once a threshold has been crossed. Instead, it is more likely, according to Swift and Moslow (1982), that barriers respond to sea level rise on a daily basis.

Shoreface retreat, as hypothesized by Fischer (1961) and Swift (1975) presents a significant caveat: sediment supply. With an adequate supply, the barrier can migrate landward as sediment is transferred landward in response to sea level rise. However, as more sand is lost in the system, the barriers would be unable to migrate. For this reason, shoreface retreat is not fully applicable to barrier systems along the sediment-starved Mississippi River delta plain. Furthermore, Swift's (1975) barriers migrate up a coastal plain with some relief, so not only are they migrating landward, but also gaining elevation as they migrate. The barriers on the Mississippi River delta plain are essentially migrating across a flat plain, and so the loss of sediment from the system has a larger effect on the ability of those barrier islands to survive subaerially.

The transgressive submergence hypothesis that invokes the three-stage evolutionary model proposed by Penland et al. (1981) was tested by Otvos (1986) using by aerial photography, historical maps, and shallow stratigraphy. Otvos (1986) suggested that the variables cited within the three-stage model, such as rates of island evolution and degradation, and shelf shoal formation are inadequately defined and thus present weaknesses in the model. Specifically, Otvos hypothesizes that barrier islands form from reworked subaqueous deltaic deposits that emerged from shoals and were never attached to the mainland.

Barrier Island Formation on the Mississippi River Delta Plain

The Penland et al. (1988) three-stage evolutionary model for Mississippi Delta transgressive barrier islands (Figure 4) invokes components from each of the three earlier proposed models of barrier island formation. In Stage 1, after the initial fluvial abandonment of the headland due to an upstream avulsion, marine processes rework the coarse fraction of the deltaic sediment into flanking spits (Penland et al., 1988). Eventually these spits are breached to form flanking barrier islands similar to the mode of barrier formation proposed by Gilbert (1885) and Fisher (1968) (Penland and Boyd, 1981; Penland et al., 1988). In Stage 2, continued subsidence and erosion of interior wetlands results in the sandy shoreline becoming detached from the headland forming a transgressive barrier island arc similar to the drowned beach ridges in Hoyt's (1967) model (Penland and Boyd, 1981; Penland et al., 1988). Continued subsidence and loss of sand to deepwater sinks results in barrier island transgressive submergence and the development of a Stage 3 submerged inner-shelf shoal (Penland et al., 1988). During the transition from Stage 2 to Stage 3, the barrier island arc may become submerged during high energy events, such as seasonal storms. Additionally, before the inner-shelf shoal becomes fully submerged, it may become subaerially exposed during fairweather conditions due to constructive wave processes (Otvos, 1970; Fearnley et al., 2009). However, the ability of the inner-shelf shoal to maintain subaerial exposure is compromised by relative sea level rise and loss of sand offshore, and thus the conversion to an inner-shelf shoal cannot be reversed in a regime of continual relative sea level rise, as stated by Otvos (1970). Modern analogs and type areas for the model proposed by Penland et al. (1988) include: the LaFourche erosional headland with Timbalier Islands and Grand Isle as flanking barriers (Stage 1); the Chandeleur Islands transgressive barrier island arc (Stage 2); and Ship Shoal (Stage 3).

The Chandeleur Islands are Stage 2 transgressive barrier islands formed by reworking of the St. Bernard delta complex of the Mississippi River. This lobe was abandoned approximately 1,800 years BP (Frazier, 1967) and has been undergoing transgression since that time. The Chandeleur Islands are arc-shaped islands, approximately 72 km in length from the southernmost spit at Breton Island to the northernmost spit at Hewes Point. Historically, the dominant direction of sediment transport is north due to the islands orientation to the dominant wave climate in the Gulf of Mexico (Penland et al., 1988), although there is some variation at the southern end of the islands. More recently, studies (Georgiou and Schindler, 2009) have shown that longshore transport is bidirectional which moves material laterally towards the flanks of the Chandeleur Islands. As a result, the northern islands sand lithosome is thicker with wide beaches and sand bars within the surf zone (Penland et al., 1988) primarily as a function of lateral spit accretion. The southern islands are much thinner and more fragmented, indicating a lack of sediment supply and accommodation, and mainly consist of shell beaches. The Chandeleur Islands are separated from the St. Bernard marsh complex by 25 km of open water, Chandeleur Sound.

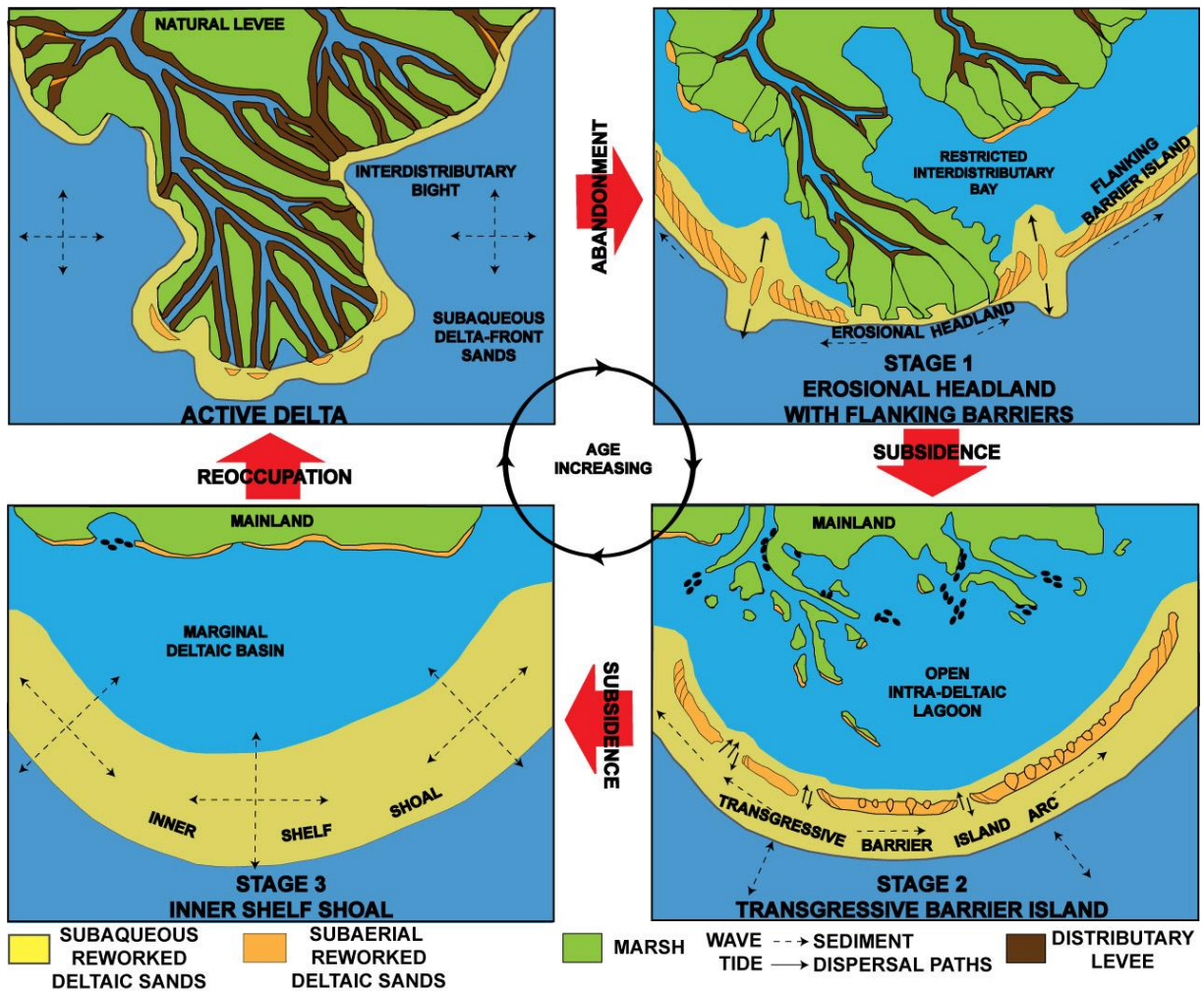


Figure 4 - Formation and evolution of barrier islands on the Mississippi River delta plain. The first stage is initiated by fluvial abandonment, and further stages are driven by the combined forces sea-level rise and subsidence. The transition from Stage 2 to Stage 3 is the primary focus of this research, and the formation of the sandy shoreline shown in Stage 3. Modified from Penland et al. , 1988.

Shoreline and bathymetric data from multiple time periods (dating to the 1850s) for the Chandeleur Islands demonstrate that large sectors of island have crossed the transgressive submergence threshold (Fearnley et al., 2009; Miner et al., 2009), a trend that was greatly accelerated by the 2004 and 2005 hurricane seasons. Recent studies predict that the Chandeleur Islands will be completely converted to ephemeral barrier islands/shoals within two decades (Fearnley et al., 2009). Studies conducted in the 1980s—prior to the increased hurricane intensity and frequency observed during the past decade—predicted that the transgressive submergence threshold conditions would not be met for another ~250 years (McBride et al., 1992). Thus, it is

important to understand the processes currently affecting the mainland marsh as well as the processes and changes that will occur once the seaward fronting Chandeleur Islands become completely submerged. This study focuses on the response of the marsh in the St Bernard delta complex as the Chandeleur Islands are progressively submerged.

As the Chandeleur Islands undergo continual thinning, breakup, and conversion to shoals, the entire system will ultimately evolve into a series of submerged sand shoals through transgressive submergence (Penland et al., 1988; Fearnley et al., 2009). The Chandeleur Islands today act as a buffer between the saltwater conditions of the Gulf and the estuarine conditions in St. Bernard Marsh and Pontchartrain Basin. In the absence of fronting barrier islands, the marshes could possibly be subjected to higher levels of salinity and greater wave energy, resulting in accelerated deterioration of the marsh. However, the changing conditions and processes affecting the marshes may also facilitate onshore movement of sand or reworking of sand at depth, producing a sandy shoreface along the marsh.

An unusual characteristic of the Chandeleur Islands is their relative stability in comparison with other barrier island systems in the Mississippi River delta plain, specifically Isles Derniere. Despite an earlier abandonment by the St. Bernard lobe (~1800 years BP; Frazier 1967), the Chandeleur Islands are in the same stage of barrier evolution as the Isles Derniere which are reworked remnants of the Lafourche delta complex which was abandoned (~700 years BP; Frazier 1967). It is likely that a difference in substrate lithology, volume of sand available for natural island maintenance, or variability in the rate of relative sea level rise between these two locations can explain the similarity in geomorphic phase yet the large age discrepancy.

The Isles Derniere were originally a single barrier chain associated with the LaFourche delta complex (Penland et al., 1988). Unlike the Chandeleur Islands, which are reworked

distributary sands from Bayou La Loutre, the source of sediment for the Isles Derniere is not necessarily from the associated distributary, but rather from updrift sources (i.e. Caminada Headland; Penland et al. 1988). In the 1850s, the Isles Derniere consisted of an attached headland with flanking barrier islands but through rapid subsidence, land loss, and bay expansion, the islands have become detached barriers (Penland et al., 1988). In the recent past, the Isles Derniere have steadily decreased in size and fragmented into multiple islands. Ship Shoal is a large subaqueous sand body offshore from the Isles Derniere that is generally migrating landward (Penland et al., 1988). Because Ship Shoal has migrated landward over a distance equal to or greater than its width, no barrier island facies are preserved in the stratigraphy of Ship Shoal; however, the presence of beachrock and an estuarine shell assemblage identified in vibracores provide evidence of barrier island origin (Penland et al., 1988). Additionally, it has been hypothesized that the Isles Derniere formed along the marsh periphery in response to the decline of Ship Shoal as a barrier island chain (Penland et al., 1988). If this holds true, then a similar shoreline is likely to form along the St. Bernard marsh as a response to the disintegration and submergence of the Chandeleur Islands.

In a study by Stone et al. (2005), Ship Shoal was analyzed as a sediment source for restoration projects. One of the goals of this study was to model the affects of different scenarios on the Isles Derniere assuming the entire removal of Ship Shoal. During storm conditions, waves generally break on Ship Shoal before they reach Isles Derniere. With the removal of Ship Shoal, the wave heights increased almost 100% (Stone et al., 2005). However, because these waves are generally larger, the surf zone associated with Isles Derniere was moved seaward and the resulting wave energy impacting the shorelines was roughly the same with Ship Shoal present. During fairweather conditions, wave height increases only 10-20% (Stone et al., 2005).

Methods and Data

Historic Datasets and Regional Stratigraphic Relationships

Kolb and van Lopik (1958a, b) produced two reports that relied upon borings and cross-sections in the Mississippi River delta plain (Figure 5) to document regional stratigraphic relationships. These borings were most likely collected using a thin-wall, or Shelby, tube sampler (J. Dunbar, personal communication). A Shelby tube sampler collects undisturbed samples in 12.7 cm (5 in) diameter tubes of 60.9 cm (24 in) to 76.2 cm (30 in) in length (Fang, 1991). Sediment samples from the Shelby tubes were analyzed according to the Unified soil classification system (USCS) which was modified to best characterize the local soil characteristics by the New Orleans District of the U.S. Army Corps of Engineers. Lithological associations and stratigraphic relationships, based on the sediment samples, were determined and described by Kolb and van Lopik (1958a, b). These borings and stratigraphic cross-sections were redrawn in graphic form using Adobe Illustrator (Appendix B - Cross-sections).

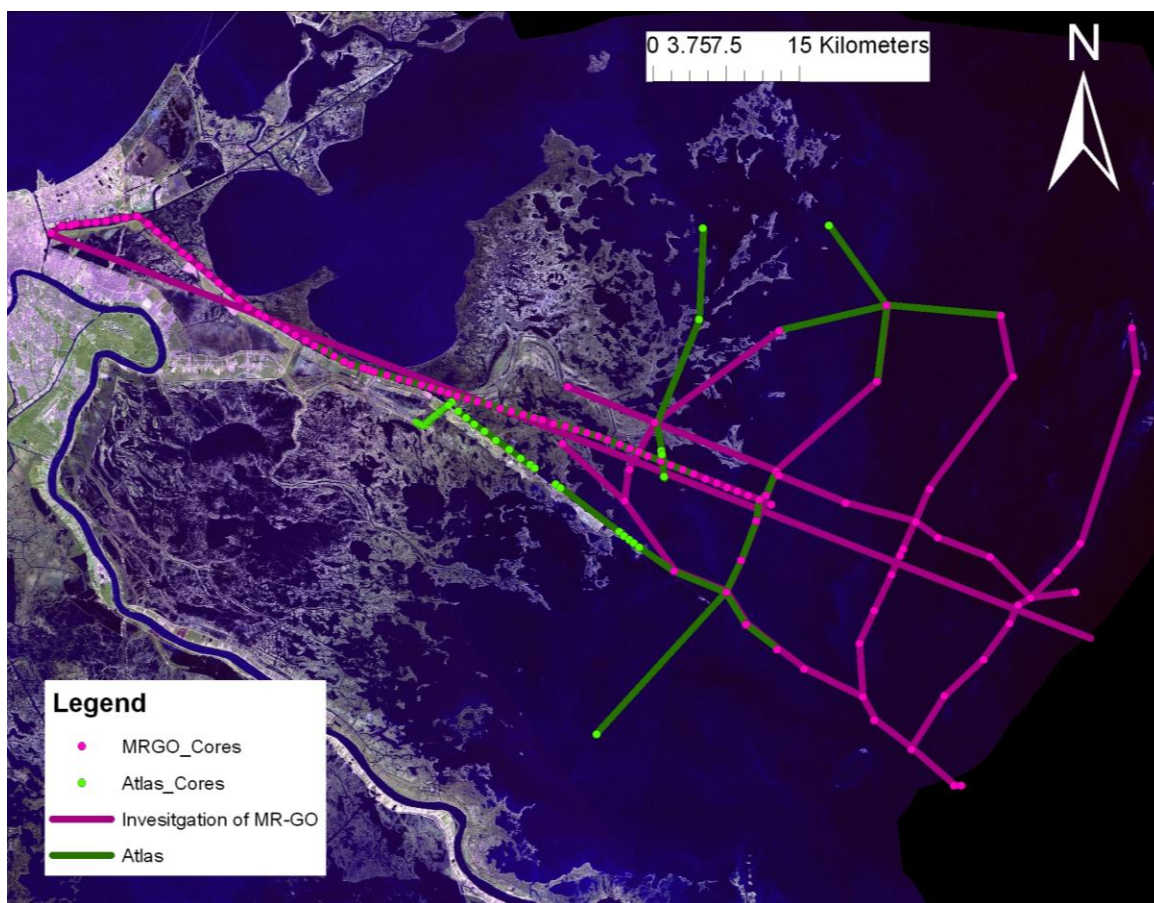


Figure 5 - Locations of borings and cross-sections. Borings and cross-sections from Kolb and van Lopik (1958a) are shown as magenta dots and lines. Borings and cross-sections from Kolb and van Lopik (1958b) are shown as green dots and lines. Satellite image is a 2005 LANDSAT image accessed through Louisiana State University's Atlas website (atlas.lsu.edu)

Stratigraphic relationships were interpolated using RockWare, Inc., Rockworks 14 (revision 2009.3.23) software which uses locations, depths, and stratigraphic characteristics to construct two-dimensional and three-dimensional models of subsurface relationships. Although there are several options for making a three-dimensional model in Rockworks 14, the most important is the method option, or algorithm because this option determines the extent of interpolation that occurs for a given model. To produce stratigraphic models using Rockworks, an inverse distance algorithm was selected for spatial interpolation. This algorithm assigns a value to a node based on a weighted average of the nodes surrounding it (RockWare, Inc., 2008). The weighting is proportional to the inverse of the distance raised to a power between data

points, and is determined by an exponent. Essentially, this algorithm along with the value of the weighting exponent determines how localized or regional the data will appear. For example, point bars and channels are highly localized data located primarily near former distributary networks. Other deposits, such as prodelta deposits, are less localized and fall into a more regional-scale of deposition. For this specific model, and because there are several stratigraphic units which are highly localized (and of particular interest due to the sand content in deposits like point bars), a weighted exponent with the value of 2.0 was selected (the lower the value, the more localized the units in the model will appear) (RockWare 2008). This value, essentially, is related to the heterogeneity of the stratigraphy in these borings. Because sand-rich strata, such as distributary channels, are highly localized, selecting a lower number effectively shows these deposits in a more realistic way. Numerous attempts were undertaken to assess how different values affected the generation of stratigraphic models. In the versions using high values, the result was sheet-like deposits of distributary channels, presenting an unrealistic representation of the deposits.

Recent Data and Shallow Stratigraphy

Vibracores were collected by the University of New Orleans Coastal Research Laboratory in 2001, 2003, 2004, and 2009 (Figure 6) within the study area using a custom-built system consisting of a vibrating cement mixer and aluminum piping. The vibrating cement mixer allows the core tubing to penetrate by essentially liquefying the surrounding sediment (Lanesky et al., 1979; Hoyt and Demarest, 1981). Additionally, the mixer can be adjusted to vibrate at various frequencies as needed to maintain sediment liquefaction and core penetration. Once the core has reached refusal, measurements are taken to calculate compaction in the core. In order to extract the core completely, suction must be created by filling the remaining pipe with water and

putting a stopper in the top of the core. A tripod and pulley system is used for extracting the vibracore. Once the core returns to the laboratory, it is split lengthwise with a circular saw: one half is archived and the other half is used for sampling and describing. Core description sheets (Appendix A - Vibracore Description Sheets) show percent sand, color, organic content, and other pertinent information to describing the core.

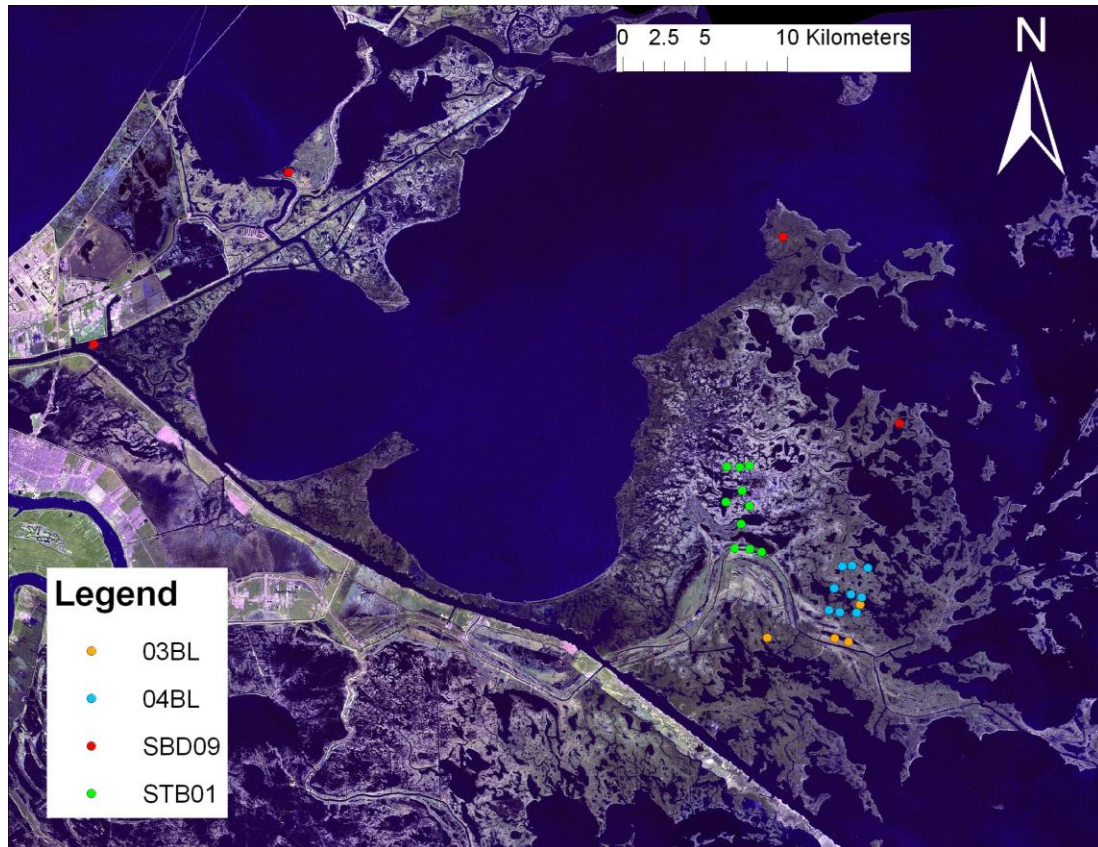


Figure 6 - Locations of vibracores in the St. Bernard Marsh from 2001 to 2009. Satellite image was accessed through LSU's Atlas website (atlas.lsu.edu)

Graphic lithologic core logs and stratigraphic cross-sections were created from these core description sheets using Adobe Illustrator. Each core was digitized individually and represented with various colors and swatches according to the description of the core. Once all the cores were digitized, they were put into cross-sections. Stratigraphic relationships were drawn on the cross-sections and labeled according to the environments to which they corresponded.

Modern Marsh Surface Data

Two marsh peat cores (SBD2 and SBD3; Figure 6) were collected in selected locations in the St. Bernard marsh in Summer 2009 using a Russian Peat Borer. Once a target depth was reached (for example, 1 meter, or 0.5 meter), the device was rotated, trapping the sample inside the core tube with a cover plate. This system is used in marshes because it minimizes vertical compaction. Once the core was extracted, it was placed into half-cylinder PVC pipes wrapped in plastic to avoid contamination, and then the core itself was wrapped in plastic and secured with a strong adhesive, such as duct-tape. Once the core returned to the lab, it was sampled in 2-cm sections, samples were placed in small bags. The samples were then dispersed depending on the processing methods, which included water content, loss-on-ignition, dry bulk density, ^{210}Pb , and ^{137}Cs .

Water content of each sample was determined by weighing the sample soon after it was collected, and then comparing this wet weight against a dry weight. The samples were typically dried in an oven set at 60° C, but some samples were also dried at room temperature. The only difference between the drying methods is the amount of time before the sample is sufficiently dry. The Loss-on-Ignition (LOI) method of Delaune et al. (2003) was used to obtain an organic content for the specific sample. The samples, which had been dried by the method discussed above, were weighed before being placed into a muffle furnace at 400° C for 16 hours. The resulting weight was subtracted from the pre-ignition weight. This "lost" weight was then divided by the starting weight to obtain a percentage of organic material that was ignited and lost during the LOI process.

One marsh core, SBD2, was processed for ^{210}Pb , ^{137}Cs and organic content by the Louisiana Universities Marine Consortium (LUMCON). ^{210}Pb and ^{137}Cs can be used

simultaneously to provide vertical accretion rates across a range of timescales (10-100 year; DeLaune et al., 1989). ^{137}Cs is an unnatural atmospheric gas isotope that exists as a result of nuclear weapons testing during the late 1950's and early 1960's (DeLaune et al., 1989). As a result, high concentrations of this isotope were present during peak times of nuclear weapons testing: specifically, the early 1950s, and again in 1963-1964 (DeLaune et al., 1989). ^{137}Cs decays with a half life of approximately 30 years to ^{137}Ba . DeLaune et al. (1989) admit that there may be migration of these isotopes within the sediment, but that peak concentrations "do not shift (vertically) substantially". ^{210}Pb is a naturally occurring atmospheric gas isotope that is trapped by rainfall with a mean atmospheric residence time of 9.6 days (DeLaune et al., 1989). The concentration of ^{210}Pb in rainwater is therefore believed to be constant (DeLaune et al., 1989; Benninger 1976). Additionally, ^{210}Pb in sediment decays to ^{226}Ra . The excess ^{210}Pb from rainwater in relation to the total ^{210}Pb activity is used for ^{210}Pb dating (DeLaune et al., 1989). These qualities of the two radioisotopes provide unique dating tools that can be applied to estimate vertical accretion rates in wetland soils. However, without an established vertical chronology from ^{137}Cs , the accretion data from ^{210}Pb is useless and for that reason, ^{210}Pb and ^{137}Cs are used together.

Unfortunately, the accretion data from SBD2 have multiple difficulties including large calculated errors for accretion rates, as well as significant outliers at specific intervals. Due to these difficulties, the data are not discussed further.

Coastwide Reference Monitoring System

The Louisiana Coastwide Reference Monitoring System (CRMS) is a program funded by the Coastal Wetlands Planning, Protection and Restoration Act (CWPPRA) and consists of 390 stations located within the marshes of Mississippi River delta (Steyer et al., 2003; Steyer et al.,

2006; USGS, 2010). Each station monitors wetland health, with data on vegetation, hydrologic index, salinity, and accretion rates. Nine locations (Figure 7), established in the Spring of 2008, were selected in the Pontchartrain Basin for this study. Data and methods for accretion rates are readily available online at www.lacoast.gov/crms. The accretion data collected from these sites results from measurements of accreted sediment thickness above a feldspar layer. The feldspar powder provides a reference marker horizon because it was sprinkled onto the marsh when the station was established (Cahoon et al., 1995; lacoast.gov/crms). The feldspar forms a vibrant white layer against which to measure vertical accretion. Once established, the site is later revisited and cores are taken from the marsh where the feldspar marker was laid down (Cahoon et al., 1995; lacoast.gov/crms). If accretion has taken place, the feldspar marker will be buried and the thickness of material represents the total magnitude of accretion. Liquid nitrogen is poured down this core before extraction to preserve the core until it can be properly analyzed. However, in some cases, the feldspar has been removed from the system perhaps by flooding of the marsh or herbivory and thus no accurate accretion data can be collected (lacoast.gov/crms).

The data collected at CRMS sites included vegetation type, hydrologic index, vertical accretion, and soil elevation change measured with a Rod Surface Elevation Table (RSET; lacoast.gov/crms). These measurements are typically collected over a short period of time (i.e. months to years) and are indicative of short term changes within the marsh.

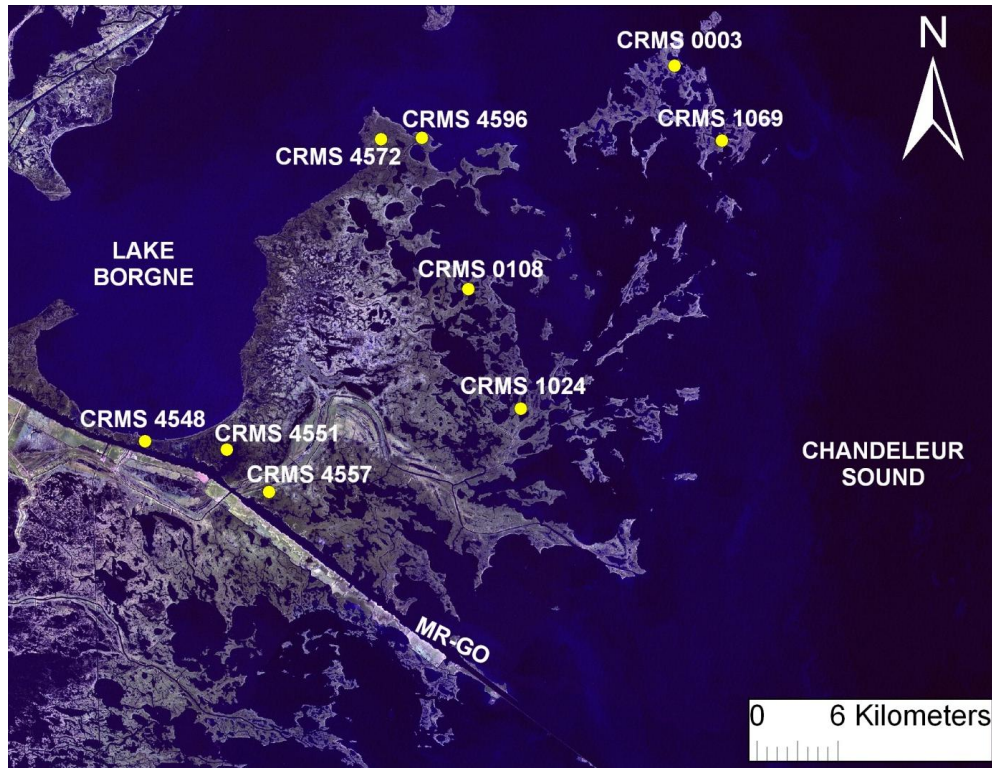


Figure 7 - Locations of CRMS sites in the St. Bernard marsh from coordinates obtained online at www.lacoast.gov/crms. CRMS data includes locations, accretion rates, vegetation types, as well as hydrologic data for a given site.

Bathymetric Data of Chandeleur Sound

Bathymetric data (Figure 8) are from the ADCIRC grid SL15v06r09 which was used in previous studies (Bunya et al., 2010; Dietrich et al., 2010; Schindler, 2010). These data were compiled using bathymetric data from a variety of sources such as The National Oceanographic and Atmospheric Association (NOAA), the National Ocean Service (NOS) and the U.S. Geological Survey (USGS). Most of these data are historic hydrographic charts from NOAA (Georgiou et al., 2009; Schindler 2010).

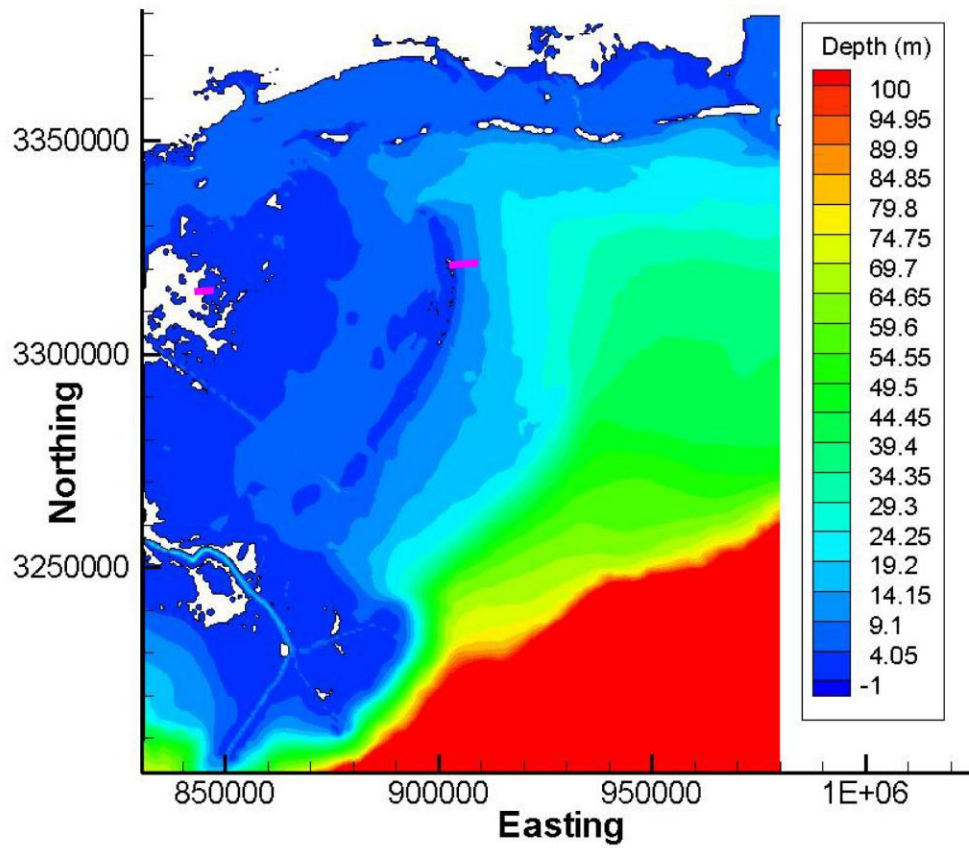


Figure 8 - Bathymetry of the north-central Gulf of Mexico (Schindler, 2010). Transects (pink) were extracted from this data to produce profiles of the marsh and Chandeleur island shoreline. Grid coordinates are in meters, Universal Transverse Mercator (UTM) Zone 15N.

Results

Regional Stratigraphy

Kolb and van Lopik (1958a) identified a suite of Holocene deltaic, coastal, and marine environments in their analysis of the Mississippi River-Gulf Outlet: prodelta clays, intradelta complex, interdistributary trough, abandoned course, abandoned distributary, point bar, natural levees, swamp, marsh, lacustrine, sand beach, bay-sound, and nearshore gulf. Of these environments, the most commonly encountered within the upper 80m of this study area are prodelta clays, intradelta complex, interdistributary trough, abandoned course, abandoned distributary, point bar, natural levee, marsh, sand beach, bay-sound, and nearshore gulf (Table 1).

In order to define the facies associations and distribution, a series of stratigraphic cross-sections were constructed in Adobe Illustrator using data from Kolb and van Lopik (1958a, b). The following sections discuss two cross-sections (Figure 9) and the overall stratigraphic framework of the delta complex. All other cross-sections can be found in Appendix B - Cross-sections.

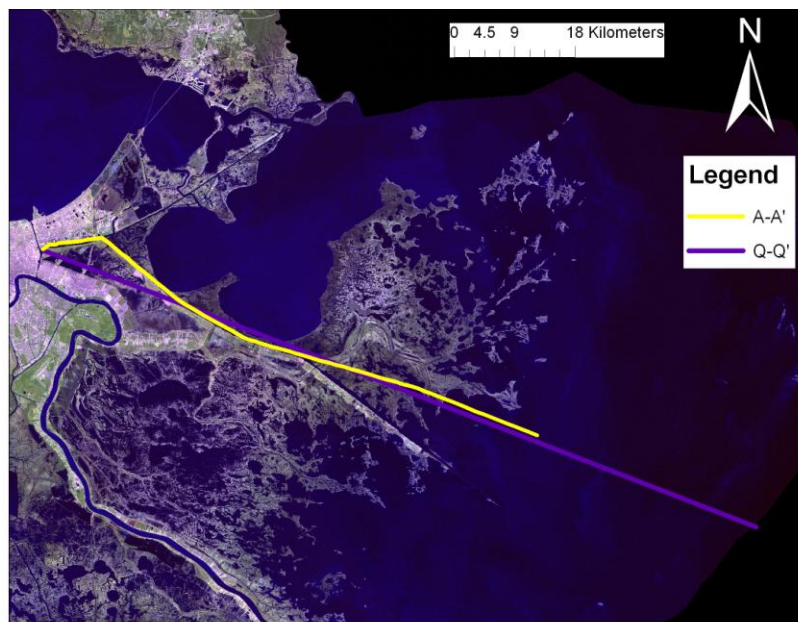


Figure 9 - Locations of cross-sections A-A' and Q-Q'.

Table 1 - Table of the stratigraphic facies as identified and described by Kolb and van Lopik (1958a). The italicized facies are sand-rich. All text is from Kolb and van Lopik (1958a), but percentages are from Kolb and van Lopik (1966).

Depositional Types	Lithology	Remarks
Prodelta Clays	95% Clay, 5% Silt	Underlies the entire deltaic sequence as homogeneous unit. Slopes and thickens toward the southeast
<i>Intradelata Complex</i>	<i>35% Clay, 40% Silt, 25% Sand</i>	<i>Relatively coarse portion of subaqueous delta. Intricately interfingered deposits. Disposed in broad wedges about abandoned courses and major distributaries.</i>
Interdistributary Trough	80% Clay, 10% Silt, 7% Sand, 3% Organic Material	Disposed in clay wedges between major distributaries. Clay sequence interrupted by silty or sandy materials associated with myriad small distributaries, but otherwise fairly homogeneous. Material will probably displace laterally under fairly light load.
<i>Abandoned Course</i>	<i>20% Clay, 35% Silt, 45% Sand</i>	<i>Forming ribbon of fairly coarse sediment in abandoned Mississippi River course. Averages 2500 ft in width and 80 to 90 ft deep. Grain size increases with depth and upstream direction</i>
Abandoned Distributary	45% Clay, 20% Silt, 35% Sand	Forming ribbons of fairly coarse sediment from a few feet to more than 1500 ft in width, 30 to 60 ft deep. Grain size increases with depth.
<i>Point Bar</i>	<i>25% Clay, 20% Silt, 55% Sand</i>	<i>Flanking major courses. Thickness 80 ft or more. Materials become coarser with depth</i>
Natural Levee	55% Clay, 40% Silt, 5% Sand	Disposed in irregular belts along abandoned courses and distributaries. Thickness averages 15 ft or less.
Marsh	32% Clay, 3% Silt, 65% Organic Material	Forms 90% of land surface within study area. Average thickness 10 ft. Very high water content. Subject to rapid compaction under load.
<i>Sand Beach</i>	<i>5% Silt, 90% Sand, 5% Shell</i>	<i>Surficial beaches of minor areal extent. Buried beaches also insignificant portion of subsurface</i>
Bay-Sound	55% Clay, 3% Silt, 37% Sand, 5% Shell	Averages 10-15 ft deep throughout Chandeleur Sound. Interfingered, characteristically silts and silty sand deposits
<i>Nearshore Gulf</i>	<i>12% Clay, 14% Silt, 55% Sand, 19% Shell</i>	<i>A transgressive basal sandy unit beneath the prodelta clays and seaward of the Chandeleur arc of islands</i>

MRGO A-A'

This cross-section (Figure 10) shows a general north-west to south-east trend from interdistributary-dominated marsh environments to more fluvial-dominated intradelta complexes and abandoned distributaries. The end of this cross section follows, essentially, the end of Bayou La Loutre, which is a former Mississippi River channel (Kolb and van Lopik 1958a, b). The prevalence of coarse-grained deposits correlate with fluvial-dominated deposits, and thus beneath the approximate modern shoreline of St. Bernard marsh is the highest concentration of sand-rich strata. However, much of these strata, in particular the intradelta complex, exist below 3m (Kolb and van Lopik, 1958a,b).

MRGO Q-Q'

The cross-section Q-Q' (Figure 11) is an idealized cross-section that is similar A-A' except that borings have been extrapolated to make a straight cross-section across the delta complex. Noticeable first is the Pleistocene deposit beneath St. Bernard marsh that gradually thins to the southeast. The base of the Pleistocene surface is not defined by Kolb and van Lopik (1958a), but rather these "thicknesses" indicated the maximum depth of penetration. The prodelta wedge is stratigraphically above the Pleistocene surface and thickens to the southeast. As noticed in previously discussed cross-sections, the distribution of intradelta complexes is limited and bounded along the southeast by the mouth of Bayou La Loutre. The presence of intradelta complexes is also correlated with the presence of modern marsh deposits. Overall, this cross-section provides a basic understanding of St. Bernard Delta complex regional stratigraphy because it highlights the smaller scale stratal relationships observed in other cross-sections, such as the interfingering of intradelta, interdistributary, and abandoned distributary channel deposits.

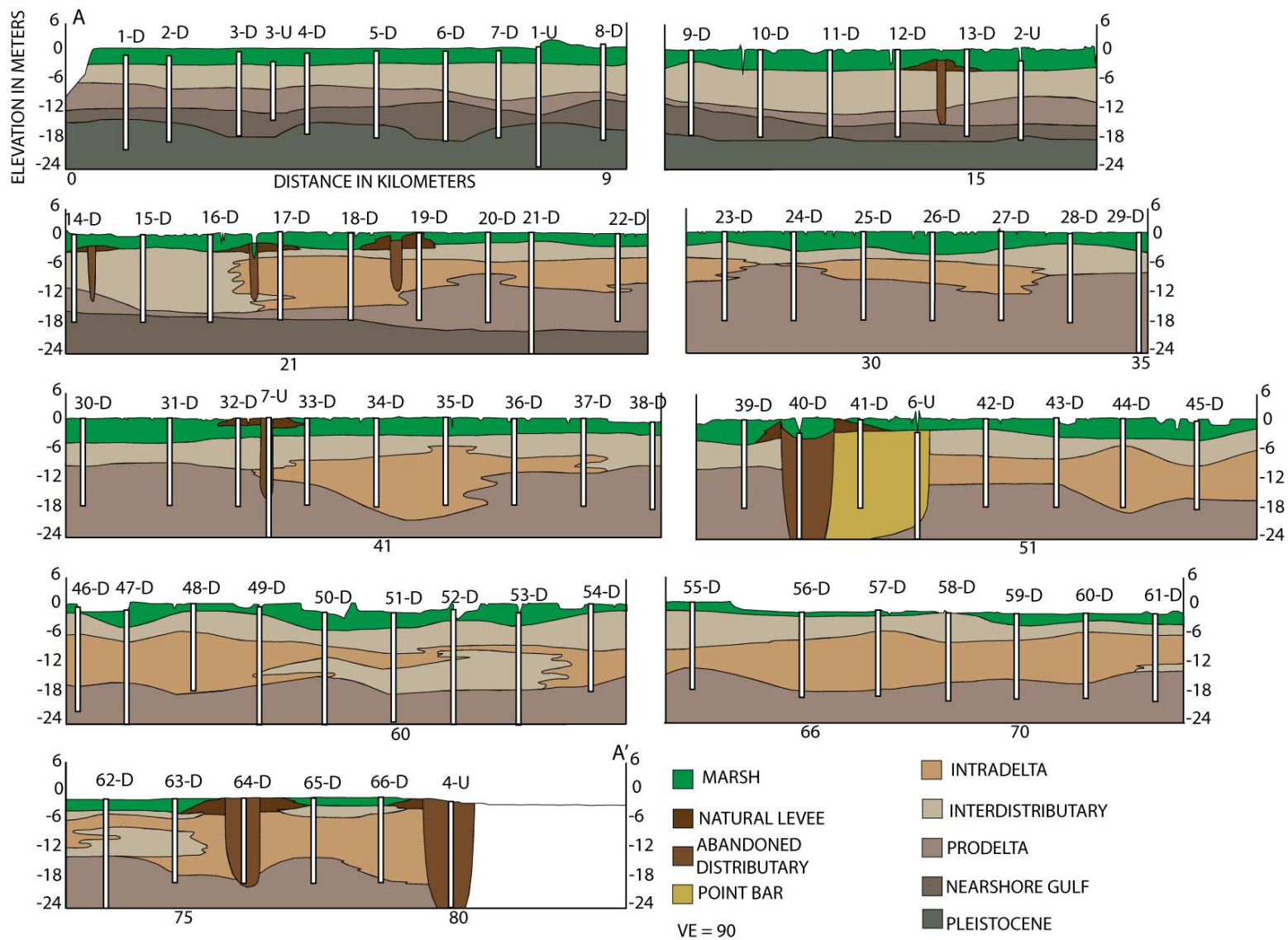


Figure 10 - Cross-section based on over 60 borings, modified from Kolb and van Lopik (1958a), showing discrete locations of deltaic deposits, including locations of formerly active distributary channels.

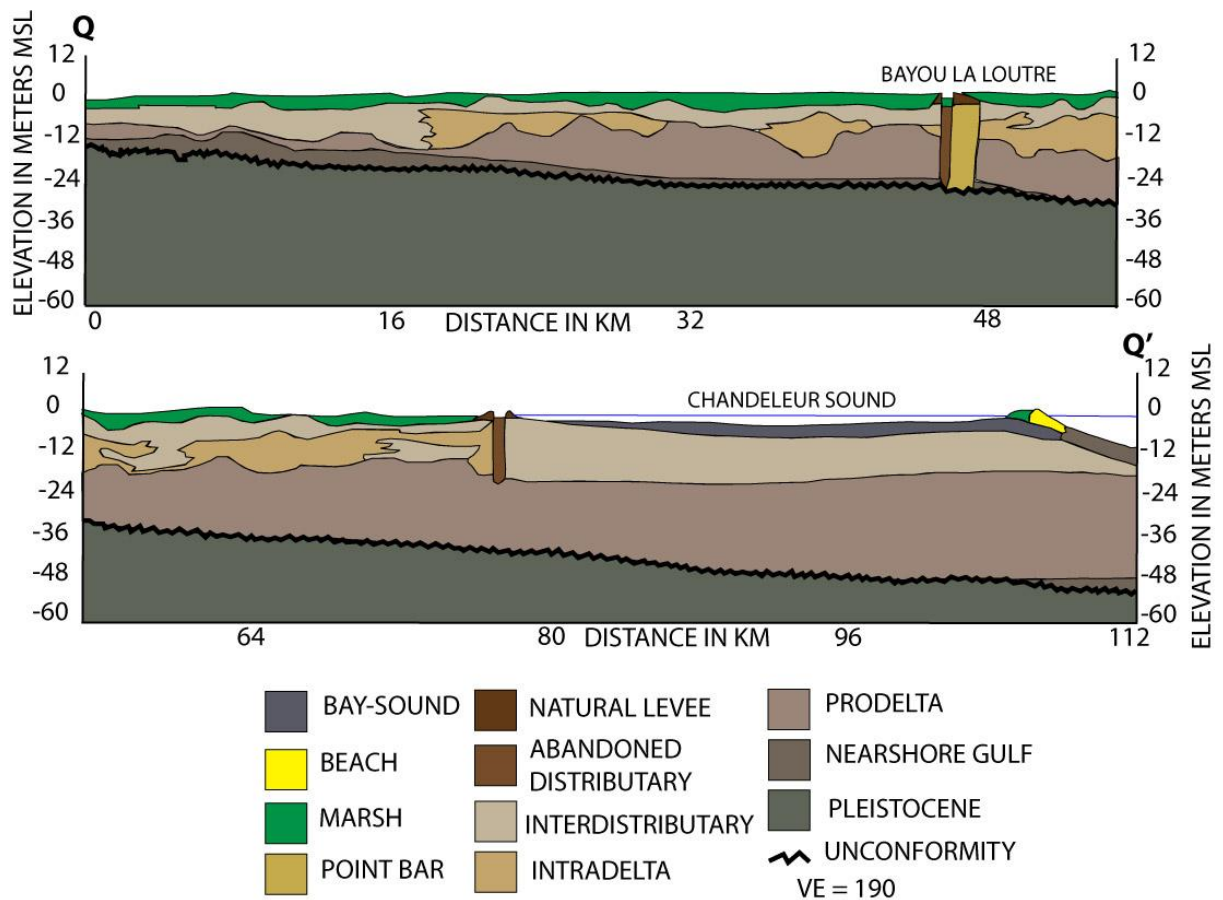


Figure 11 - Idealized cross-section of the St. Bernard delta complex showing the distribution and location of deltaic deposits. Modified from Kolb and van Lopik (1958a).

Interpretation

The overall stratigraphy of the St. Bernard Delta complex, from the previously described cross-sections, is dominated by interdistributary deposits. The coarse-grained deposits, such as intradelata complexes, natural levees, and abandoned distributary channels are limited. Natural levees and their corresponding abandoned distributary channels are highly localized and spatially variable features. These features have been exposed during ravinement and were likely responsible for the initial sandy supply to the Chandeleur Island system (Penland et al 1988). The volume of sediment in intradelata complex deposits is much greater than in natural levees, less spatially variable, and more likely to be released during ravinement in large quantities.

However, it appears that the majority of intradelta complex deposits are confined between the southwestern most extent of Bayou La Loutre and the intersection between the Gulf Intracoastal Waterway and the Mississippi River-Gulf Outlet.

Stratigraphic Models

Two fence diagrams (Figure 12 and Figure 13) and a three dimensional model (Figure 14) were created using Rockworks 14 (revision 2009.3.23, RockWare Inc., 2008) from the data provided by Kolb and van Lopik (1958a, b). Fence diagram 1 (Figure 12) was created by mapping cross-sections in similar locations to cross-section locations in Kolb and van Lopik (1958). Also, the longest cross-section from Kolb and Lopik was included because it follows the depositional strike of the St. Bernard delta complex. The shorter perpendicular cross-sections follow the dip. This fence diagram shows very similar stratigraphy to the cross-section it was derived from. However, there is significant error in the distribution of the sediments. In the model it appears that abandoned distributary and point bar deposits are located throughout the delta and are not particularly associated with any known distributary networks. The model extrapolated the presence of these deposits that are known to be isolated to the immediate vicinities of abandoned distributary channels. What can be gleaned from this model is the complexity and interfingering of intradelta complex and interdistributary deposits.

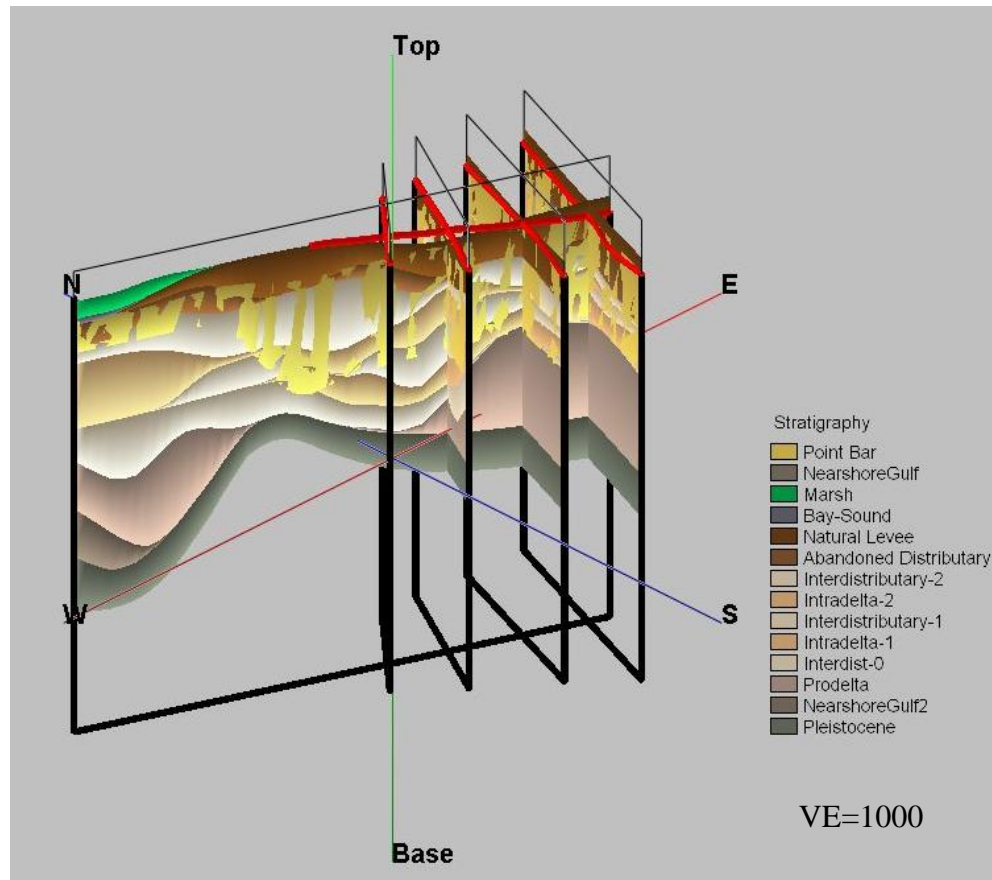


Figure 12 - Fence diagram of the St. Bernard delta complex showing the location and relationship between stratigraphic units based on the cross-sections provided by Kolb and van Lopik (1958a, b). This model contains spatial inaccuracies (i.e. the location of point bar deposits), but does provide a useful conceptual model for the St. Bernard delta. Vertical Exaggeration is 1000.

Fence diagram 2 (Figure 13) was created using the cross-sections from the seaward end of fence diagram 1 and is essentially a sub-section of Fence diagram 1. The purpose of this was to obtain better resolution on delta stratigraphy and ignore the stratigraphy updip of the delta complex. Because the area of interest is the stratigraphy directly below the modern shoreline, the stratigraphy updip (i.e. closer to New Orleans) is not relevant in this study. As in the first diagram, this diagram shows an inaccuracy in the distribution of point bar and abandoned distributary deposits, but displays the complex nature of the relationship between intradelta complex and interdistributary deposits. What is more prominent in this diagram is that the interdistributary and intradelta complex deposits seem to be concentrated in the updip direction

(i.e. they thin towards the distal edge of the delta complex). This is also observed in the cross-section, but is clearer in this diagram.

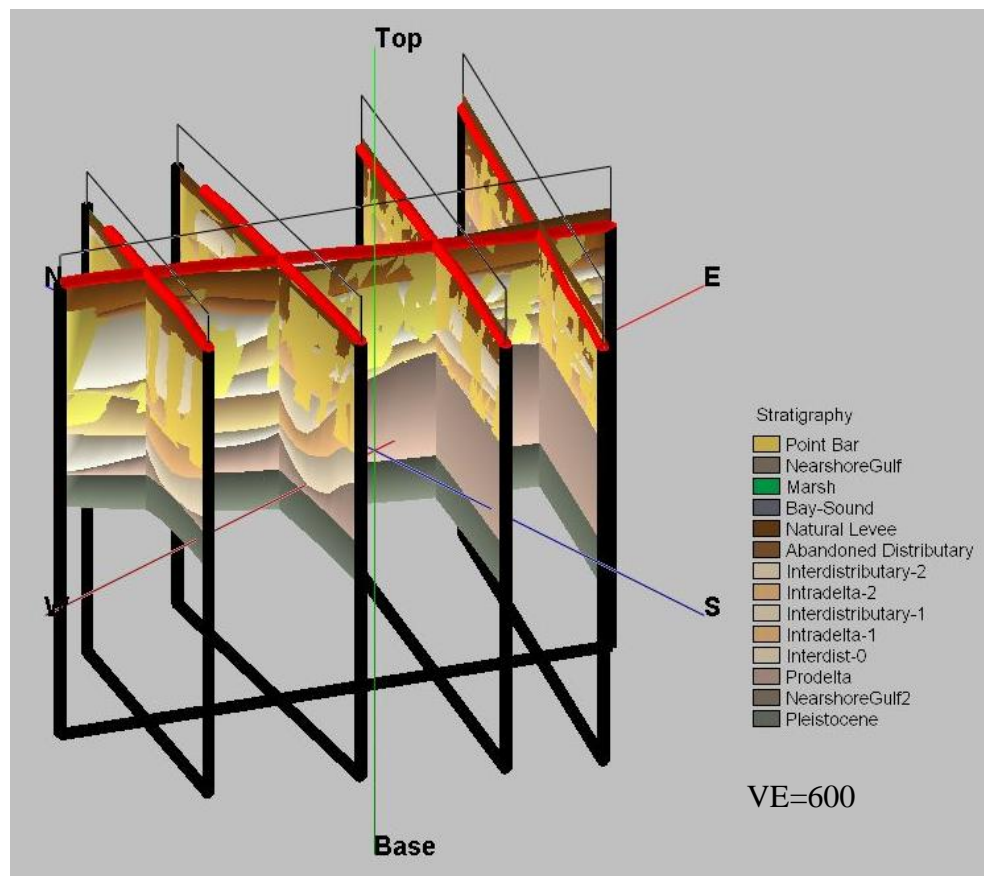


Figure 13 - Fence diagram of the lower St. Bernard delta complex showing a more detailed view of the lower-delta complex. Vertical Exaggeration is 600.

The three-dimensional model (Figure 14) is a solid block representation of the fence diagrams. Interestingly, the marsh surface in this diagram looks fairly accurate (i.e. a semi-continuous mainland with some islands). However, the abandoned distributary and point bar deposits are not realistically displayed (as noted in the fence diagrams). What is different in this model from the fence diagrams is that the relative thicknesses of deposits can be estimated. For example, the prodelta deposits are quite thick in comparison to interdistributary and intradelata complex deposits. Once again, the thickest deposits of intradelata complex and interdistributary are located in the middle of the model, beneath the marsh "shoreline".

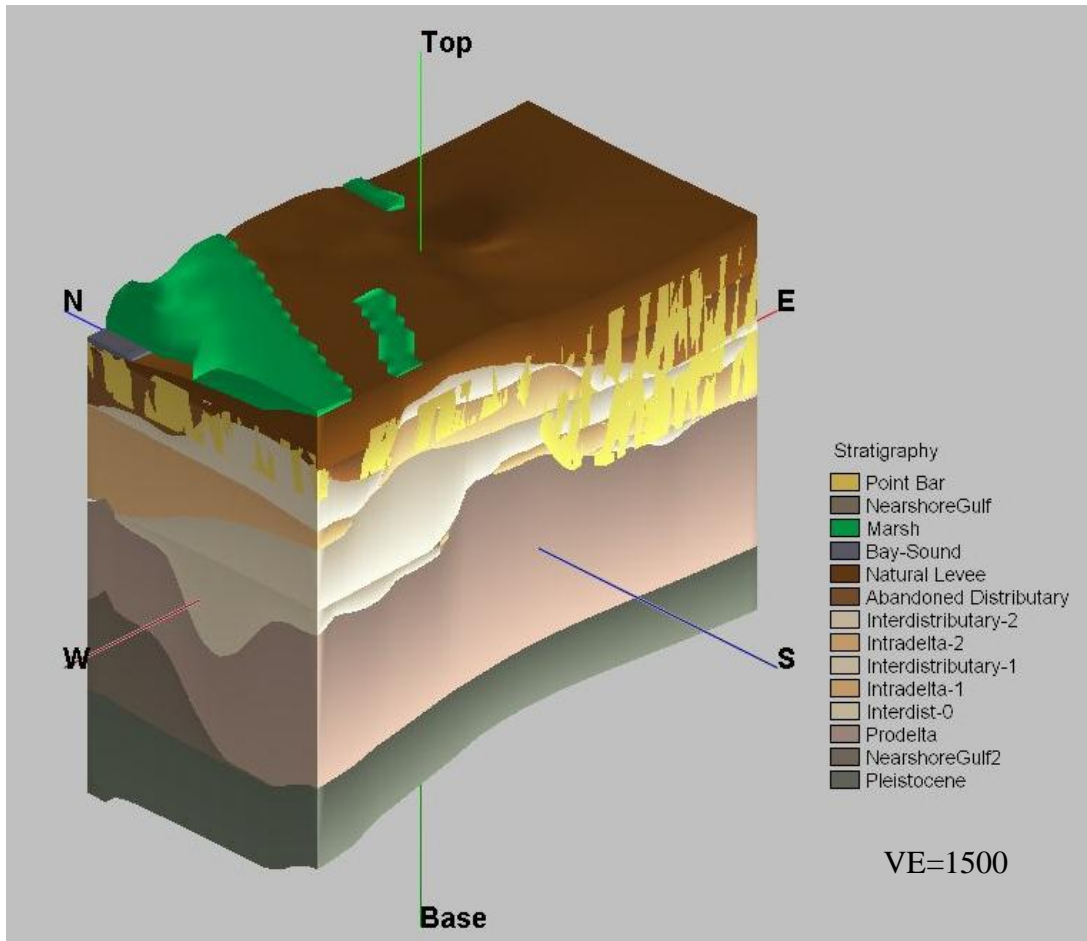


Figure 14 - Three dimensional block diagram of the St. Bernard delta complex based on cores and cross-sections provided by Kolb and van Lopik. Vertical Exaggeration is 1500.

Shallow Stratigraphy

The sections below describe cross-sections created in Adobe Illustrator from vibracores taken by the University of New Orleans Coastal Research Laboratory in 2003 and 2004. All other vibracore description sheets can be found in Appendix A - Vibracore Description Sheets and other cross-sections can be found in Appendix B - Cross-sections. Additionally, some of these vibracores and cross-sections can be found in Calvin (2002).

C-C'

04BL-08, 04L-09, 03BL-10, 04BL-03, and 03BL-3 are cores that make up the cross-section BL_C-C'. In the core 04BL-08, from 4.60m to 5.60m is dark gray sand with shell

fragments. Above this unit from 3.89m to 4.60m is light gray clay. Further above from 3.89m to 2.80m is a gray unit of clay and sand. The topmost unit from 2.80m is tan clay with abundant roots and organics. 04BL-09 begins in light gray clay from 5.98m to 3.14m. From 2.54m to 3.14m is dark gray to black clay. 1.22m to 2.54 m contains brown clay with organics. From 1.22m to the top of this core is dark brown clay with massive rooting. 03BL-10 contains two units: gray clay and sand from 2.98m to 6.47m, and organic clay from the surface to 2.98m. In the core 04BL-03 from 5.18m to 5.91m is light gray massive sand. 2.99m to 5.18m is light gray clay. This unit coarsens into light gray sand from 2.42m to 2.99m with numerous wood fragments. 1.19m to 2.42m is brown gray clay with wood fragments. From 1.19m to the surface is gray-black organic clay with rooting throughout. 03BL-3 contains two units: clay and sand from 0.40m to 4.00m and organic clay with rooting from 0.40m to the surface.

Z-Z'

Four cores make up the cross-section Z-Z': STB-01-I, STB-01-G, STB-01-D, and STB-01-B. STB-01-B was previously described in X-X'. STB-01-I has a total length of 7.13m and begins in cross-bedded fine sand that grades into horizontal beds of medium sand at 6.13m. Overlying this from 5.96m to 6.13m is fine sand. Above this from 5.82m to 5.96m is a massive bed of medium sand. From 5.54m to 5.82m is gray and brown silt. The next interval from 5.40 to 5.54 is horizontally laminated tan fine sand. Overlying this from 5.32 to 5.40m is gray and brown fine sand to silt. Above this from 4.97 to 5.32m is a unit of horizontal laminations of tan fine sand with a sharp bottom contact. From 4.71m to 4.97m is a unit of interbedded silt, fine sand, and clay with clay content increasing with depth as sand content decreases. The interval from 4.31 to 4.71m is a massive bed of fine sand with an interbedded unit and some shell fragments. Overlying this from 3.31 to 4.97m is interbedded silt and fine sand with some organic material.

Above this from 2.70m to 3.31m is interbedded organic material with silt which grades into clean tan silt. From 2.29m to 2.70m is a massive bed of dark gray silt with some shell fragments. Numerous shell fragments in gray silt occur from 2.22m to 2.29m. Above this from 1.71m to 2.22m is interbedded tan and light gray silt and fine sand. Overlying this from 0.49m to 1.71m is organic clay that grades into silt. The top most unit of this core from 0.49m is organic rich clay and peat with abundant rooting. STB-01-G has a total length of 7.13m and the bottommost unit from 5.75m to 7.13m is silt and fine sand with abundant shell fragments that grades into a massive bed of silt and clay. Overlying this from 4.47 to 5.75m is interbedded silt and fine sand with horizontal laminations. Above this from 4.39 to 4.47m is a unit of shell fragments. From 2.70m to 4.39m is interbedded clay and silt with horizontal laminations. The interval between 0.70 to 2.70m is gray and brown interbedded silt and fine sand with horizontal laminations. Overlying this from 0.21m to 0.70m is a massive silt bed with rooting. The topmost unit of this core from 0.21m is marsh vegetation and peat. STB-01-D has a total length of 7.71m and the bottommost unit from 5.51m to 7.71m is a massive bed of silt and clay. Above this from 4.78m to 5.51m is interbedded silt and fine sand. Overlying this from 4.51 to 4.78m is silt which grades upwards into clay. From 3.77m to 4.51m is silt that grades into fine sand with some coarser component. The interval from 3.55m to 3.77m is interbedded silt and fine sand. From 3.18m to 3.55m is silt which grades upwards into fine sand. Above this from 2.39m to 3.18m is organic clay with numerous plant fragments. Overlying this from 1.74m to 2.39m is interbedded organic clay and peat. From 1.44m to 1.74m is organic clay and peat. The interval from 0.78m to 1.44m is organic clay and plant fragments. The topmost unit from 0.78m is marsh vegetation and peat.

Interpretation

C-C' contains considerably more sand than the other cross-sections in this area (Appendix B - Cross-sections), particularly in the cores closer to Bayou La Loutre (Figure 15). The lower sand units of 04BL-03 and 03BL-3 have been interpreted as a crevasse splay mostly because they are sandy clays that contain multiple sand-rich layers. Coeval with this deposit is an interdistributary bay at the base of 04BL-08, 04BL-09, and 03BL-10. The presence of shell material and the absence of sand in these units differentiate the interdistributary bay deposits from crevasse splay deposits. Above the crevasse splay deposits in 04BL-03 there is a unit containing several woody fragments, and thus this has been interpreted as a backswamp. Like most of the aforementioned cross-sections, this cross-section is capped by salt marsh deposits containing organic-rich clay, rooting, and peat.

Cross-section Z-Z' (Figure 16) shows a range of interdistributary and distributary associated depositional environments, typically interdistributary bay deposits overlain by crevasse-splay deposits. This cross-section lies on the cut-bank side of a meander, and thus would likely be a site of levee-breaching events and overbank deposits. Most of the cores sampled in this area display a consistent fining upward trend of overbank deposits grading vertically upward into muddy, organic marsh deposits (Figure 16). This vertical transition is marked by a gradational contact at approximately 1 m depth in most cores.

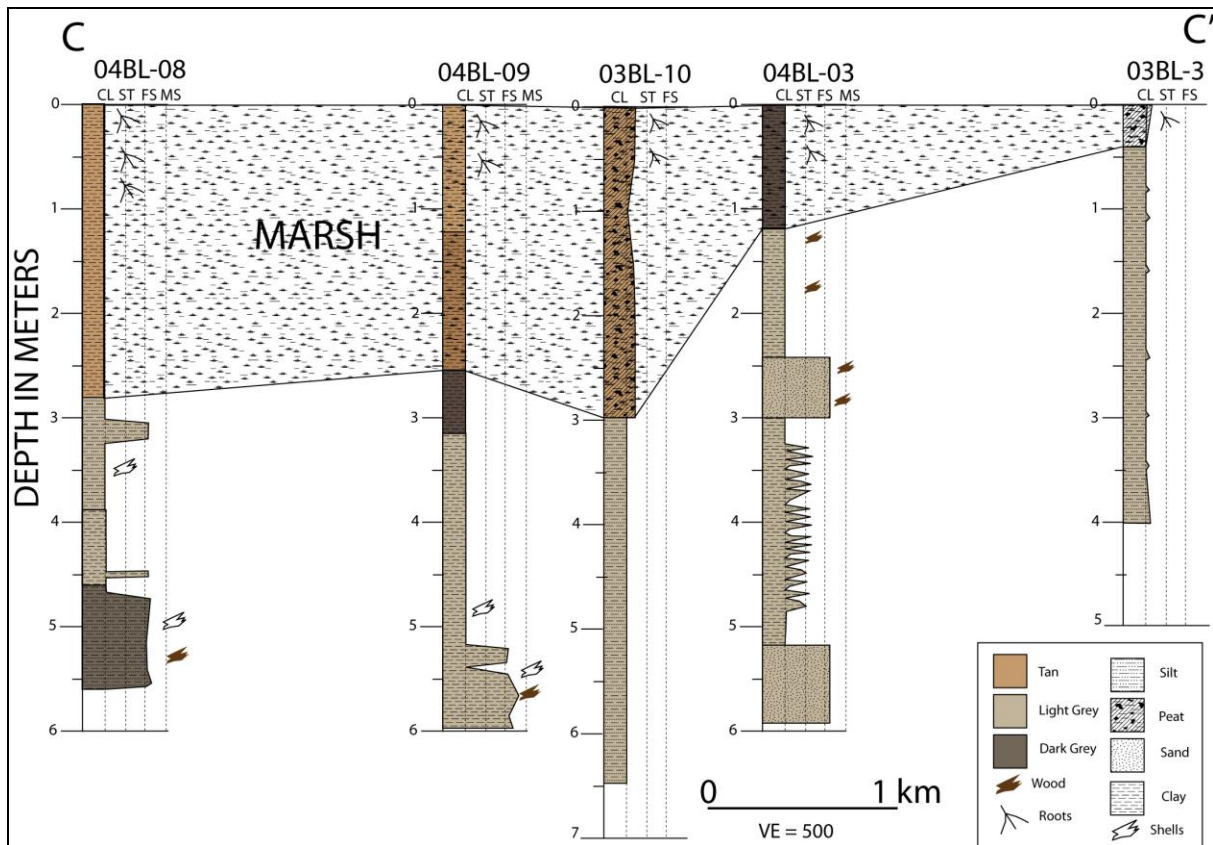


Figure 15 - C-C' trending north to south along Bayou La Loutre for 5 kilometers. Notice the lack of sand-rich material in the cores and also in the cross-section in general. CL is clay, ST is silt, FS is fine sand, and MS is medium sand. The vertical scale is in meters.

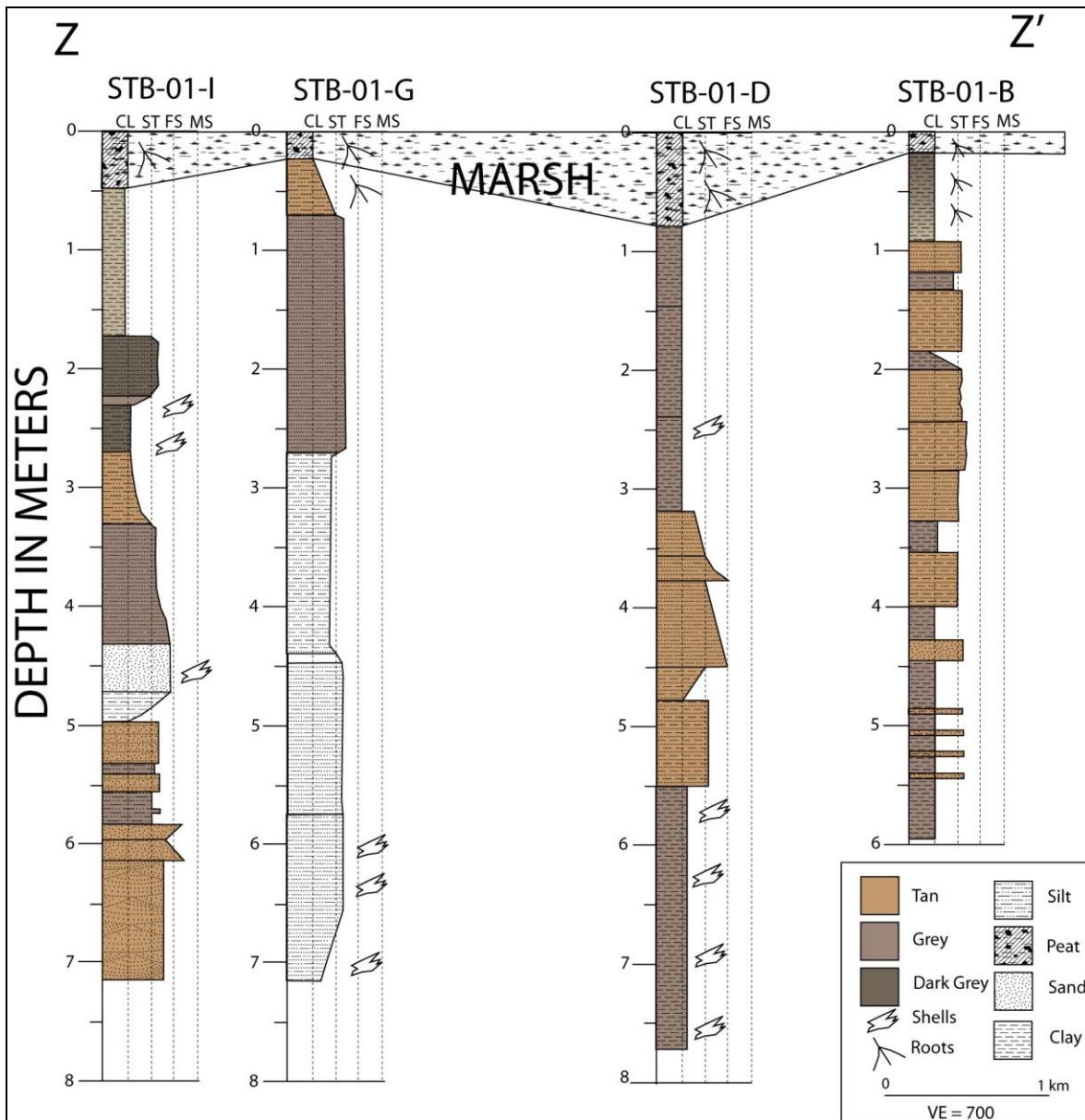


Figure 16 - Cross-section Z-Z' that trends north-south across the study area for a distance of 6 km. This cross section indicates the high sand content and the range of lithologies that are present in this area. Lithofacies have been interpreted to show the depositional environments.

Modern Marsh Surface

The Coastwide Reference Monitoring System (CRMS) site 0003 is located near Isle au Pitre in saline marsh dominated by *Spartina alterniflora* at N30.0994, W89.2528. The site was measured four times: once in late 2008, once in early 2009, again in the fall of 2009, and finally in early 2010. The average elevation change is 0.15 cm yr^{-1} and vertical accretion rates estimated

since is 1.25 cm yr^{-1} . CRMS0108 is located in a more central area of the St. Bernard marsh, but it is still saline marsh dominated by *Spartina alterniflora* at N29.9551, W89.4159. This site was measured twice: once in October of 2009 and again in April of 2010. Unfortunately, this site does not have accurate accretion data, but the reasons for the absence of data are not explained. CRMS site 1024 is a similar situation to CRMS 0108; neither of these cores have elevation data against which to measure the accretion rates. The site 1069 is located just south of 0003 in a saline marsh dominated by *Spartina alterniflora* at N30.0485, W89.2183. CRMS site 1024 was measured once in October of 2009 and again in April of 2010. The average elevation change is 0.7 cm yr^{-1} and the average vertical accretion is 2.47 cm yr^{-1} . CRMS site 4548, located at W29.8607, N89.6667, is saline marsh dominated by *Spartina alterniflora*. This site was measured three times: once in early 2009, once in late 2009, and again in early 2010. The average elevation change is 1.19 cm yr^{-1} and the average accretion rate is 0.3 cm yr^{-1} . The CRMS site 4551 is located at N29.8535, W89.6042 in *Spartina alterniflora*-dominated saline marsh. This site was measured only once in early 2009. Unfortunately, there are no data for this site. CRMS 4557 is also in a *Spartina alterniflora*-dominated saline marsh located at N29.8244, W89.573. This site was measured once in early 2009, once in late 2009, and again in early 2010. This site has an average elevation change of 2.02 cm yr^{-1} . However, there are no accretion data for this site. The site 4572 is located at N30.0567, W89.4792 in a *Spartina alterniflora*-dominated saline marsh. This site was measured once in early 2009, once in late 2009, and again in late 2010. The average elevation change at this site is 0.78 cm yr^{-1} . The average accretion rate is 0.95 cm yr^{-1} . CRMS 4596 is located at N30.0567, W89.448 and is in a *Spartina alterniflora*-dominated saline marsh. This site was measured four times: once in late 2008, once in early 2009, once in late

2009, and again in early 2010. The average elevation change at this site is 0.02 cm yr^{-1} . The average accretion rate is 0.42 cm yr^{-1} .

Bathymetric Profiles of Chandeleur Sound and Seaward of the Chandeleur Islands

Six profiles were extracted from the bathymetric data (Figure 8) using Tecplot (version 10.0-6-012, Tecplot, Inc., 2005) and imported into Microsoft Excel (version 12.0.6557.5000, Microsoft Corporation, 2006). The bathymetric data are based on NOAA hydrographic charts, possibly including historical data. The bathymetric data are extrapolated by the ADCIRC model onto elevation data of the land surface. What this indicates is that there are no empirical data for the shoreface. As a result, these profiles should to be considered a model of the shoreface, and do not represent actual shoreface profiles. That being said, the profiles do provide an acceptable base to attempt this experiment. Three profiles were extracted from the marsh shoreline and were selected based on reliability of the data (i.e. no errors were visible) and position of the shoreline in relation to the stratigraphic cross-sections in this study. Three profiles were extracted from the seaward side of the Chandeleur Islands: one in the north, one transect in the middle, and one on the southern part of the islands. These data are displayed as graphs (Figure 17) in Microsoft Excel along with the equilibrium profile established by Wilson and Allison (2008) which is described by the following equation:

where y is the depth below mean sea level and x is the horizontal distance from the marsh surface.

In order to clarify and simplify the plot, only one extract profile from the St. Bernard Marsh and one from the Chandeleur Islands are shown. The profiles were selected by visually estimating the average shape of the profile and eliminating the profiles that appeared to contain

outliers (Figure 17). Based on these profiles, relative depths of ravinement were established at 2 m for the marsh and 12 m for the Chandeleur Islands.

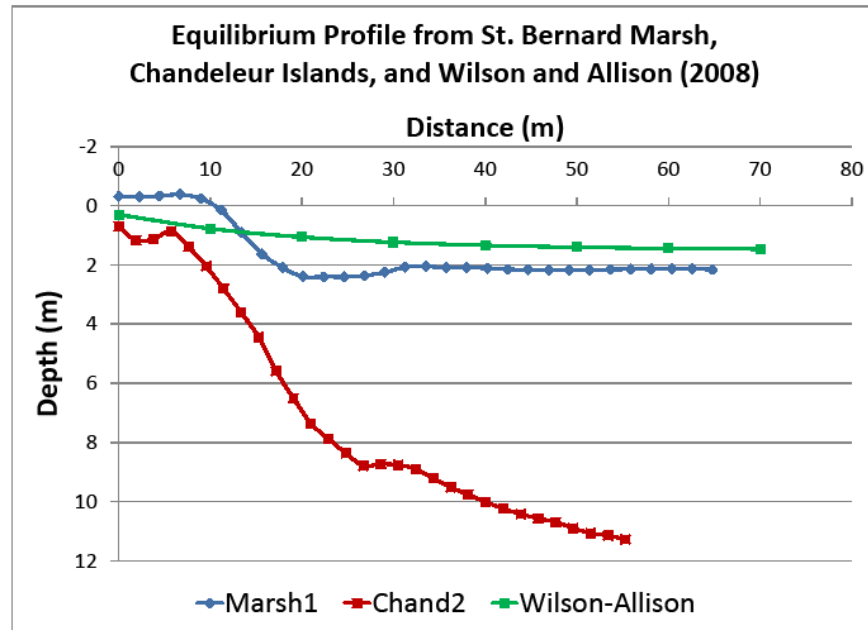


Figure 17 - Shoreface profiles, both from bathymetric data (Schindler, 2010) in red and blue, and an empirically derived equation (blue; Wilson and Allison, 2008; $y = -1.5e^{(-0.05x)}$), showing the window of ravinement between the blue and red profiles. The blue and green lines are considered the current shoreline profiles of the St. Bernard marsh. The red profile, which was extracted from the Gulf side of the Chandeleur Islands, is considered to be the profile to which the current marsh profiles will equilibrate as the Chandeleur Islands disintegrate and submerge.

Discussion

Stratigraphic Models

The fence diagrams (Figure 12 and Figure 13) and the three-dimensional model (Figure 14) are not perfect models of the delta complex, but they do contribute to the understanding of the stratigraphy within the marsh. All three of these diagrams agree with the stratigraphic cross-sections from Kolb and van Lopik (1958a, b) that the thickest deposits of intradelta complexes are located beneath the modern shoreline (or approximately in the middle of the delta complex). This indicates that if Chandeleur Sound deepens in response to increased fetch and resulting depth-limited waves, there are thick sand-rich deposits into which a ravinement surface may erode.

Volumetric Calculations

Volumetric and spatial information are of importance for these intradelta and other sand-rich deposits (>25% sand). As previously mentioned, these deposits were sourced during the initial construction of the Chandeleur Island system, and will likely be sourced during the formation of a new sandy shoreline along the marsh fringe. Using the profiles created by extracting bathymetric data, a "window of ravinement" was established. Ravinement, as defined by Stamp (1922), is a disconformity resulting from a retrograding surf zone which intersects pre-existing coastal deposits. This "window of ravinement" is the depth to which Chandeleur Sound will likely equilibrate as wave heights in the Sound increase due to the submergence of the Chandeleur Islands. The marsh profiles were asymptotic to approximately 2 meters depth. The profiles from the Gulf side of the Chandeleur Island system were asymptotic to approximately 12 meters depth. These profiles were overlain on all the aforementioned stratigraphic cross-sections. These cross-sections were then edited, removing all deposits considering sand-poor (less than

25% sand). Cross-sections that did not contain sand above 12m depth or that were significantly distal from the modern shoreline were ignored. The locations of these sand-rich strata in map view were drawn using ESRI, Inc. ArcMap (version 9.2, 2006) based on the "window of ravinement" overlain on the following cross-sections: A-A', C-C', F-F', and PC_B (Figure 18; Table 2).

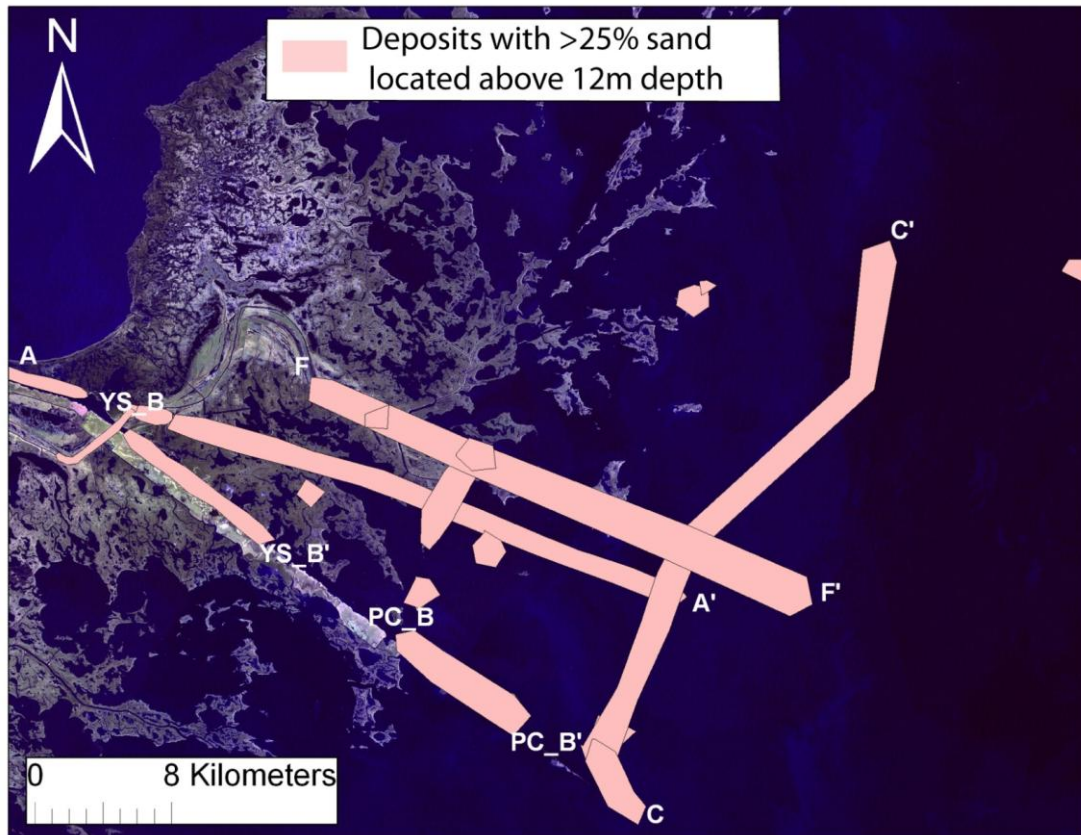


Figure 18 - Locations of sand bodies in the St. Bernard delta complex located above the window of ravinement depth (12 m).

Using this information, minimum and maximum volumes of sediment to be liberated during ravinement were calculated. All calculations are based on a given length (that is, the lateral extent of the deposits along the transect; Table 2). Thickness values were based on thicknesses observed in cross-sections, and minimum values for each calculation used the minimum thickness, and vice versa for maximum values. A standard width of 1 km was used for

the minimum width. Considering that the length in a dip direction of some of these deposits exceeds 40 km, 1 km width in a strike direction is relatively thin. The maximum width values were simply the minimum values doubled (2 km). A final variable was added in to all calculations: sand percentage. Based on the information from Kolb and van Lopik (1958a, b), intradelta complex deposits contain 25% sand and abandoned distributaries contain 45% sand. Since these are the most common deposits in the delta lobe, the lowest sand percentages were factored into the minimum sand volume, and likewise for the maximum sand percentage and volume.

The error for these volumes was calculated by doubling the width variable for both minimum (25% sand) and maximum (45% sand) values, producing a value of 0.10 km³.

One caveat of this is intradelta complex deposits are more widespread in the system, and abandoned distributary deposits occur locally. This affects the results because the maximum volumes calculated are likely much greater than the actual volumes, and the minimum volumes are more trustworthy calculations.

Table 2 - This table shows volumetric calculations for various sand bodies located in the cross-sections A-A', C-C', F-F', and PC_B.

A-A'	Length (m)	Thickness (m)	Width (m)	% Sand	Volume (km ³)
Min	10834	3	1000	0.25	0.01
Max	10834	9	1000	0.45	0.08
C-C'					
Min	39277	6	1000	0.25	0.05
Max	39277	10	1000	0.45	0.35
F-F'					
Min	18044	6	1000	0.25	0.03
Max	18044	10	1000	0.45	0.08
PC_B					
Min	8490	3	1000	0.25	0.01
Max	8490	6	1000	0.45	0.02
Total Volume					
Min	0.10				
Max	0.55				

Modern Marsh Surface

Geomorphology of Erosion in the St. Bernard Marsh

Land-loss maps produced by Britsch and Dunbar (2006) indicate that, in comparison to other, younger deltaic complexes, the St. Bernard complex has lower rates of land loss. Land loss rates in Terrebonne and Barataria basins (Lafourche delta complex) were between 19.6 and 24.0 km²yr⁻¹ from 1956 to 1978 and 26.4 and 28.7 km²yr⁻¹ from 1978 to 1990 (Barras et al., 1994).

The St. Bernard delta complex had land loss rates between 5.9 and 6.7 km²yr⁻¹ from 1956 and 1978 and between 4.1 and 4.9 km²yr⁻¹ from 1978 to 1990 (Barras et al., 1994). The relatively low rates in this area are likely due to the age of the complex and the nature of erosion in brackish marshes relative to freshwater marshes (Howes et al., 2010). Ideally, deltaic subsidence is most rapid during fluvial occupation and early abandonment because sediment compaction and dewatering rates decrease through time (Tornqvist et al 2008; Mesri and Godlewski 1997). Erosion in St. Bernard Marsh occurs primarily by interior ponding and bay expansion and the marsh becomes fringed by irregular shaped islands along bay margins (Reed 1989). Once these marsh islands are formed, they are subject to wave attack and erode quickly. In the St. Bernard Marsh, many of the remaining marsh islands overlie distributary channel natural levee deposits (Kolb and van Lopik 1958a). The coarse-grained nature of these distributary natural levee deposits and the topographic highs of relict natural levees make them more-resistant to ponding and erosion. Many of the marsh islands along the fringes of the St. Bernard complex are rimmed with shell beaches.

Accretion Rates (CRMS)

Average accretion rates from CRMS sites 0003, 1069, 4548, 4572, and 4596 are approximately 12.5 mmyr⁻¹. Conservative estimates for Holocene subsidence in the Mississippi River delta plain by Tornqvist et al. (2006) are between 0.06 to 0.12 mmyr⁻¹. However, Penland and Ramsey (1990) used U.S. Army Corps of Engineer tide gage stations to obtain relative sea level rise rates in the St. Bernard delta complex between 1.01 cmyr⁻¹ and 1.09 cmyr⁻¹. Because the St. Bernard delta complex was abandoned ~1800 years BP, it can be assumed that compaction rates (and thus subsidence rates in general) are lesser (Mesri and Godlewski, 1997) strictly based on the age of the deposits. Therefore, subsidence rates in the St. Bernard marshes

are lower than the Mississippi River delta plain in general. If the rate of relative sea level rise (subsidence and sea level rise combined) is equal to approximately 1.00 cm yr^{-1} (Penland and Ramsey, 1990) and the average accretion rate of 1.25 cm yr^{-1} (CRMS), then marsh is currently maintaining an appropriate elevation relative to sea level change. However, predicted ongoing accelerations (IPCC; Bindoff et al., 2007) in sea level rise will challenge the ability of this salt marsh to maintain an elevation above sea level.

Shell-Rimmed Shorelines

Presently, sandy shorelines and sandy islands in Chandeleur Sound are rare. Along some sections of mainland fringing marsh, shell-lag (primarily *Crassostrea virginica*) shorelines and pocket beaches have developed from winnowing of shell material contained within interdistributary deposits. Modeling experiments validated with field data have demonstrated that once shells are deposited, they become more difficult to entrain than typical spherical particles due to imbrication of the shells (Allen, 1984; Weill et al., 2010).

Other authors (e.g. Weill et al., 2010; Allen, 1984) have studied the hydrodynamic properties of shells. Allen (1984) concluded that whole bivalve shells settle slowly relative to other similarly sized particles because of their large surface area and large drag. However, once the shells are settled, in non-turbulent environments, they become imbricated and are extremely difficult to entrain. Additionally, shells settling in a sediment-rich slurry, such as a turbidite, create a void space in which sand material can be trapped by the shell and thus settle along with the shell. Weill et al. (2010) studied shells further in a chenier system in France. In this system, shells are isolated from other material and deposited in sheets. Weill et al. (2010) conclude that the imbricated shells form a protective armor on the shoreline, resisting entrainment. Additionally, because of the high porosity in shelly shorelines, they can serve as a trap for finer

grained sediment (in this case, sand and clay). This is extremely relevant to the St. Bernard delta complex because of the abundance of shell-rich shorelines and islands is abundant and lack of sand. It is likely that, in the future, if sand is introduced to the system, it will be trapped on these shorelines.

Models of Shell-Shoreline Formation and Evolution

Based on the geomorphic evolution of the St. Bernard marsh and the current regime dominated by sandy shorelines, three conceptual models were created. The first stage of the model (Figure 21) describes how shell pocket beaches are converted to subaqueous shell mounds. This model was based on observations during an flight over the study area in November 2009. Pictures from this flight showed important processes, such as waves washing into the marsh behind shell shorelines (Figure 19) and retrograding shell beaches (Figure 20).



Figure 19 - Oblique aerial photograph near Isle Au Pitre in the northernmost extent of the St. Bernard marshes, looking south. Notice the evidence of waves washing into the marsh and overwash platforms behind the shell shoreline.



Figure 20 - Oblique aerial photograph of Martin Island, located in Chandeleur Sound, looking west. Notice the marsh platform exposed seaward of the shell shoreline on the southern shoreline.

In this model (Figure 21), shell pocket beaches are formed by winnowing and deposition on the marsh surface. As the marsh continues to fragment, sparing more resistant landmasses (like natural levee deposits), these pocket beaches become shell-rimmed marsh islands. Eventually, due to the

combined pressures of subsidence and sea-level rise, the marsh becomes submerged and the shells accumulate in the shallow water above, forming a mound. After continued subsidence, the

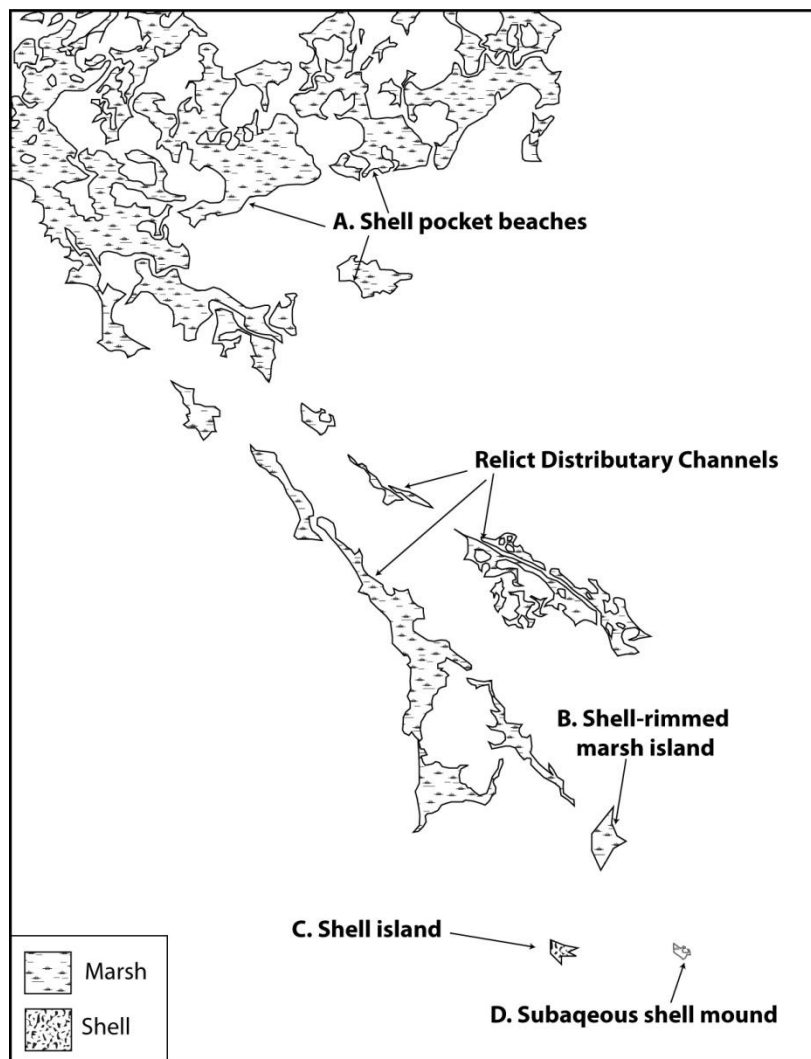


Figure 21 - Plan-view conceptual geomorphic model suggesting a progression of shell pocket beaches to submerged shell mounds, note the shell pocket beaches occur more inland than the shell-rimmed marsh islands and the subaqueous shell mounds. Relict distributary channels are preferentially preserved due to their lithology (compacted silts and clays more resistant to erosion). As these channels become isolated, shell-rimmed islands form, which eventually become shell islands due to the inability of the marsh to accrete vertically. Eventually, subsidence forces the entire mass to submerge as a shell mound.

shells too become submerged and form a subaqueous shell mound. The second and third conceptual model describe the effects of shell material on marsh shorelines (Figure 22) and the effects of the ravinement of sandy material on the marsh shorelines (Figure 23). Both models are based on the model proposed by Wilson and Allison (2008) for marsh shorelines on the

Mississippi River delta plain, which was derived from empirical data. Both models are divided into four stages, beginning in Stage A, a slowly subsiding marsh. In the shell-dominated system,

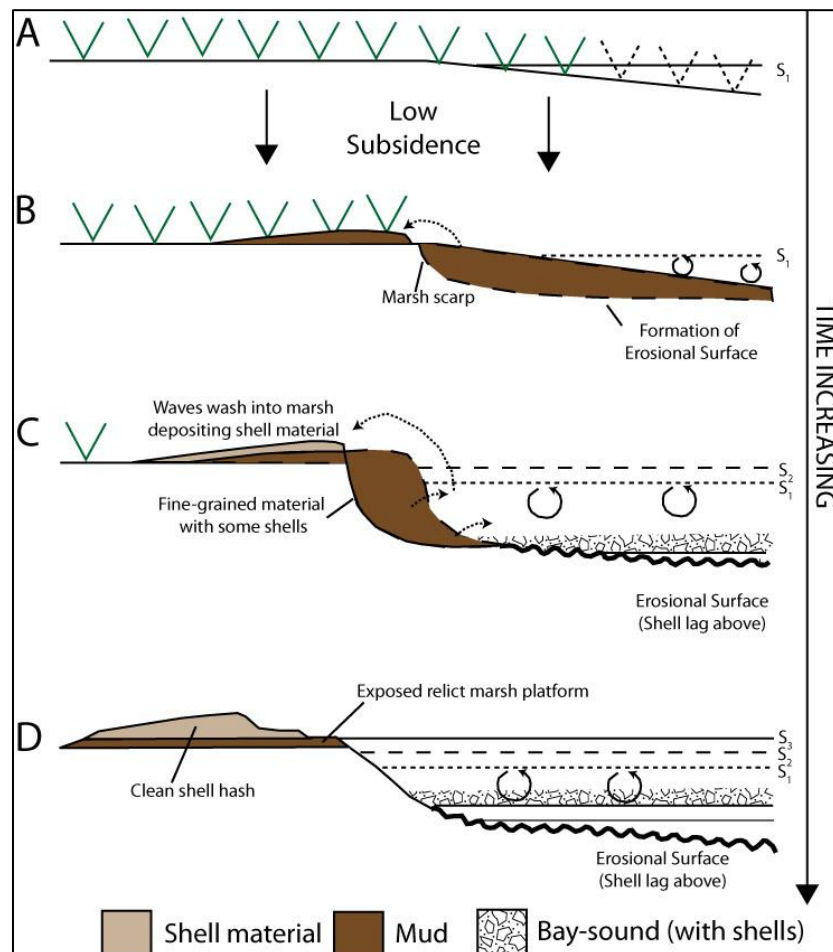


Figure 22 - Conceptual model of marsh-edge processes contributing to the formation of shell pocket beaches. B is initiated when a marsh scarp is formed, producing sediment that can be placed on the marsh surface by wave action. Eventually, as this marsh scarp deepens, shells and shell material are eroded from the bay-bottom deposits and the fine sediment is winnowed, leaving behind a shell pocket beach. Eventually, this shells smother the marsh, but also serve to armor the shoreline and fundamentally change the equilibrium profile. S1, S2, and S3 are subsidence lines indicating the progression of subsidence in the marsh system.

Stage B is initiated when an erosional scarp forms on the edge of the marsh and sediment becomes re-suspended. Some of this material is placed on the marsh surface during periods of high wave and tidal activity. The material left in suspension is winnowed until the largest particles (in this case, shells) remain. These shells are placed on the marsh surface during

extreme events (spring tides, cold fronts, and tropical cyclones). Through time, as depicted in stages C-D, the marsh surface is covered in shells which simultaneously protects the marsh by forming a type of pavement and inhibits accretion. This model complements the aforementioned conceptual geomorphic model describing how a shell pocket beach evolves into a subaqueous shell mound. Unlike the shell-dominated model, the source for sediment of the sand-dominated model is within the marsh itself. This model is based fundamentally on the idea that material located at depth within the marsh is liberated during ravinement and placed on the marsh surface. In Stage B of this model, a marsh scarp forms and the marsh shoreline begins retreating as a function of increased wave energy associated with the increased depth created by the marsh scarp. In Stage C, the ravinement surface, or the marsh scarp, has intersected a sand-rich body. This material is entrained, suspended, and transported by waves to the marsh surface, creating a sandy beach. In stage D, the shoreline continues to retreat, and the sand-body beneath the marsh surface continues to supply the beach on the surface. Eventually, a new equilibrium profile will be attained due to the fundamental differences in lithology (i.e. slope stability) between clay, silt, and sand. This new profile, in turn, changes the wave dynamics and begins a cycle observed on most beaches between reflective profiles and run-up profiles.

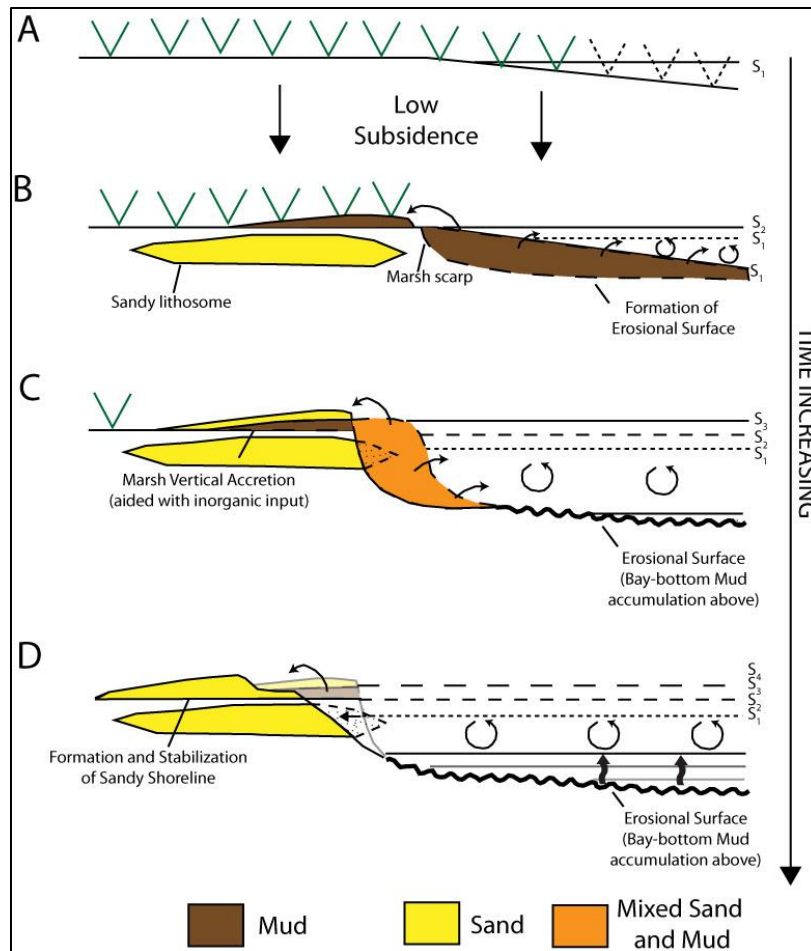


Figure 23 - Conceptual model showing the influence of sandy material on the shoreline. C is initiated when the marsh scarp intersects a sand-rich body, and waves move the material to the surface of the marsh. Eventually, this deposit on the marsh thickens as more of the deposit at depth is eroded, and a sandy-shoreline is formed. S1, S2, and S3 are subsidence lines indicating the progression of subsidence in the marsh system.

Conclusion

Regional Stratigraphic Relationships

(1) Is there enough sandy material in the shallow subsurface to contribute to building of a sandy shoreline?

Results indicate that much of the delta complex is composed of fine-grained material with limited sand-rich units. The volumetric calculations of the sand-rich units (>25% sand) are between 0.10 km^3 and $0.55 \text{ km}^3 \pm 0.10 \text{ km}^3$. There are large potential errors in these calculations, but they do give an appropriate volumetric range for the amount of sediment potentially in the system.

Erosional patterns in the marsh will determine how and when this sediment is liberated. The shoreline is not likely, based on historical erosional patterns, to erode uniformly, even as the marsh is exposed to open gulf conditions. The dominant pattern of erosion begins with ponding on the marsh surface, followed by marsh disintegration in the same circular patterns formed by the ponding process. This pattern of erosion dictates the amount and the preferential release of the sediment at specific times. If a pulse of sand-rich sediment is introduced into the system, and there is a significant hiatus before the next pulse is released, the first pulse may be eroded by wave and tidal activity. If this process continues, then sand will not accumulate and therefore be unable to form a continuous shoreline. This is a big caveat for forming a sand-rich shoreline, assuming that sand-rich material is present in the subsurface of the marsh.

Modern Marsh Surface

(2) Is the marsh stable enough to enable a shoreline to form against it if sandy sediments are liberated during shoreface ravinement in a regime of increasing wave energy?

Data from the Coastwide Reference Monitoring System (CRMS) indicates that accretion rates in the St. Bernard marsh are 12.5 mm yr^{-1} . Relative sea level rise (which is the combined

forcing of subsidence and eustatic sea level rise) is approximately 1.00 cm_{yr}⁻¹ (Penland and Ramsey, 1990). From these numbers, it is clear that the St. Bernard Marsh is able to accrete and survive present rates of relative sea-level rise. However, as eustatic sea-level rise accelerates, these marshes will find it increasingly difficult to accrete (Bindoff et al., 2007) if they continue to accrete at a rate similar to that indicated by the CRMS data.

(3) What do historical to recent marsh fragmentation patterns and mode of marsh shoreline erosion tell us about response to increasing wave energy, tidal current and prism evolution, and zones of relative stability?

In the current regime of interior wetland loss landward of Chandeleur Sound, natural levee deposits associated with distributary channels have high preservation potential relative to surrounding interdistributary marsh deposits due to higher initial elevation, lower compactional subsidence, and higher concentrations of coarse-grained (silty to sandy) inorganic sediment. This has resulted in preferential preservation natural levee deposits that form linear headland features extending through open bays and into Chandeleur Sound. As erosion and retreat continue, the location of sand-rich pocket beaches and shorelines will likely be localized to natural levee deposits, and other sand-rich strata (Otvos 1986). However, this is not expressed in the geomorphology of the modern marsh.

More resistant landmasses associated with natural levee deposits become isolated as marsh islands with shell-rimmed beaches but ultimately, become submerged to form shell mounds. Without adequate sand supply from subsurface liberated during ravinement this regional erosional behavior will likely continue and accelerate in the future under increased wave and tidal energy associated with the transgressive submergence of the Chandeleur Islands.

Initially, marsh surface exists in a regime of subsidence-driven relative sea level rise. As the bay expands, fetch increases, and thus wave heights increase, creating depth-limited waves

and allowing these waves to scour deeper (Feagin et al., 2009). The marsh scarp and shoreface retreats due to wave attack. Fine material eroded from the marsh shoreface is removed from the system and shell material from both within the underlying stratigraphy and in the bay is reworked onshore to form a shell shoreline (e.g. Weill et al., 2010). Additionally, overwash during storm events flattens the marsh behind the shell shoreline and pushes the shell material further into the marsh producing a perched shell beach fronted by an erosional marsh scarp.

(4) Will shoreface processes be active along the marsh shoreline soon (within ~50 years)? Or will the subaqueous sand shoals protect the marsh from open marine conditions for many years (>1000 years)?

In a study by Stone et al. (2005), Ship Shoal, an offshore transgressive deposit, was analyzed as a sediment source for restoration projects. The study concluded that the removal of Ship Shoal did not have a significant effect on the Isles Derniere. One caveat with this study is that the model assumes instantaneous removal of Ship Shoal, and is not coupled to adjust for changing hydrodynamic conditions. In a natural setting, if Ship Shoal were removed, storm waves would scour the area landward of Ship Shoal, allowing for larger waves to break close to the Isles Derniere through time. Eventually, Isles Derniere would face significantly different hydrodynamic conditions than those presented in Stone et al. (2005).

What is the effect of shell material on the marsh?

Currently, shell material is the dominant beach-forming material in the marsh, forming shell-pocket beaches, shell-rimmed marsh islands, shell islands, and shell mounds. As the Chandeleur islands become submerged, changing hydrodynamic conditions (fetch, wave height, depth) in Chandeleur Sound will force a response from the fringing marsh shoreline. The increased ravinement depths in this scenario will likely liberate the deeper sand-rich strata in the marsh for sandy shoreline development. If however, these sand-rich strata are not liberated or

perhaps their volume is not significantly large enough to form a sandy shoreline, the geomorphic pattern described herein: the conversion of shell-pocket beaches to shell mounds will continue to be the dominant erosional behavior in this marsh.

References

- Allen J.R.L., 1984, Experiments on the settling, overturning and entrainment of bivalve shells and related models: *Sedimentology*, v. 31, p. 227-250.
- Barras, J., Beville, S., Britsch, D., Hartley, S., Hawes, S., Johnston, J., Kemp, P., Kinler, Q., Martucci, A., Porthouse, J., Reed, D., Roy, K., Sapkota, S., and Suhayda, J., 2003, Historical and projected coastal Louisiana land changes: 1978-2050: United States Geological Survey, Open File Report, 03-334, 39 p. (Revised January 2004).
- Benninger, L.K., 1976, The uranium-series radionuclides as tracers of geochemical processes in Long Island Sound, Ph.D. Dissertation, Yale University, New Haven, Connecticut, 161 p.
- Bindoff, N.L., Willebrand, J., Artale, V., Cazenave, A., Gregory, J., Gulev, S., Hanawa, K., Le Quéré, C., Levitus, S., Nojiri, Y., Shum, C.K., Talley, L.D., and Unnikrishnan, A., 2007, Observations: Oceanic Climate Change and Sea Level. In: *Climate Change 2007: The Physical Science Basis. Contribution of Working Group I to the Fourth Assessment Report of the Intergovernmental Panel on Climate Change* [Solomon, S., D. Qin, M. Manning, Z. Chen, M. Marquis, K.B. Averyt, M. Tignor and H.L. Miller (eds.)]. Cambridge University Press, Cambridge, United Kingdom and New York, NY, USA.
- Blum, M.D., and Roberts, H.H., 2009, Drowning of the Mississippi Delta due to insufficient sediment supply and global sea-level rise: *Nature Geoscience*, v. 2, p. 488-491.
- Bristch, L.D., and Dunbar, J.B., 2006, Land loss in coastal Louisiana: 1930's to 2001: Technical Report TR-05-13, Engineer Research and Development Center, Vicksburg, MS.
- Bunya, S., Dietrich, J.C., Westerink, J.J., Ebersole, B.A., Smith, J.M., Atkinson, J.H., Jensen, R., Resio, D.T., Leutlich, R.A., Dawson, C., Cardone, V.J., Cox, A.T., Powell, M.D., Westerink, H.J., Roberts, H.J., 2010, A high-resolution coupled riverine flow, tide, wind,

- wind wave, and storm surge model for Southern Louisiana and Mississippi. Part 1: model development and validation: *Monthly Weather Review*, v. 138, p. 345-377.
- Cahoon, D., and Reed, D., 1995, Relationships among marsh surface topography, hydroperiod, and soil accretion in a deteriorating Louisiana salt marsh: *Journal of Coastal Research* v. 11, n. 2, p. 357–369.
- Cahoon, D.R., Reed, D.J., and Day, Jr., J.W., 1995, Estimating shallow subsidence in microtidal salt marshes of the southeastern United States: Kaye and Barghoorn revisited: *Marine Geology*, v. 128, n. 1, p. 1-9.
- Calvin, J., 2002, What processes control marsh elevations within the St. Bernard Delta?, Master's Thesis, University of New Orleans, New Orleans, Louisiana, 166 p.
- Coleman, J.M., 1980, *Deltas - Processes of deposition and models for exploration*, 2nd Edition: Burgess Publishing, Minneapolis, MN, 123 p.
- Coleman, J.M., Roberts, H.H., and Stone, G.W., 1998, Mississippi River delta: an overview: *Journal of Coastal Research*, v. 14, p. 698-716.
- Couvillion, B.R., Barras, J.A., Steyer, G.D., Sleavin, W., Fischer, M., Beck, H., Trahan, N., Griffin, B., Heckman, D., 2011, Land area change in coastal Louisiana from 1932-2010: United States Geological Survey Scientific Investigations Map 3164, scale 1:265,000, 12 p.
- deBeaumont, E., 1845, *Leçons de géologie pratique*: Paris, p. 223-252.
- DeLaune, R.D., Whitcomb, J.H, Patrick. W.H., Jr., Pardue, J.H., Pezeshiki, S.R., 1989, Accretion and canal impacts in a rapidly subsiding wetland: ^{137}Cs and ^{210}Pb techniques: *Estuaries*, v. 12, n. 4, p. 247-259.

- Delaune, R.D., Jugsujinda, A., Peterson, G.W., Patrick Jr., W.H., 2003, Impact of Mississippi River freshwater reintroduction on enhancing marsh accretionary processes in a Louisiana estuary: *Estuarine, Coastal, and Shelf Science*, v. 58, p. 653-662.
- Dietrich, J.C., Bunya, S., Westerink, J.J., Ebersole, B.A., Smith, J.M., Atkinson, J.H., Jensen, R., Resio, D.T., Leutlich, R.A., Dawson, C., Cardone, V.J., Cox, A.T., Powell, M.D., Westerink, H.J., Roberts, H.J., 2010, A high-resolution coupled riverine flow, tide, wind, wind wave, and storm surge model for Southern Louisiana and Mississippi. Part II: Synoptic description and analysis of Hurricanes Katrina and Rita: *Monthly Weather Review*, v. 138, p. 378-404.
- Fang, Hsai-Yang, 1991, *Foundation Engineering Handbook*, 2nd Ed., Kluwer Academic Publishers: Norwell, MA, 923 p.
- Feagin, R.A., Lozada-Bernard, S.M., Ravens, T.M., Moller, I., Yeager, K.M., and Balrd, A.H., 2009, Does vegetation prevent wave erosion of salt marsh edges?: *Proceedings of the National Academy of Science*, v. 106, n. 25, p. 10109-10113.
- Fearnley, S.M., Miner, M.D, Kulp, M., Bohling, C., Penland, S., 2009, Hurricane impact and recovery shoreline change analysis of the Chandeleur Islands, Louisiana, USA: 1855-2005: *Geo-Marine Letters*, v. 29, p. 455-466.
- Fischer, A.G., 1961, Stratigraphic record of transgressing seas in light of sedimentation on Atlantic coast of New Jersey: *American Association of Petroleum Geologists Bulletin*, v. 45, p. 1656-1666.
- Fisher, J.J., 1968, Barrier island formation: discussion, *Geological Society of America Bulletin*, 78, p. 1125-1136.

- Fisk, H.N., 1944, Geological investigation of the alluvial valley of the lower Mississippi River: U.S. Army Corps of Engineers, Mississippi River Commission, Vicksburg, MS, 78 p.
- Frazier, D.E., 1967, Recent deltaic deposits of the Mississippi River: their development and chronology: Gulf Coast Association of Geological Societies, Transactions, v. 27, p. 287-315.
- Georgiou, I.Y., McCorquodale, J.A., Schindler, J., Retana, A.G., FitzGerald, D.M., Hughes, Z., Howes, N., 2009, Impact of multiple freshwater diversions on the salinity distribution in the Pontchartrain estuary under tidal forcing: Journal of Coastal Research, SI 54, p. 59-70.
- Georgiou, I.Y., and Schindler, J.K., 2009, Wave forecasting and longshore sediment transport gradients along a transgressive barrier island: Chandeleur Islands, Louisiana: Geo-Marine Letters, v. 29, p. 467-477.
- Gilbert, 1885, The topographic feature of lake shores: United States Geological Survey, 5th Annual report, p. 69-123.
- Howes, N.C., FitzGerald, D.M., Hughes, Z.J., Georgiou, I.Y., Kulp, M.A., Miner, M.D., Smith, J.M., and Barras, J.A., 2010, Hurricane-induced failure of low salinity wetlands: Proceeding of the National Academy of Sciences of the United States of America, v. 107, n. 32, p. 14014-14019.
- Hoyt, J.H., 1967, Barrier island formation: Geological Society of America Bulletin, v. 78, p. 1125-1135.
- Hoyt, W.H., and Demarest, J.H., 1981, Vibracoring in coastal environments: a description of equipment and procedures. NOAA Sea Grant College Program, University of Delaware, p. 20-31.

- Johnson, D., 1919, Shore processes and shoreline development: Wiley, New York, 584 p.
- Kolb, C.R., and van Lopik, J.R., 1958a, Geological Investigation of the Mississippi River-Gulf Outlet Channel: U.S. Army Corps of Engineers, Waterways Experiment Station, Miscellaneous Paper 30259, Vicksburg, MS, 43 p.
- Kolb, C.R., and van Lopik, J.R., 1958b, Geology of the Mississippi River deltaic plain, southeastern Louisiana: U.S. Army Corps of Engineers, Waterways Experiment Station, Technical Report 3-483 and 3-484, Vicksburg, MS, 122 p.
- Kolb, C.R., and van Lopik, J.R., 1966, Depositional environments of the Mississippi River deltaic plain - Southeastern Louisiana, p. 17-61, in Shirley, M.L. (ed.), Deltas in their geologic framework, Houston Geological Society.
- Kulp, M., FitzGerald, D.M., and Penland, S., 2005, Sand-rich lithosomes of the Holocene Mississippi river delta plain, in Bhattacharya, J.P. and Giosan, L., eds., River Deltas- Concepts, Models, and Examples, Society of Economic Mineralogists and Paleontologists Special Publication, n. 83, p. 227-291.
- Lanesky, D.E., Logan, B.W., Brown, R.G., and Hine, A.C., 1979, A new approach to portable vibracoring underwater and on land: Journal of Sedimentary Petrology v. 49, n. 2, p. 654-657.
- McGee, W.J., 1890, Encroachments of the sea: The Forum, L.S. Metcalf (ed.), v. 9, p. 437-449.
- Meade, R.H., Yuzyk, T.R., and Day, T.J., 1990, Movement and storage of sediment in rivers of the United States and Canada, in Surface Water Hydrology, Geological Society of America, Boulder, Colorado, p. 255-280.
- Mesri, G., and Godlewski, P.M., 1977, Time- and stress-compressibility interrelationship: Journal of the Geotechnical Engineering Division, v. 103, n. GT5, p. 417-430.

- Miner, M.D, Kulp, M., Weathers, H.D., and Flocks, J., 2009, Historical (1869-2007) sea floor evolution and sediment dynamics along the Chandeleur Islands, in Lavoie, D. (ed.), Sand Resources, Regional Geology, and Coastal Processes of the Chandeleur Islands Coastal System: an Evaluation of the Breton National Wildlife Refuge: Scientific Investigations Report 2009-5252, United States Geological Survey, 33 p.
- Nyman, J., Walters, R., DeLaune, R.D., Patrick, Jr., W.H., 2006, Marsh vertical accretion via vegetative growth: Estuarine, Coastal, and Shelf Science, v. 69, p. 370-380.
- Otvos, E.G., 1970, Development and migration of Barrier Islands, Northern Gulf of Mexico: Geological Society of America Bulletin, v. 81, p. 241-246.
- Otvos, E.G., 1986, Island evolution and "stepwise retreat": Late Holocene transgressive barriers, Mississippi delta coast - Limitations of a model: Marine Geology, v. 72, p. 325-340.
- Penland, S., and Ramsey, K.E., 1990, Relative sea-level rise in Louisiana and the Gulf of Mexico: 1908-1988: Journal of Coastal Research, v. 6, n. 2, p. 323-242.
- Penland, S., and Suter, J.R., 1988, Barrier island erosion and protection in Louisiana: a coastal geomorphological perspective: Gulf Coast Association of Geological Societies, Transactions, v. 38, p. 331-342.
- Penland, S., Boyd, R., and Suter, J.R., 1988, Transgressive depositional systems of the Mississippi delta plain: a model for barrier shoreline and shelf sand development: Journal of Sedimentary Petrology, v. 58, no. 6, p. 932-949.
- Penland, S., Roberts, H.H., Williams, S.J., Sallenger, Jr., A.H., Cahoon, D.R., Davis, D.W., Groat, C.G., 1990, Coastal land loss in Louisiana: Gulf Coast Association of Geological Societies, Transactions, v. 40, p. 685-700.

- Rampino, M.R., and Sanders, J.E., 1981, Evolution of the barrier islands of southern Long Island, New York: *Sedimentology*, v. 28, p. 37-48.
- Reed, D.J., 1989, The role of salt marsh erosion in barrier island evolution and deterioration in coastal Louisiana: *Transactions-Gulf Coast Association of Geological Societies*, v. 39, p. 501-510.
- RockWare, Inc., 2008, *RockWorks 14 User Manual*, 371 p.
- Roberts, H.H., 1997, Dynamic changes of the Holocene Mississippi River delta plain: the delta cycle: *Journal of Coastal Research*, v. 13, n. 3, p. 605-627.
- Rybczyk, J., and Cahoon, D., 2002, Estimating the potential for submergence for two wetlands in the Mississippi River delta: *Estuaries* v. 25, n. 5, p. 985–998.
- Schindler, J., 2010, Estuarine dynamics as a function of barrier island transgression and wetland loss: understanding the transport and exchange processes, Master's Thesis, University of New Orleans, 94 p.
- Stamp, L.D., 1922, An outline of the Tertiary geology of Burma: *Geology Magazine*, v. 59, p. 481-501.
- Steyer, G.D., Sasser, C.E., Visser, J.M., Swensen, E.M., Nyman, J.A., and Ranie, R.C., 2003, A proposed coast-wise reference monitoring system for evaluating wetland restoration trajectories in Louisiana: *Environmental Monitoring and Assessment*, v. 81, p. 107-117
- Steyer, G.D., Twilley, R.R., Raynie, R.C., 2006, An integrated monitoring approach using multiple reference sites to assess sustainable restoration in coastal Louisiana. In: Aguirre-Bravo, C., Pellicane, P.J., Burns, D.P., and Draggan, S., Eds. 2006. *Monitoring Science and Technology Symposium: Unifying Knowledge for Sustainability in the Western Hemisphere Proceedings RMRS-P-42CD*. Fort Collins, CO: U.S. Department of Agriculture, Forest Service, Rocky Mountain Research Station, p. 326-333.

- Stone, G.W., Zhang, X., and Sheremet, A., 2005, The role of barrier islands, muddy shelf and reefs in mitigating the wave field along coastal Louisiana: *Journal of Coastal Research*, Special Issue n. 44, p. 40-55.
- Swift, D.J.P., 1975, Barrier island genesis: evidence from the central Atlantic shelf, eastern USA: *Sedimentary Geology*, v. 14, p. 1-43.
- Törnqvist, T.E., Bick, S.J., van der Borg, K., de Jong, A.F.M., 2006, How stable is the Mississippi Delta?: *Geology*, v. 34, n. 8, p. 697-700.
- Törnqvist, T. E., González, J. L., Newsom, L. A., Van der Borg, K., De Jong, A. F. M. and Kurnik, C.W., 2004, Deciphering Holocene sea-level history on the U.S. Gulf Coast: A high-resolution record from the Mississippi Delta: *Geological Society of America Bulletin*, v. 116, p. 1026-1039.
- Törnqvist, T.E., Kidder, T.R., Autin, W.J., van der Borg, K., de Jong, A.F.M., Klerks, C.J.W., Snijders, E.M.A., Storms, J.E.A., van Dam, R.L., Wiemann, M.C., 1996, A revised chronology for Mississippi River subdeltas: *Science*, v. 273, p. 1693-1696.
- Törnqvist, T.E., Wallace, D.J., Storms, J.E.A., Wallinga, J., van Dam, R.J., Blaauw, M., Derkse, M.S., Klerks, C.J.W., Snijders, E.M.A., 2008, Mississippi Delta subsidence primarily caused by compaction of Holocene strata: *Nature Geoscience*, v. 1, p. 173-176.
- Weill P., Mouaze, D., Tessier, B., Brun-Cottan, J-C., 2010, Hydrodynamic behavior of coarse bioclastic sand from shell cheniers: *Earth Surface Processes and Landforms*, v. 35, p. 1642-1654.
- Williams, S.J., Arsenault, M.A., Buczkowski, B.J., Reid, J.A., Flocks, J.G., Kulp, M.A., Penland, S., and Jenkins, C.J., 2006, Surficial sediment character of the Louisiana offshore

Continental Shelf region: a GIS Compilation, U.S. Geological Survey Open-File Report 2006-1195, 49 p.

Wilson, C.A., and Allison, M.A., 2008, An equilibrium profile model for retreating marsh shorelines in southeast Louisiana: *Estuarine, Coastal, and Shelf Science*, v. 80, p. 483-494.

Appendix A - Vibracore Description Sheets

UNIVERSITY OF NEW ORLEANS

DEPARTMENT OF GEOLOGY AND GEOPHYSICS

VIBRACORE DESCRIPTION SHEET

CORE ID: 03BL-1

DATE: 8-25-04

DESCRIBED BY: myke b.

ELEVATION: -0.25m

LOCATION: Bogal's Lake

CORE LENGTH: 4.27m

LAT/LONG: 29°50'16"N 89°29'57"W


TOTAL DEPTH: 4.27m

COMPACTION: 0.97m

SEDIMENTARY TEXTURE AND STRUCTURES					% SAND	PHYSICAL CHARACTERISTICS					STRATIFICATION TYPE					SAMPLE					PHYSICAL DESCRIPTION									
CLAY	SILT	FINE SAND	MEDIUM SAND	COARSE SAND	GRAVEL	INTERVAL	0	50	100	COLOR	DEFORMATION	BED THICKNESS	% SHELL	% ORGANIC	% BIOTURBATION	WAVE	FLASER	LENTICULAR	GROSS BED	MASSIVE BED		INCLINED BED	HORIZ. LAMINATION	GRAIN-SIZE	HEAVY MINERAL	MICRO FOSSILS	RADIO-METRIC	RADIOGRAPH	PHOTOGRAPH	
																														0-0.83m Clay/silt Dark Brown Organics - olive gray clays. Massive bedding. Thin (17cm) marsh deposit with rooting to a depth of 1.03m. Bottom contact gradational.
																														0.83-4.27m Clay-SAND Olive gray clays with tan SANDS. Bedding is lenticular and highly deformed due to corring.

DEPARTMENT OF GEOLOGY AND GEOPHYSICS
VIBRACORE DESCRIPTION SHEET

DATE: 8-26-04 DESCRIBED BY: myke b
LOCATION: Bayou LaLoutre
LAT/LONG: 29° 50' 10 N 89° 27' 24 W
COMPACTION: 0.74m

SEDIMENTARY TEXTURE AND STRUCTURES						Σ SAND		PHYSICAL CHARAC- TERISTICS		STRATI- FICATION TYPE		SAMPLE		PHYSICAL DESCRIPTION														
CLAY	SILT	FINE SAND	MEDIUM SAND	COARSE SAND	GRANULE	INTERVAL	0	50	100	COLOR	DEFORMATION	BED THICKNESS	Σ SHELL		Σ ORCHARD	Σ BIOTURBATION	WAVEY	FLASHER	LENTICULAR	CROSS BED	MASSIVE BED	INCLINED BED	HORIZ. LAMINATION	GRAN. SIZE	HEAVY MINERAL	MICRO FOSSILS	RADIOMETRIC	RADIOGRAPH
																												

DEPARTMENT OF GEOLOGY AND GEOPHYSICS
VIBRACORE DESCRIPTION SHEET

DATE: 8-26-04

DESCRIBED BY: myke b

LOCATION: 3000 Island

LAT/LONG: 29° 51' 15" N 89° 16' 24" W

COMPACTION: 1.18 m

PHYSICAL DESCRIPTION

DEPARTMENT OF GEOLOGY AND GEOPHYSICS
VIBRACORE DESCRIPTION SHEET

DESCRIBED BY: Elizabeth Rydrewski

LAT/LONG: 29° 51' 49.5" 89° 27' 21.6"

COMPACTION: 93.98%

PHYSICAL DESCRIPTION

UNIVERSITY OF NEW ORLEANS

DEPARTMENT OF GEOLOGY AND GEOPHYSICS

VIBRACORE DESCRIPTION SHEET

CORE ID: 04BL-02

DATE: 11-23-04

DESCRIBED BY: Elizabeth Rydzewski

ELEVATION: 3 + 15.24 m

LOCATION: Bayou la Batre

CORE LENGTH: 4.88 m

LAT/LONG: 29° 51' 36.20" 89° 26' 44.36"

TOTAL DEPTH: _____

COMPACTION: 39.37 cm

SEDIMENTARY TEXTURE AND STRUCTURES						% SAND	PHYSICAL CHARAC- TERISTICS				STRATI- FICATION TYPE				SAMPLE				PHYSICAL DESCRIPTION						
CLAY	SILT	FINE SAND	MEDIUM SAND	COARSE SAND	GRAVEL	INTERVAL (m)	COLOR	DEFORMATION	BED THICKNESS	% SHELL	% ORGANIC	% BIOTURBATION	WAVEY	FLASER	LENTICULAR	CROSS BED	MASSIVE BED	INCLINED BED		HORIZ. LAMINATION	GRAN-SIZE	HEAVY MINERAL	MICRO FOSSILS	RADIO-METRIC	PHOTOGRAPH
						0																			
						1.5																			
						3																			
						3.27																			
						4																			
						4.88																			

0						0																			
1.5						1																			
3.27						3																			
4.88						4																			

0-1.5m) Massive Clay, Dusky Yellowish brown (10YR 9/2) to 0.62m, Black (N1) to 0.77m, Grayish Black (N2) 0.77m to base of unit. Spartina roots abundant to 0.55m. Organics throughout unit.

(1.5m - 3.27m) Massive Clay, Dark greenish gray (5GY 7/1) 1.5m to 1.50m, Brownish gray (5YR 7/1) 1.50m to 2.64m, Olive black (5Y 9/1) 2.64m to 2.88m, Black (N1) 2.88m to 2.93m, Brownish black (5YR 9/1) 2.93m to base of unit. Organics throughout unit. Wood fragments at 2.33m. Base of unit ending with sharp contact.

(3.27m - 4.88m) Massive Clay, Brownish gray (5YR 7/1) 3.27m to 3.62m, Light olive gray (5Y 5/2) 3.62m to 3.74m, Dark yellowish brown (10YR 4/2) 3.74m to 3.79m, Light olive gray (5Y 5/2) 3.79m to base of unit. Organics at 3.34, 3.45, 3.58, 3.68, 4.09, and 4.84. Sand at base of unit 0.6m thick.

(0-1.5m) Massive Clay, Dusky Yellowish brown (10YR 5/2) to 0.62m, Black (N1) to 0.77m, Grayish Black (N2) 0.77m to base of unit. *Spartina* root abundant to 0.55m. Organics throughout unit.

(1.5m-3.27m) Massive Clay, Dark greenish gray (5Y 4/1) 1.5m to 1.52m, Brownish gray (5YR 4/1) 1.52m to 2.64m, Olive black (5Y 3/1) 2.64m to 2.88m, Black (N1) 2.88m to 2.93m, Brownish black (5YR 3/1) 2.93m to base of unit. Organics throughout unit. Wood fragments at 2.33m. Base of unit ending with sharp contact.

(3.27m-4.88m) Massive Clay, Brownish gray (5YR 4/1) 3.27m to 3.62m, Light olive gray (5Y 5/2) 3.62m to 3.74m, Dark yellowish brown (10YR 4/2) 3.74m to 3.79m, Light olive gray (5Y 5/2) 3.79m to base of unit. Organics at 3.34, 3.45, 3.58, 3.68, 4.09, and 4.84. Sand at base of unit. 0.6m thick.

UNIVERSITY OF NEW ORLEANS

DEPARTMENT OF GEOLOGY AND GEOPHYSICS

VIBRACORE DESCRIPTION SHEET

CORE ID: 04BL-03

DATE: 11-23-04

DESCRIBED BY: Dorothy R. Riedewald

ELEVATION: +15.24m

LOCATION: Bayou Labarre

CORE LENGTH: 5.91m

LAT/LONG: 29° 50' 59.24" N 89° 26' 32.75" W

TOTAL DEPTH: 5.91m

COMPACTION: 20.32cm

SEDIMENTARY TEXTURE AND STRUCTURES				% SAND	PHYSICAL CHARAC- TERISTICS	STRATI- FICATION TYPE	SAMPLE	PHYSICAL DESCRIPTION
CLAY	SILT	FINE SAND	MEDIUM SAND	COARSE SAND	GRAVEL	INTERVAL (m)		
						0		
						50		
						100		
						COLOR		
						DEFORMATION		
						BED THICKNESS		
						% SHELL		
						% ORGANIC		
						% BIOTURBATION		
						WAVE		
						FLASER		
						LENTICULAR		
						CROSS BED		
						MASSIVE BED		
						INCLINED BED		
						HORIZ. LAMINATION		
						GRAIN SIZE		
						HEAVY MINERAL		
						MICRO FOSSILS		
						RADIOMETRIC		
						RADIOGRAPH		
						PHOTOGRAPH		

0m						0		(0-1.19m) Massive Clay. Olive black (5Y 3/4). 0 to 0.72m. Grayish black (N2). 0.72m to base of unit. <u>Spartina</u> roots 0-0.58m. Organics throughout unit. Base of unit ending with sharp contact.
1.19m						1		(1.19m-2.42m) Massive Clay. Brownish gray (5YR 4/1). Wood fragments present.
2.42m						2		(2.42m-2.99m) Massive Sand. Light olive gray (5Y 6/1). Wood fragments present.
2.99m						3		(2.99m-5.18m) Massive Clay. 2.99m to 3.0m. Light olive gray (5Y 6/1). Horizontal lamination at 3.31m, 1cm wide, Grayish Orange (10YR 7/4). Lenticular bedding throughout unit. Organics present. Grayish orange (10YR 7/4). 2cm Horizontal lamination at 4.32m.
5.18m						5		(5.18m to btm) Massive Sand. Light olive gray (5Y 6/1).
5.91m								

VIBRACORE DESCRIPTION SHEET

DESCRIBED BY: Elizabeth Rdziewski

LOCATION: Bayou La Loutre

LAT/LONG: 29° 51 01.42 89° 27 11.44

COMPACTION: 71.76 cm

PHYSICAL DESCRIPTION

VIBRACORE DESCRIPTION SHEET

DESCRIBED BY: Elizabeth Ryzewski

LAT/LONG: 29° 51' 05.85"

COMPACTION: 1002.97 cm

COMPACTION: 1002.97 cm

PHYSICAL DESCRIPTION

0-20 Grayish brown (5YR 3/2) massive clay with roots and organics throughout unit, to Dusky yellowish brown (10YR 2/2) with roots and organics becoming less apparent at base of unit. (mostly Spartina rhizomes)

20-27 Med. dark gray (N4) to Medium gray (N5) mottled massive clay throughout unit.

27-3.38 medium gray (N5) massive clay containing wood fragments and peices (could be Spartina frags & roots)

3.38-3.5 medium grey (N5) and Black (N2) laminated clay with organic horizons. ~ 1cm thick

3.5-6tm Medium grey massive clay throughout unit.

DEPARTMENT OF GEOLOGY AND GEOPHYSICS
VIBRACORE DESCRIPTION SHEET

TOTAL DEPTH: _____

COMPACTION: 109.22cm

DESCRIBED BY: Elizabeth Ridzewska

PHYSICAL DESCRIPTION

DEPARTMENT OF GEOLOGY AND GEOPHYSICS
VIBRACORE DESCRIPTION SHEET

DATE: 11/19/04

DESCRIBED BY: Elizabeth Rotzewska

LOCATION: Bayou La Loutre

LAT/LONG: 29° 52' 32.03 N 89° 26' 39.55 W

COMPACTION: 34.29 cm

PHYSICAL DESCRIPTION

VIBRACORE DESCRIPTION SHEET

DESCRIBED BY: Elizabeth Rudzewski

LOCATION: Bayou la Boute

LAT/LONG: 29° 52 2701 89° 26 03.90

COMPACTION: 129.54/.

PHYSICAL DESCRIPTION

DEPARTMENT OF GEOLOGY AND GEOPHYSICS
VIBRACORE DESCRIPTION SHEET

DESCRIBED BY: Elizabeth Ridgway

LOCATION: Bayou baloutre

LAT/LONG: 29° 51 29.67 89° 26 20.13

COMPACTION: 96.52 %

PHYSICAL DESCRIPTION

UNIVERSITY OF NEW ORLEANS

DEPARTMENT OF GEOLOGY AND GEOPHYSICS

VIBRACORE DESCRIPTION SHEET

CORE ID: STB-01-A

DATE: 8/29/01

DESCRIBED BY: John Calvin

ELEVATION: _____

LOCATION: N. Bank off of Bayou La Loutre, 50 ft. from natural levee & channel

CORE LENGTH: 202.5 cm

LAT/LONG: 29°53.226' N 89°31.078' W

TOTAL DEPTH: 266 cm

COMPACTION: 25" or 63.5 cm

SEDIMENTARY TEXTURE AND STRUCTURES					% SAND	PHYSICAL CHARACTERISTICS					STRATIFICATION TYPE					SAMPLE					PHYSICAL DESCRIPTION				
CLAY	SILT	FINE SAND	MEDIUM SAND	COARSE SAND	GRAVEL	INTERVAL	COLOR	DEFORMATION	BED THICKNESS	% SHELL	% ORGANIC	% BOTRYDATION	WAVE	FLASER	LENTICULAR	CROSS BED	MASSIVE BED	INCLINED BED	HORIZ. LAMINATION	GRAIN SIZE	HEAVY MINERAL	MICRO FOSSILS	RADIOGRAPH	PHOTOGRAPH	
						0																			0-11 cm Marsh veg. w/ clay
						11-99.5 cm																			11-99.5 cm clay/silt massive bed w/ fine organic particulates. Color grades from dark-grey to light grey w/ small lenses of oxidized sed.
						99.5-188.4 cm																			99.5-188.4 cm silty sand grades into silt/clay. Reddish-tan to light-grey w/ small lenses of oxidized sed.
						188.4-202.5 cm																			188.4-202.5 cm Sharp contact w/ sand bed. No visible structures.
						0-188.4 cm																			0-188.4 cm Marsh unit heavily rooted w/ a gradational change in lithology around 32 cm (dark grey - light grey) and again around 99.5 cm (light grey - tan) where some sand is present.
						188.4-202.5 cm																			188.4-202.5 cm Sand unit w/ some rooting.

UNIVERSITY OF NEW ORLEANS

DEPARTMENT OF GEOLOGY AND GEOPHYSICS

VIBRACORE DESCRIPTION SHEET

CORE ID: STB-D1-B

DATE: 9/4/01

DESCRIBED BY: John Calvin

ELEVATION: _____

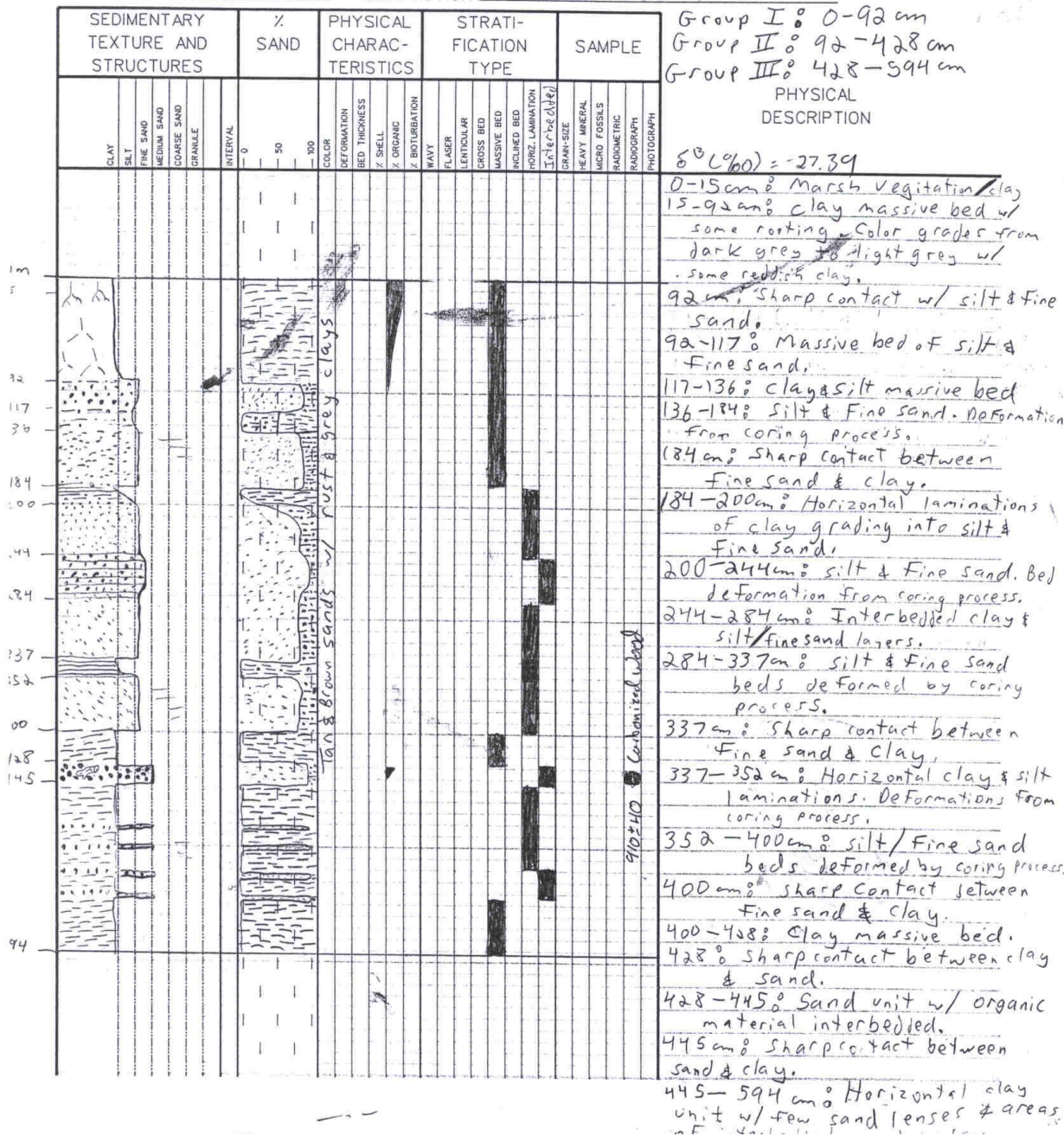
LOCATION: N Bank off Bayou LaLoutre 100 ft. from natural levee

CORE LENGTH: 594 cm

LAT/LONG: 29° 53.196' N, 89° 30.510' W

TOTAL DEPTH: 690 cm

COMPACTION: 37 1/4" or 96 cm



UNIVERSITY OF NEW ORLEANS

DEPARTMENT OF GEOLOGY AND GEOPHYSICS

VIBRACORE DESCRIPTION SHEET

CORE ID: STB-01-c

DATE: 8/29/01

DESCRIBED BY: John Calvin

ELEVATION: _____

LOCATION: N. Bank of Bayou LaLoutre 75ft. from natural levee channel

CORE LENGTH: 215 cm

LAT/LONG: 29°53.090' N 89°30.060' W

TOTAL DEPTH: 286.2 cm

COMPACTION: 28" or 71.2 cm

SEDIMENTARY TEXTURE AND STRUCTURES					% SAND	PHYSICAL CHARACTERISTICS					STRATIFICATION TYPE					SAMPLE					PHYSICAL DESCRIPTION								
CLAY	SILT	FINE SAND	MEDIUM SAND	COARSE SAND	GRAVEL	INTERVAL	0	50	100	COLOR	DEFORMATION	BED THICKNESS	% SHELL	% ORGANIC	% BIOTURBATION	WAVEY	FLASER	LENTICULAR	CROSS BED	MASSIVE BED		INCLINED BED	HORIZ. LAMINATION	GRAN-SIZE	HEAVY MINERAL	MICRO FOSSILS	RADIOMETRIC	PHOTOGRAPH	
																													0-16 cm: Marsh Veg.
																													16-164 cm: clay (dark grey) grades into clay/silt (light grey & tan) w/ rooting throughout. Massive bed. Gradational contact from about 64-71 cm
																													164-190 cm: Interbedded silt & fine sand w/ rooting throughout. Sand lense between 164-168 cm.
																													190-215 cm: Massive clay bed.
																													0-215 cm = Marsh unit heavily rooted gradational change in lithology between 64-71 cm (dark grey - light grey) and again around 190 cm where more clays are present.

UNIVERSITY OF NEW ORLEANS

DEPARTMENT OF GEOLOGY AND GEOPHYSICS

VIBRACORE DESCRIPTION SHEET

CORE ID: STB-D1-D

DATE: 9/4/01

DESCRIBED BY: John Calvin

ELEVATION: _____

LOCATION: S. Shore of Pete's Lagoon on middle transect near a small channel

CORE LENGTH: 715 cm

LAT/LONG: 29°54.032'N, 89°30.800'W

TOTAL DEPTH: 783.5 cm

COMPACTION: 27" or 68.5 cm

SEDIMENTARY TEXTURE AND STRUCTURES					% SAND	PHYSICAL CHARAC- TERISTICS	STRATI- FICATION TYPE	SAMPLE																	
CLAY	SILT	FINE SAND	MEDIUM SAND	COARSE SAND	GRAVEL	INTERVAL	COLOR	DEFORMATION	BED THICKNESS	% SHELL	% ORGANIC	% BIOTURBATION	WAVEY	FLASER	LENTICULAR	CROSS BED	MASSIVE BED	INCLINED BED	HORIZ. LAMINATION	Interbedded	GRAIN-SIZE	HEAVY MINERAL	MICRO FOSSILS	RADIOGRAPH	PHOTOGRAPH
<p>0cm</p> <p>78cm</p> <p>144cm</p> <p>174cm</p> <p>189cm</p> <p>318cm</p> <p>355cm</p> <p>377cm</p> <p>451cm</p> <p>478cm</p> <p>551cm</p> <p>573cm</p> <p>637cm</p> <p>653cm</p> <p>685cm</p> <p>715cm</p> <p>771cm</p>																									
<p>0-78cm = Marsh vegetation & peat.</p> <p>78-144cm = organic clay & plant fragments.</p> <p>144-174 = organic clay & peat</p> <p>174-239 Interbedded organic clay & peat</p> <p>239-318 = organic clay w/ plant fragments</p> <p>241-245 = two Rangia shell halves. Each about 2cm in width - about 1cm apart from each other.</p> <p>Group II.</p> <p>318 = sharp contact between organic clay & silt.</p> <p>318-355 = silt grades into fine sand.</p> <p>355-377 = Interbedded silt & fine sand</p> <p>366-377 = Coarser sand unit</p> <p>377-451 = Silt grades into fine sand & coarser sand</p> <p>451 = sharp contact between sand & silt</p> <p>451-478 = Silt grades into laminated clay</p> <p>478-551 = Interbedded silt & fine sand</p> <p>551-771 = clay/silt massive bed w/ Rangia shell fragments</p> <p>573-580 = Rangia shell fragments randomly distributed.</p> <p>637 = large fragment of Rangia shell</p> <p>653-659 = Rangia shell fragments randomly distributed.</p> <p>685-715 = Rangia shell fragment randomly distributed.</p>																									

90

COMPACTION: 34" or 86.5 cm

91

VIBRACORE DESCRIPTION SHEET

DESCRIBED BY: John Calvin

LOCATION: N. shore of lake above Pete's lagoon adjacent to oil & gas road

LAT/LONG: 29°55.113'N, 89°30.731'W

COMPACTION: 13" or 33 cm

589 cm $\delta^{13}\text{C} = 130 \pm 40$ $\delta^{13}\text{C}(\text{‰}) = -6.13$

PHYSICAL DESCRIPTION

UNIVERSITY OF NEW ORLEANS

DEPARTMENT OF GEOLOGY AND GEOPHYSICS

VIBRACORE DESCRIPTION SHEET

CORE ID: STB-01-H

DATE: 9/14/01

DESCRIBED BY: John Calvin

ELEVATION: _____

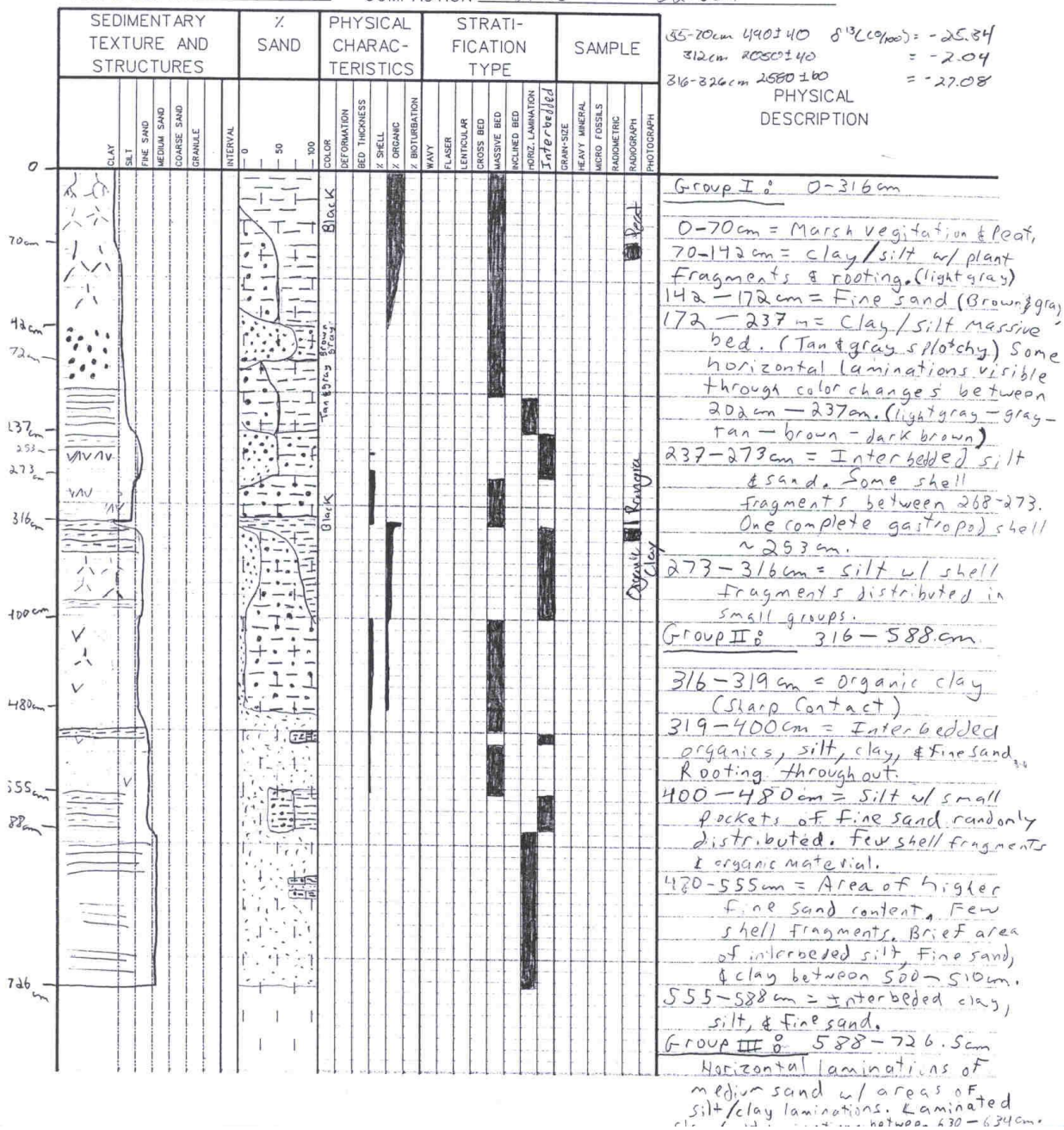
LOCATION: N. Point on W. transect; U. shore of small channel.

CORE LENGTH: 726.5cm

LAT/LONG: 29°55.924'N, 89°31.276'W

TOTAL DEPTH: _____

COMPACTION: 24.5" or 62.5cm



UNIVERSITY OF NEW ORLEANS

DEPARTMENT OF GEOLOGY AND GEOPHYSICS

VIBRACORE DESCRIPTION SHEET

CORE ID: STB-01-I

DATE: 9/21/01

DESCRIBED BY: John Calvin

ELEVATION: _____

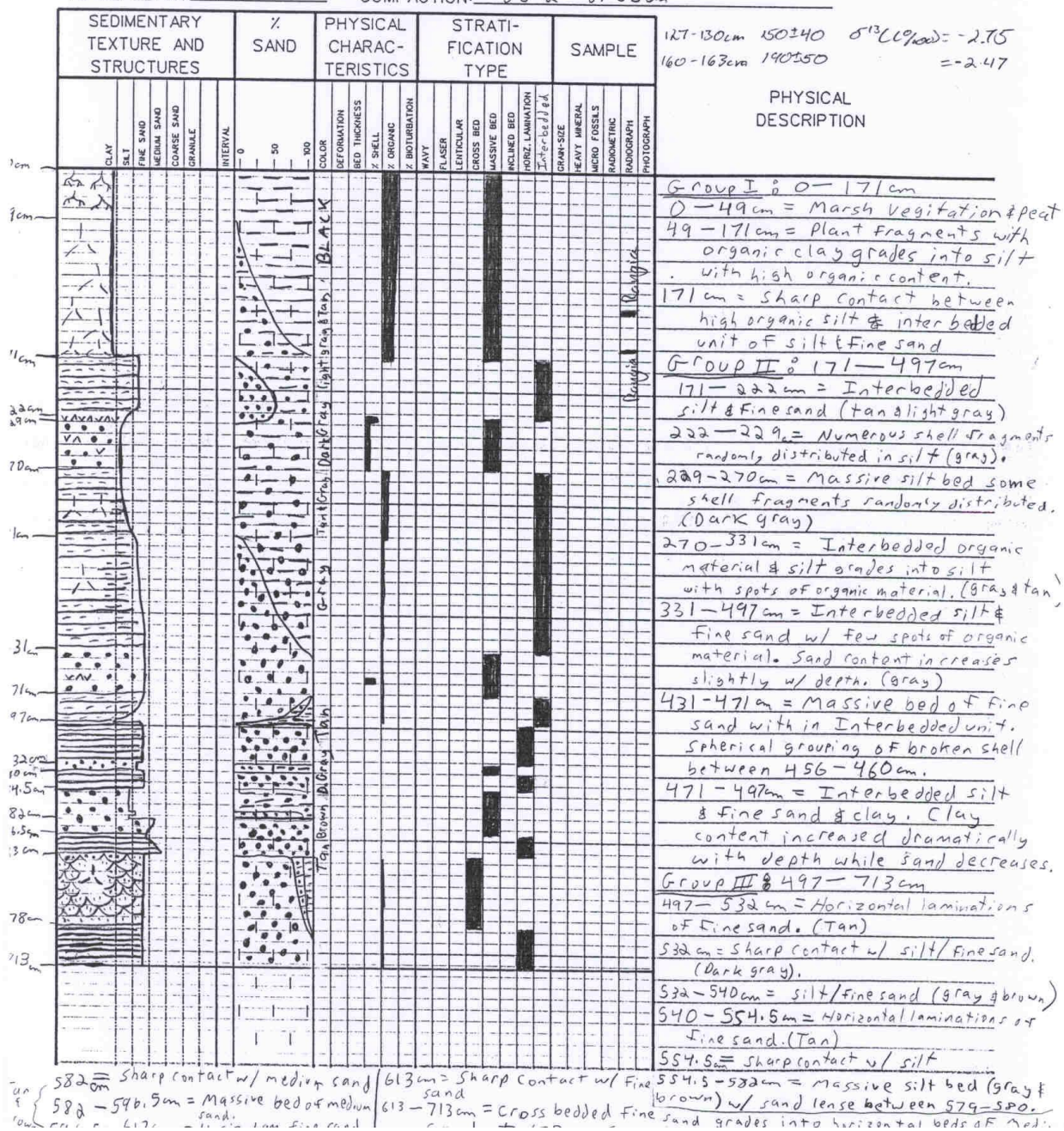
LOCATION: N. Point on middle transect; E. bank of bayou

CORE LENGTH: 713 cm

LAT/LONG: 29°55.895' N; 89°30.792' W

TOTAL DEPTH: 798 cm

COMPACTION: 33 1/2" or 85 cm



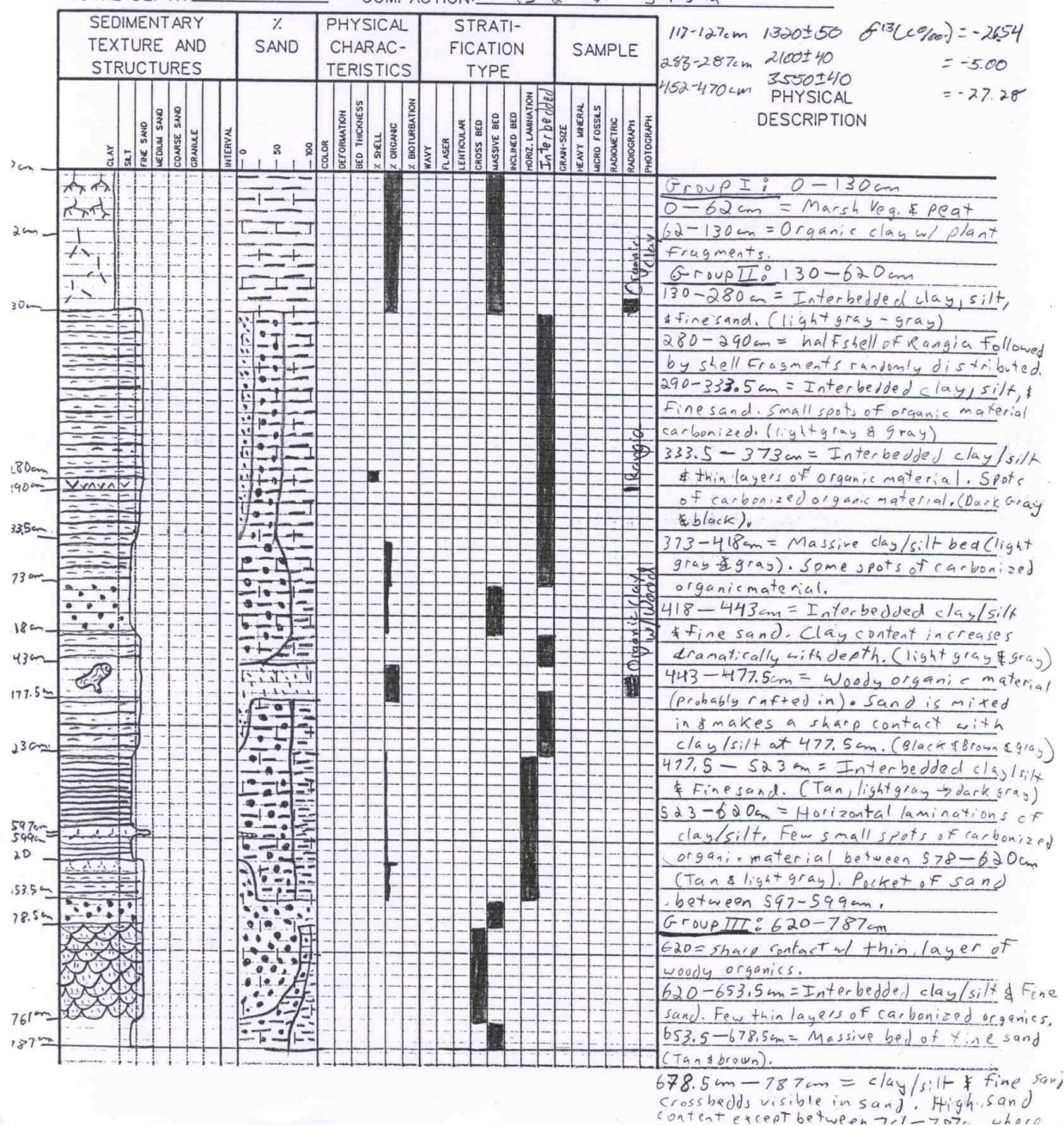
UNIVERSITY OF NEW ORLEANS

DEPARTMENT OF GEOLOGY AND GEOPHYSICS VIBRACORE DESCRIPTION SHEET

CORE ID: STB-01-J
ELEVATION: _____
CORE LENGTH: 787cm
TOTAL DEPTH: 826.5cm

DATE: 9/21/01
LOCATION: N. point of E. transect; E. bank of bayou
LAT/LONG: 29°55.925' N; 89°30.427' W
COMPACTION: 15 1/2" or 39.5cm

DESCRIBED BY: John Calvin



VIBRACORE DESCRIPTION SHEET

DESCRIBED BY: PL: 1

LOCATION: Wedge between Intracoastal and MRGO

LAT/LONG: 30° 00' 32.3" 89° 55' 01.5"

COMPACTION: 73.7 in = 60.2 cm

PHYSICAL DESCRIPTION

VIBRACORE DESCRIPTION SHEET

ELEVATION: _____

CORE LENGTH: 2.29m

TOTAL DEPTH: _____

LOCATION: Wed. 2 between Intracoastal & MRGO

LAT/LONG: 30° 00' 72.3" 70° 55' 01.5"

COMPACTION: 68 c.m.

PHYSICAL DESCRIPTION

141

VIBRACORE DESCRIPTION SHEET

DESCRIBED BY: *Mary E*

LOCATION: 24 Belmont Delta Complex / CRMS 540

LAT/LONG: 1) 38° 3' 25.03" N 89° 28' 52.86" W

COMPACTION:

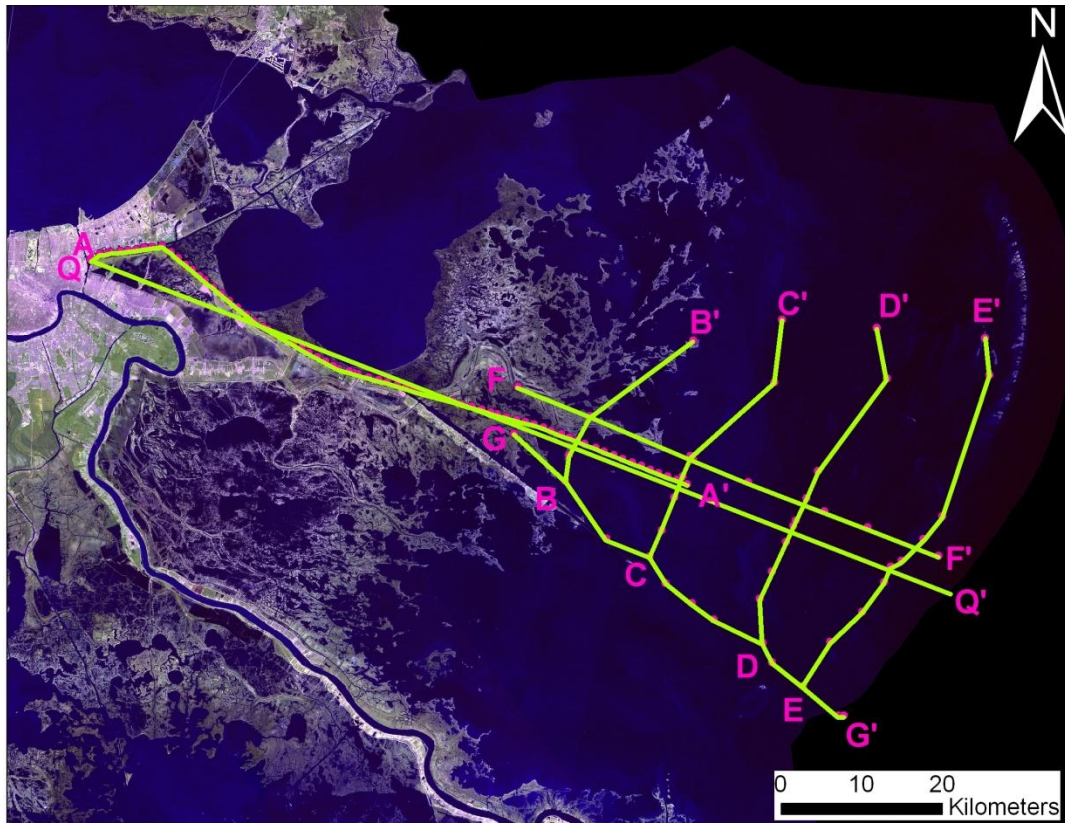
PHYSICAL DESCRIPTION

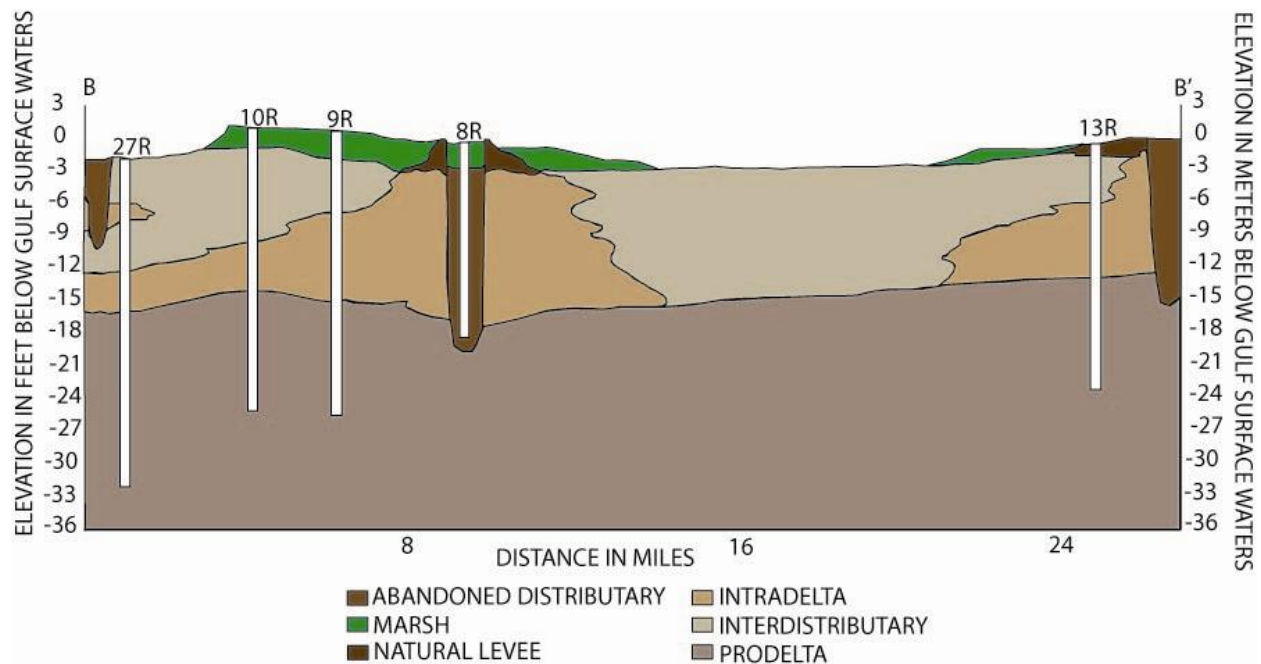
1-4.7 cm - dark brown - black ^{normal}
 organic rich clay, heavy rooting
 above 2.7 cm, sharp bottom
 contact.
4.7-5.5 light grey clay. ^(pink)
 grading to ...
5.5-11.7 cm - brown organic
 rich clay, massive rooting ^{normal}
 silty lens at 13-14, bottom
 contact gradual
11.7-15.5 cm - dark grey
 clay, mottled with light and
 dark clay, bottom contact
 gradual
15.5-23.0 cm - light grey
 clay with organic lenses @
 19.3, 21, 22.8, bottom contact
 gradual
23.0-31.0 cm * light grey silty
 clay, bottom contact gradual ^{20%}
31.0-48.0 cm
 darker grey clay with some
 small shells @ 39.4, 42.6 ^{very}
 large pocket of organic material
 at 44.0 cm.
48.0-54.0 cm - dark grey clay
 with some small silt laminations
 and lenses, few shells ^(U-4)
54.0-60.0 cm - dark grey clay
 with no silt ^{silty}
60.0-81.0 cm - grey clay with
 numerous silt laminations @
 60.3, 61.6, 62.0, 62.4, 63.0, ^(mottled)
 64.0, 65.3, 66.1, 69.5, 70.1,
 71.8, 73.9, 75.1, 76.8 (now hard)
 some fine rusty grey laminations
81.0-87.0
 light grey clay with small brown
 and blue laminations

C-14 sample @ 118 cm } roots
C-14 sample @ 65 cm }

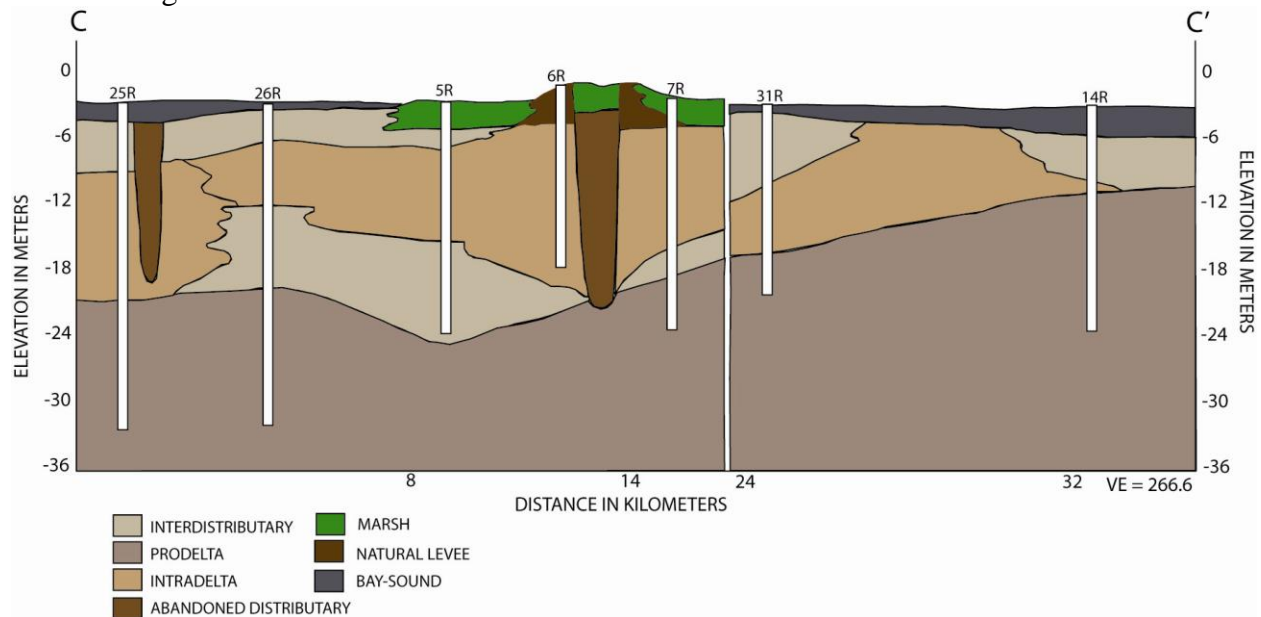
Appendix B - Cross-sections

MRGO

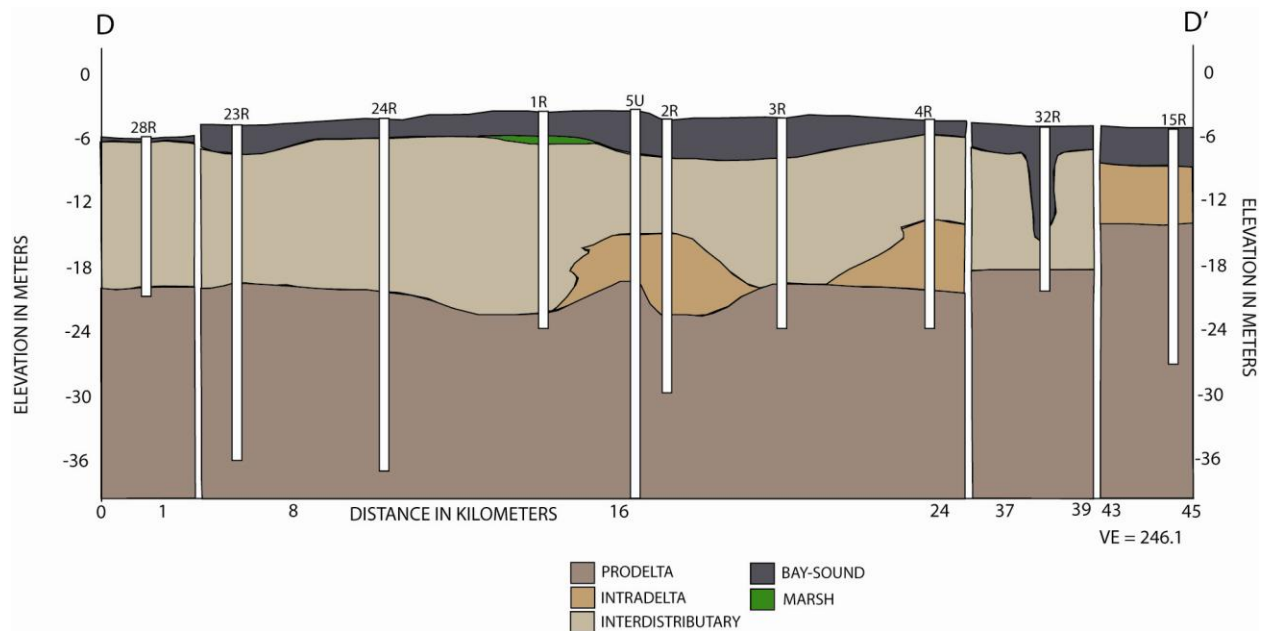




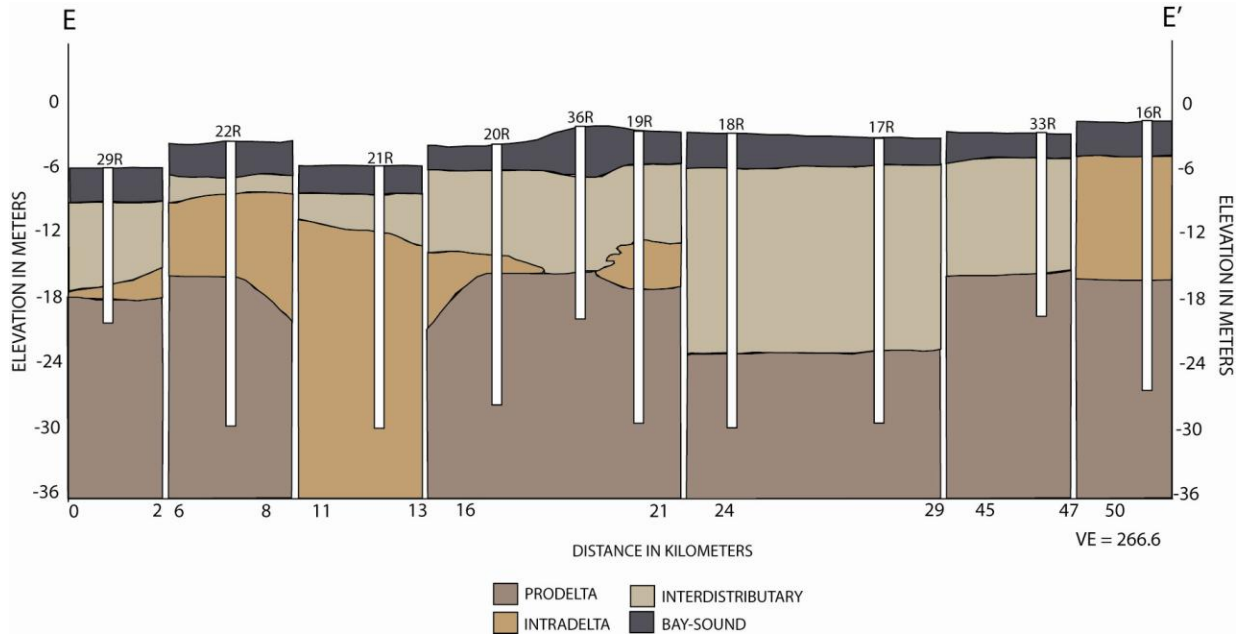
The cross-section B-B' shows a very typical deltaic cross-section for fluvially dominated delta systems. At the depicted interval, the base is a large deposit of prodelta material that extends for more than 24 kilometers and is approximately 18 meters thick. However, the cross-section does not extend more than 36 meters, and it is possible that this prodelta deposit extends to the Pleistocene surface below. Intradelta complexes occur near abandoned distributary channels, and between these channels, interdistributary clays are present. Natural levees are present along abandoned distributary channels and modern marsh has formed on those higher surfaces. This pattern of prodelta overlain by interfingering interdistributary and intradelta deposits with abandoned distributary channels seen in this cross-section is repeated in most of the following cross-sections.



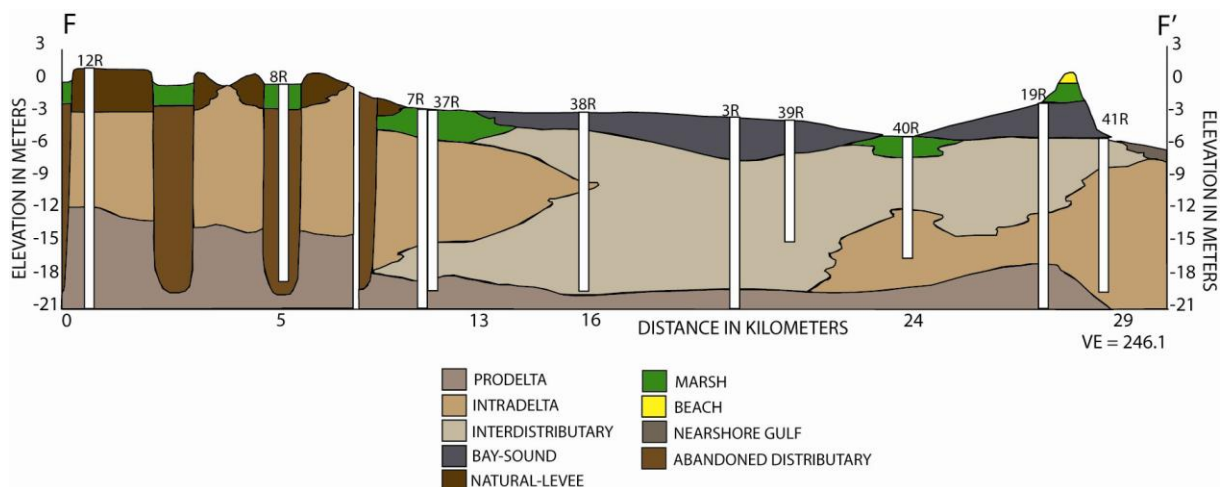
As mentioned previously, the typical pattern of prodelta deposits overlain by interdistributary clays and intradelta complex juxtaposed with abandoned distributary channels is common in fluviially-dominated delta systems. This cross-section, C-C', similarly shows this sort of relationship; however the surface of this cross-section has been covered by bay-sound deposits (Appendix B - Cross-sections). Modern marsh deposits in this cross-section are localized to natural levees and abandoned distributary channels. This relationship of modern marsh deposits on natural levee deposits is a common pattern in the geomorphology of the St. Bernard marsh due to the coarse grain size of the natural levees as well as their resistance to compaction.



D-D' is an unusual cross-section because it not only covers an area larger than the previous north-south trending cross-sections, but it also does not intersect the cross-section A-A'. This cross-section has little evidence of fluvial deposits because the majority of the deposits are prodelta and interdistributary clays, which are distal deltaic deposits, as well as modern bay-sound deposits. The intradelta complexes noted in three locations occur despite the absence of abandoned distributary channels. In their study, Kolb and van Lopik (1958a) note that distinctions between intradelta complexes and interdistributary clays can be made "only when working with very closely spaced borings". This is likely due to the presence of intradelta complexes near even the smallest distributaries, and likewise interdistributary clays captured between small distributaries or crevasses (Kolb and van Lopik, 1958a). Based on this, it is possible that more coarse-grained intradelta complexes exist in the gaps of this cross-section (between 24 and 37 kilometers), but are difficult to discern without higher-resolution data.

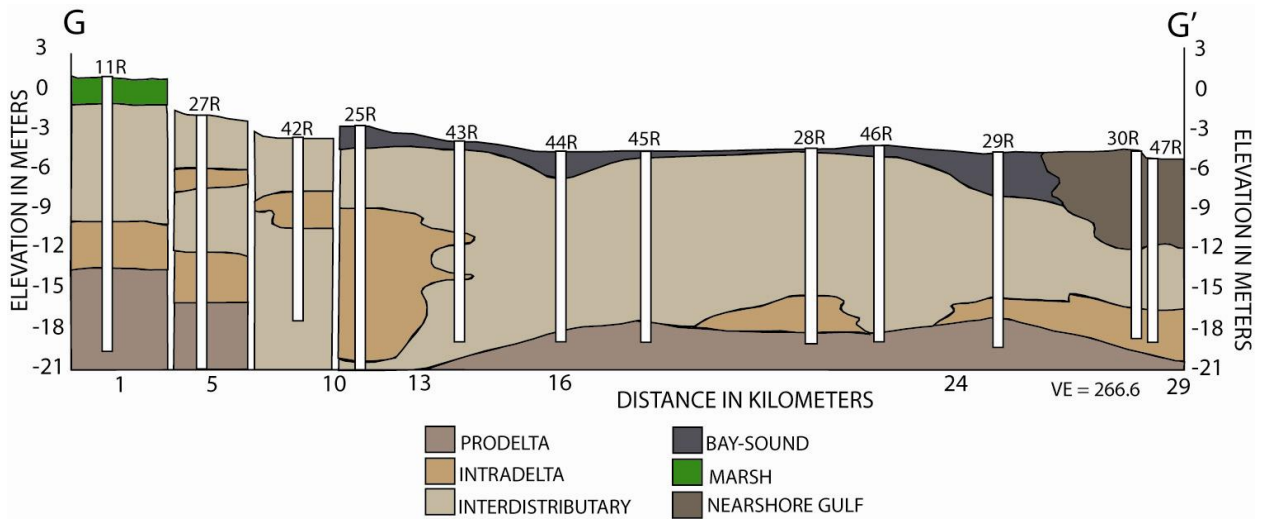


The cross-section E-E' is the eastern most cross-section that trends north-south in this group. Unlike the earlier discussed cross-sections, there are more intradelta complex deposits, though they are unrelated to abandoned distributary channels. In particular, the boring 21R is composed almost entirely of intradelta complex deposits. Additionally, the majority of these deposits are located near the southern end of the cross-section. In the previous cross-section, the majority of intradelta complex deposits were located in the north. Those deposits are also, in general, deeper than the intradelta complex deposits in this cross-section (E-E'). This may be a result of small-scale delta lobe switching within the St. Bernard Delta complex. Perhaps a northern course was occupied, then abandoned in favor of a southern course. In general, however, E-E' is lacking in significant shallow coarse (sandy) deposits.



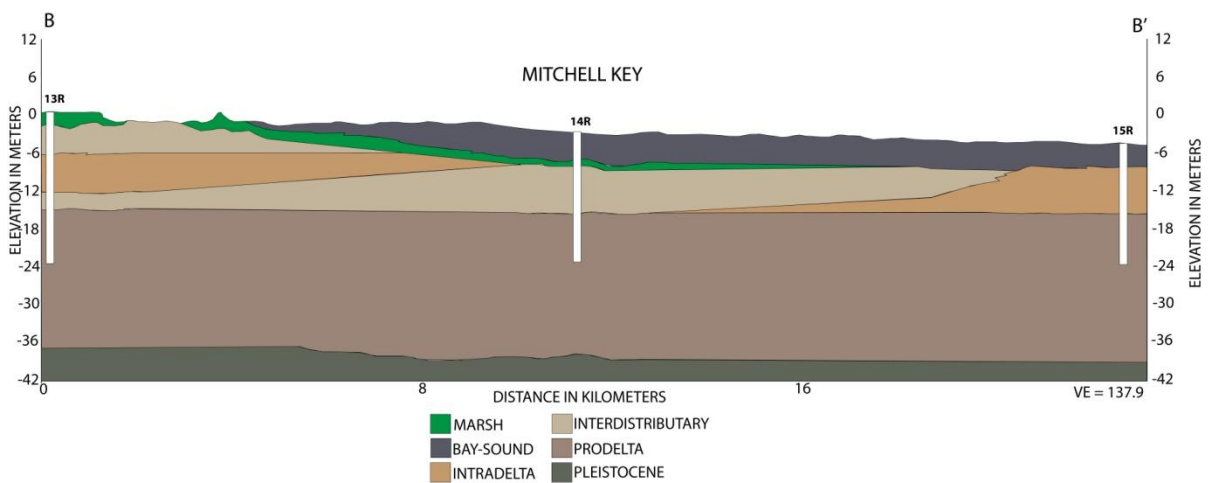
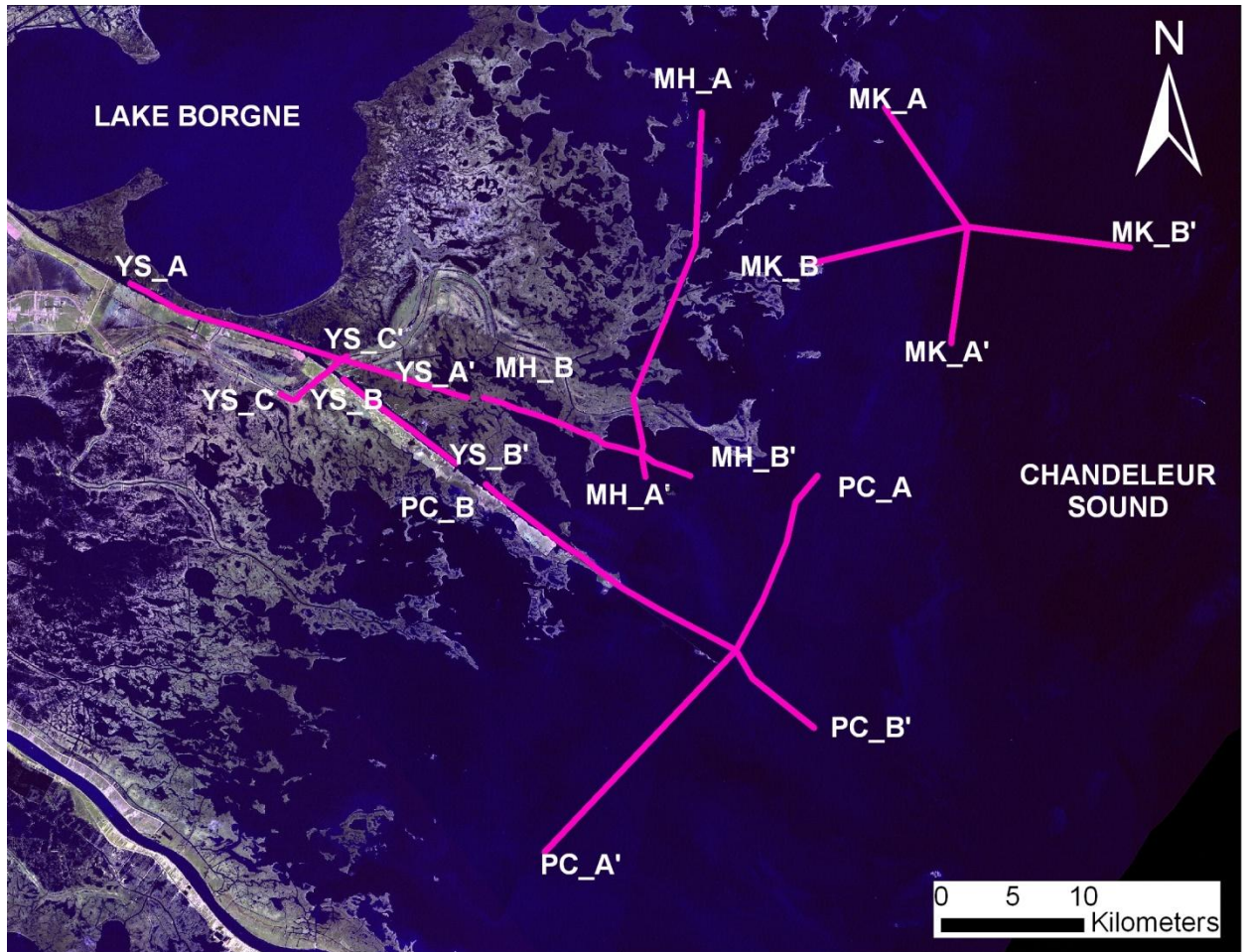
F-F' is the first of the east-west trending cross-sections. The western part of the cross-section (boreings 12R and 8R) are dominated by fluvial deposits (abandoned distributary channels, natural levees, and intradelta complex deposits). This part of the cross-section is sand-rich and lacking in clay-rich interdistributary deposits. As the cross-section continues east, the intradelta complex and abandoned distributary channel deposits become more scarce, and in the

case of the intradelta complex deposits, pinch out. In the absence of these deposits, interdistributary clays dominate. Additionally, in the surface deposits of this cross-section, the natural levees and marsh deposits transition into bay-sound deposits. The far eastern side of this cross-section is unusual in that it contains a large deposit of intradelta complex at depth beneath the modern Chandeleur Islands. The St. Bernard Delta Complex has been suggested to extend beyond the Chandeleur Islands (Tornqvist et al.1996; Rogers et al. 2009; and others) and these deposits indicate that farthest extension of the complex.



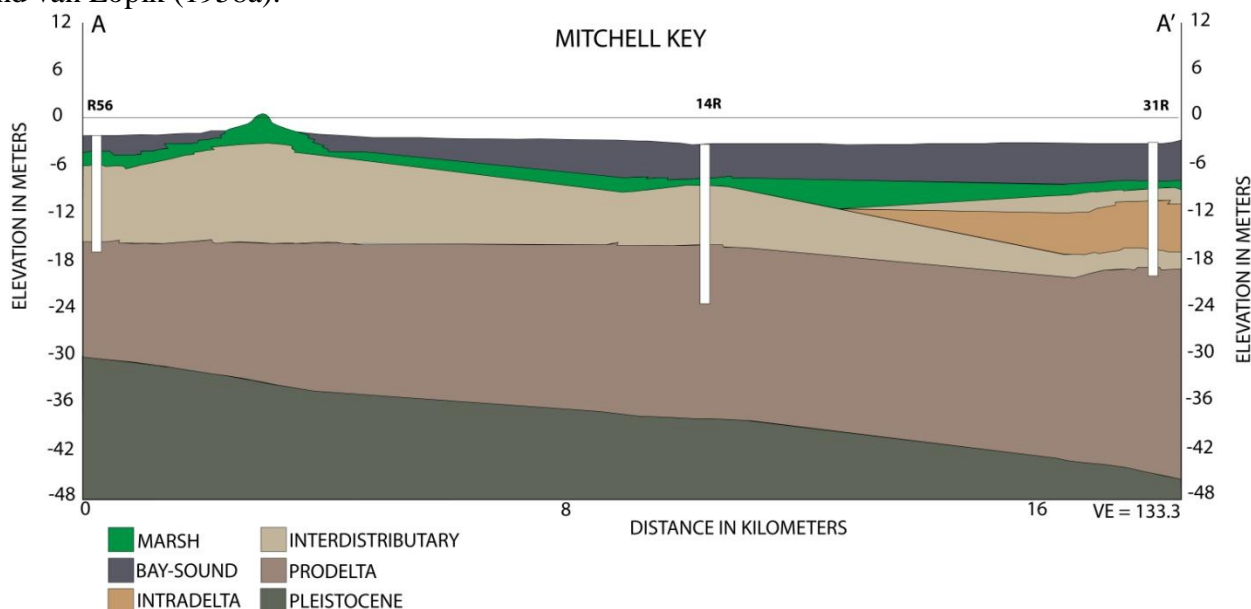
This cross-section, G-G', is the southernmost of the east-west trending cross-sections. In cross-sections D-D' and E-E', the majority of intradelta complex deposits were located along the southern end of those transects (i.e. the intersection with G-G'). However G-G' does not display the same intradelta complex deposits seen in cross-sections D-D' and E-E'. The intradelta complex deposits that do exist are at depths near to or greater than 6m, and some are even at depths of as much as 18m. The cross-section dominantly consists of interdistributary clay deposits. Unlike the previous cross-section, F-F', this cross-section shows very few fluvial deposits and indicates that the distributary channel responsible for deposition of this delta complex must have existed north of this cross-section due to the absence of abandoned channels and widespread intradelta complex deposits.

Atlas

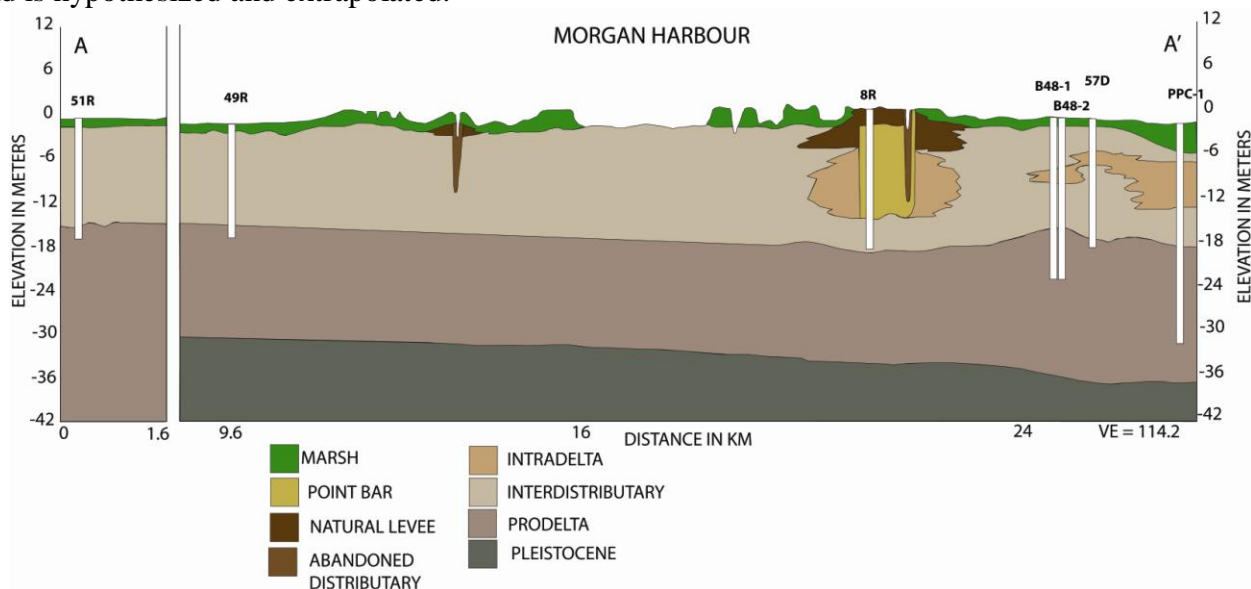


The cross-section MK A-A' is a north-south trending cross-section. Two of the three borings that compose this cross-section are shared with MRGO_C-C'. The only boring not

shown on MRGO_C-C' is R56, at the northern end of the cross-section. The general trend of this cross-section shows more fluvial deposits (i.e. intradelta complex) at the southern end of the cross-section; a trend that was typical of the MRGO cross-sections. Additionally, this cross-section shows the Pleistocene surface at approximately 30m depth extending to more than 40m depth along a southern dip trend. As no borings penetrate the Pleistocene in this cross-section, the depth and location of this deposits is considered questionable, and was likely inferred by Kolb and van Lopik (1958a).

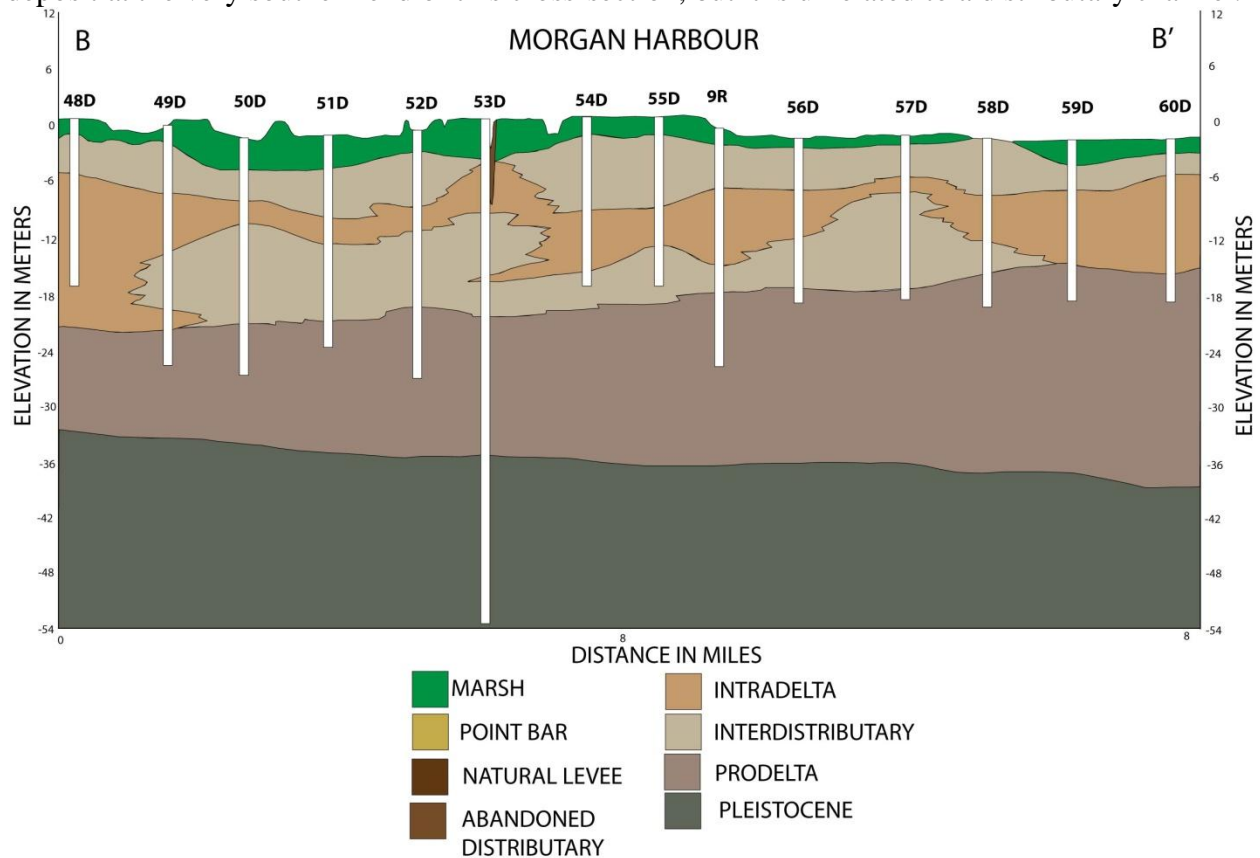


MK_B-B' crosses MK_A-A' at the boring 14R and trends west-east. This cross-section shows more intradelta complex deposits than MK_A-A', suggesting that intradelta deposits can be discontinuous and possess little lateral continuity. Both 13R and 15R in this cross-section intersect these deposits, but the extent of the intradelta deposits is unknown without additional data and is hypothesized and extrapolated.

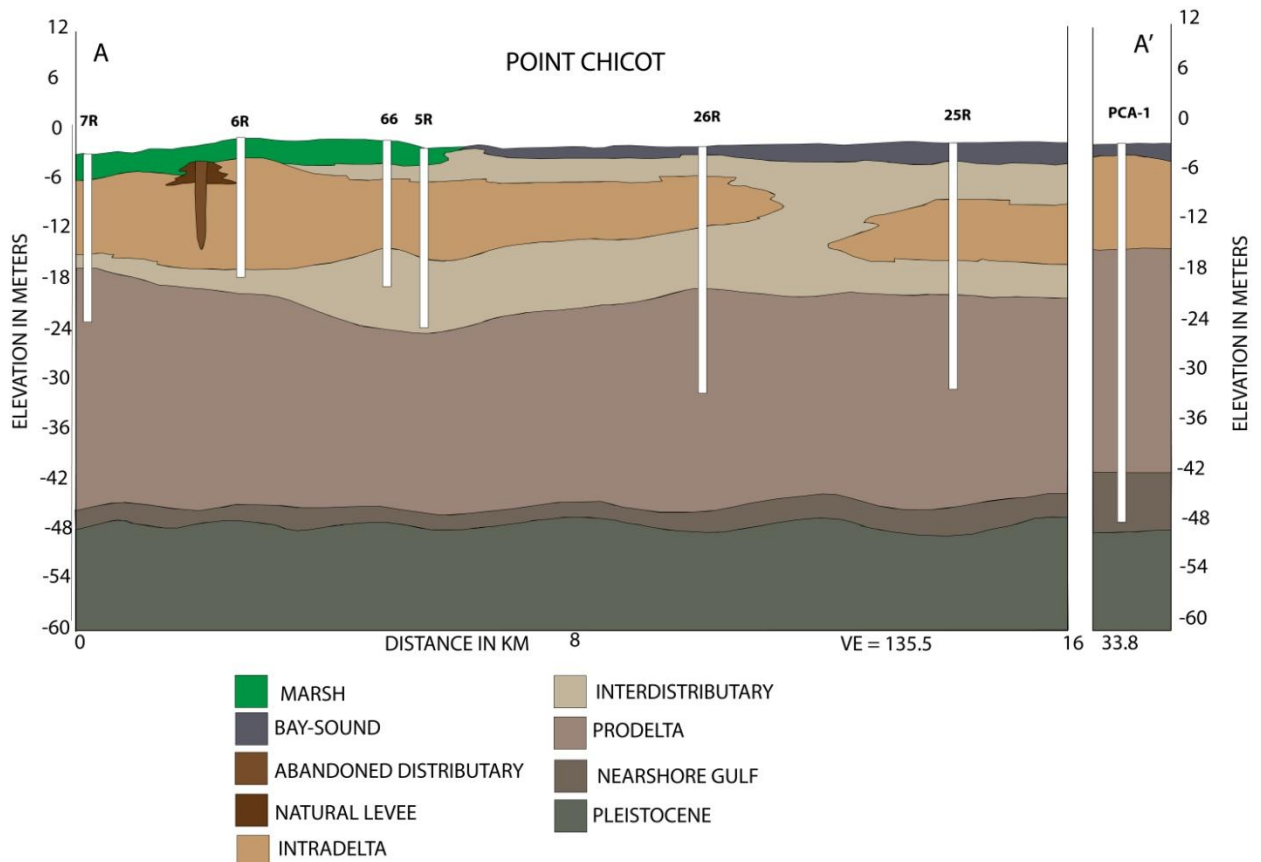


MH_A-A' is parallel to MK_A-A' in the St. Bernard Marsh and crosses Bayou La Loutre on the southern end of the cross-section. The northern part of this cross-section (i.e. north of 8R)

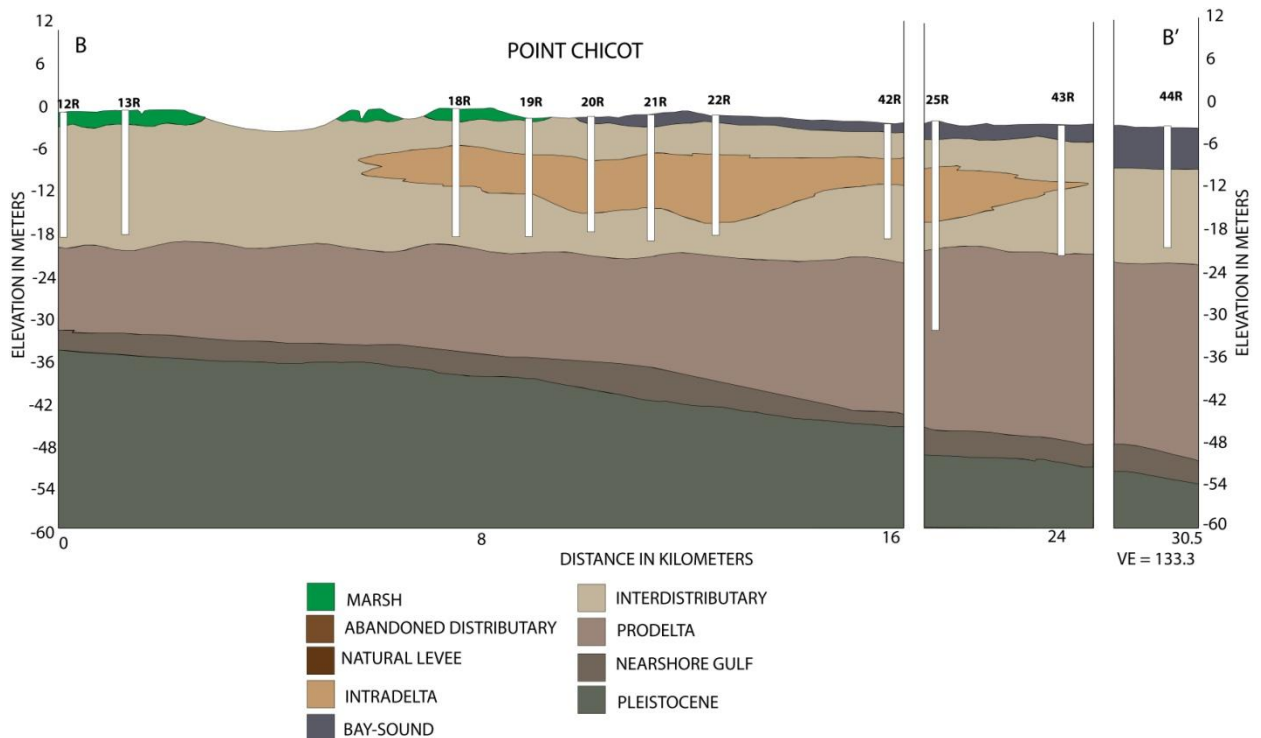
is marked by a lack of intradelta complex deposits. There is a small abandoned distributary channel that was mapped by Kolb and van Lopik (1958a), although there is no data from the borings to supplement this idea. Also, the depth of this channel is not well constrained because of a lack of data. In the southern part of the cross-section, the presence of intradelta complex deposits is associated with Bayou La Loutre. There is another identified intradelta complex deposit at the very southern end of this cross-section, but it is unrelated to a distributary channel.



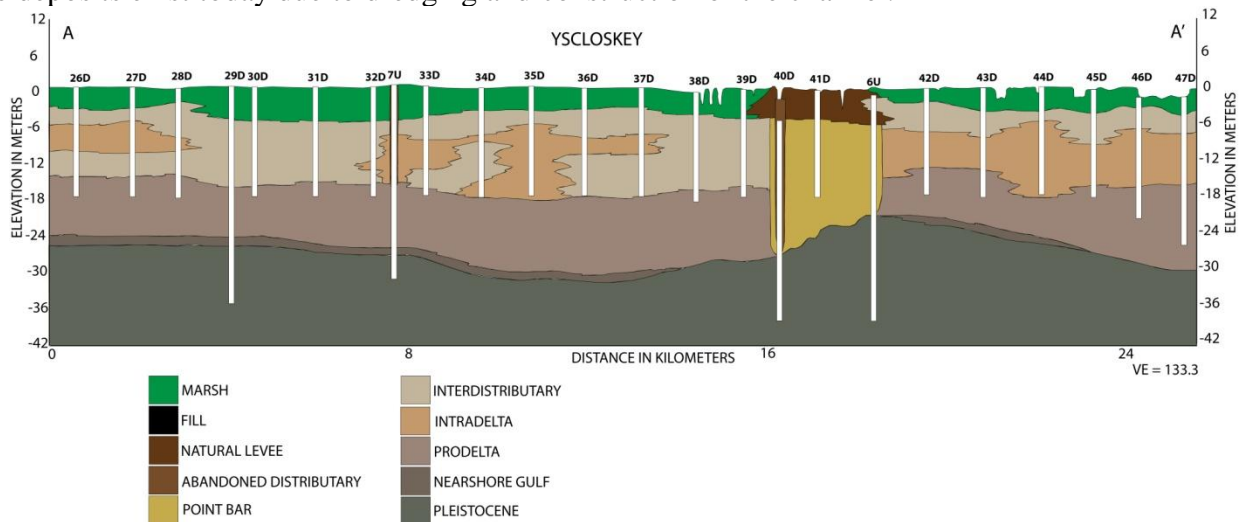
MH_B-B' is a very well constrained cross-section with fourteen approximately equally-spaced borings. The high number of borings and spacing provides a part of MRGO_A-A' in higher resolution. What is noticeable about this cross-section is the lateral extent of intradelta complex deposits and varying thicknesses of these deposits in the cross-section. The majority of these deposits are located below 6m, with a small anomaly above 6m near 53D and a small abandoned distributary channel. The Pleistocene in this cross-section is constrained by one boring only, and thus the contact between prodelta deposits and the Pleistocene surface is questionable in other locations.



The cross-section PC_A-A' trends from the northeast to the southwest, crossing the entrance to the Mississippi River Gulf Outlet. This cross-section is the southernmost cross-section and marked by thick intradelta complex deposits. There is a small distributary channel near the boring 6R, but the data supporting this channel is unknown. Perhaps it is an extension of Bayou La Loutre. The northern boring, 7R, contains by interdistributary clays both stratigraphically above and below intradelta complex deposits, but the southernmost boring (PCA-1) shows no interdistributary deposits. This trend has been seen in previously discussed cores: the existence of interdistributary deposits instead of intradelta complex deposits. Also, this cross-section has a thin interval of nearshore gulf deposits separating the Pleistocene surface from prodelta deposits, but the data for this does not exist outside of the boring PCA-1.

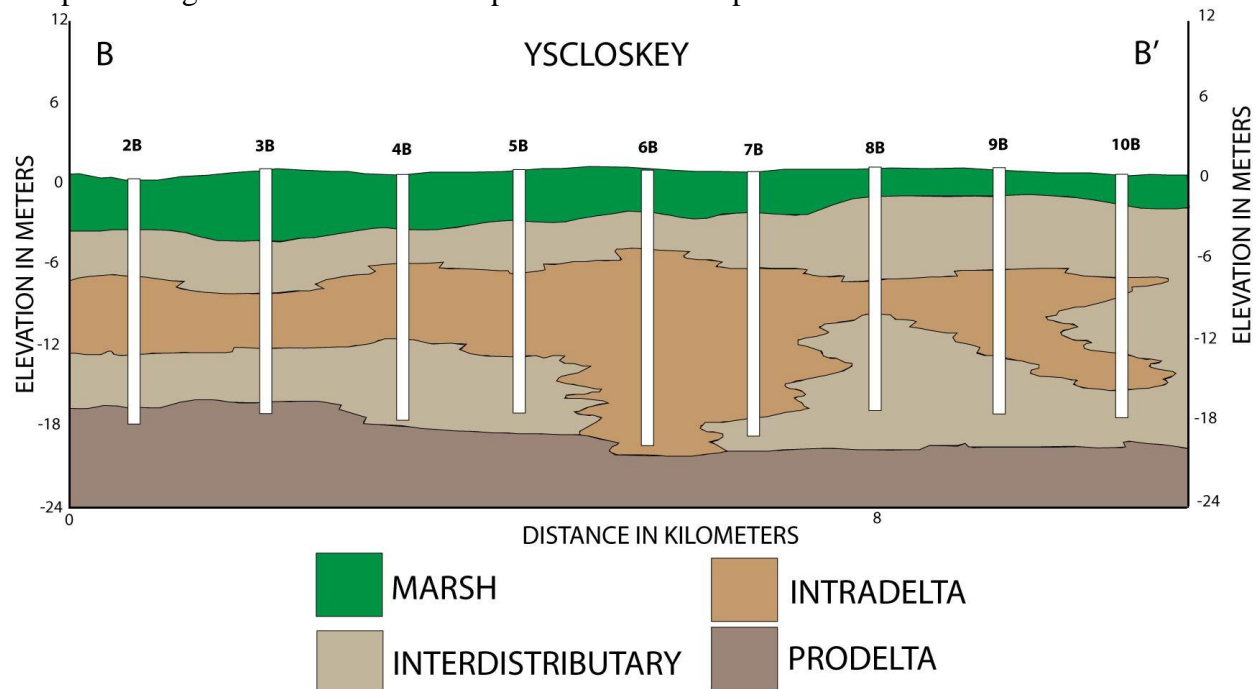


Interestingly, PC_B-B' shows a relatively small (in both thickness and lateral extent) intradelta complex at the mouth of the Mississippi River Gulf Outlet. PC_A-A' and PC_B-B' cross at boring 25R, which shows a 6m thick deposit of intradelta complex. Because these borings and cross-sections were made before the Mississippi River Gulf Outlet was built (or during its construction), they capture the marsh as it existed previously. It is unclear how much of these deposits exist today due to dredging and construction of the channel.

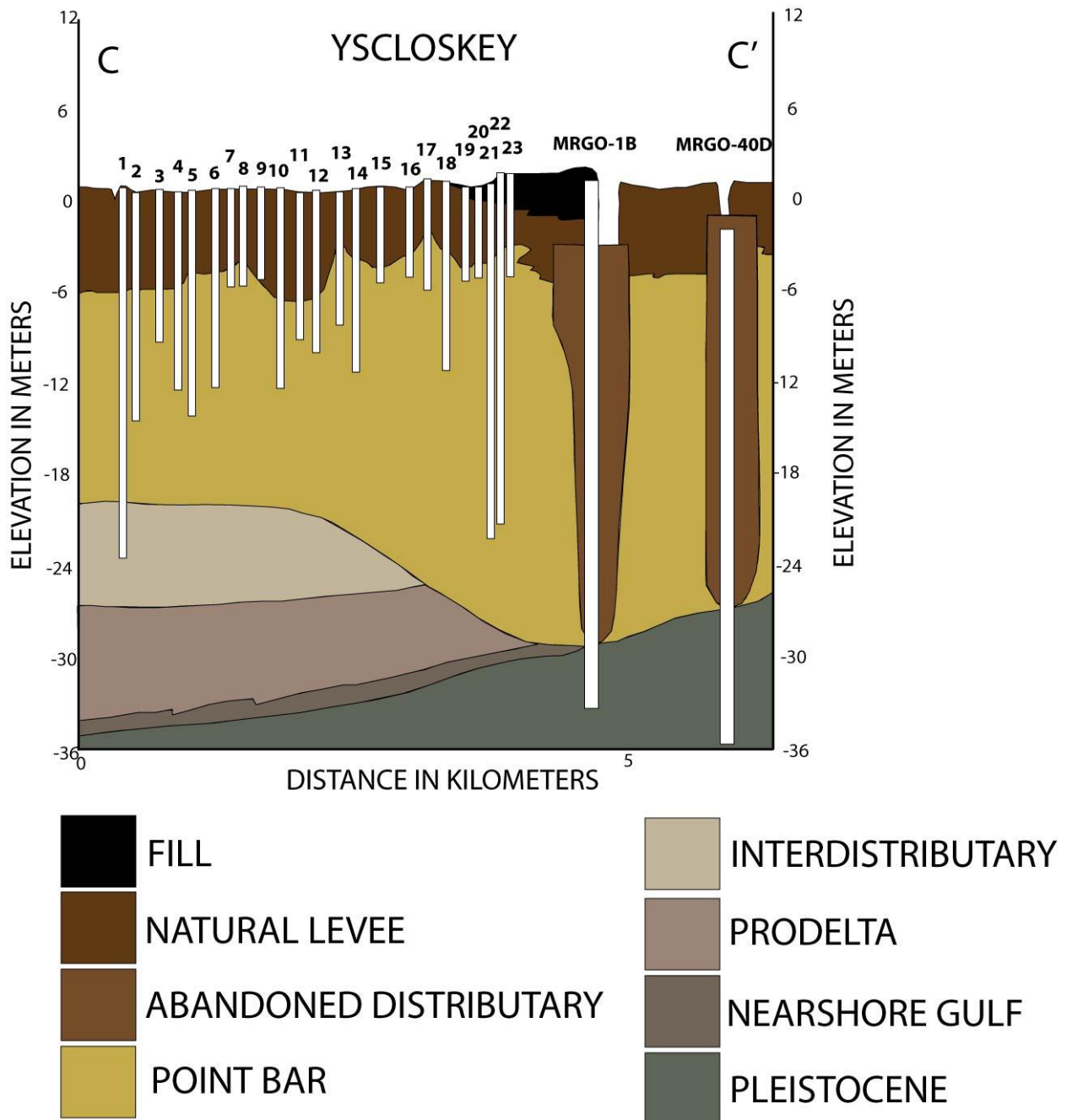


This cross-section follows the modern MR-GO channel before diverging where Bayou La Loutre meets the channel. The trend of this section is from northwest to southeast. Like MH_B-B', YS_A-A' follows a section of MRGO_A-A' in greater detail due to the larger amount of equally spaced borings. This cross-section, YS_A-A', is well constrained because of a high density of borings approximately equally spaced. There are two small intradelta complex deposits in the western end of this cross-section. The eastern intradelta complex deposit is

closely associated with Bayou La Loutre. Additionally, there are sand-rich point bar deposits located on the eastern side of this distributary channel. Interestingly, this cross-section shows Bayou La Loutre possibly incising the Pleistocene at the very base of the channel. The Pleistocene surface, in general, in this cross-section, is very shallow (~24m). Most other delta complexes in the Mississippi River delta plain are stacked on previous delta complexes (Frazier, 1967). The shallow Pleistocene surface is a fundamental difference about the St. Bernard Delta complex in regards to other delta complexes in the delta plain.

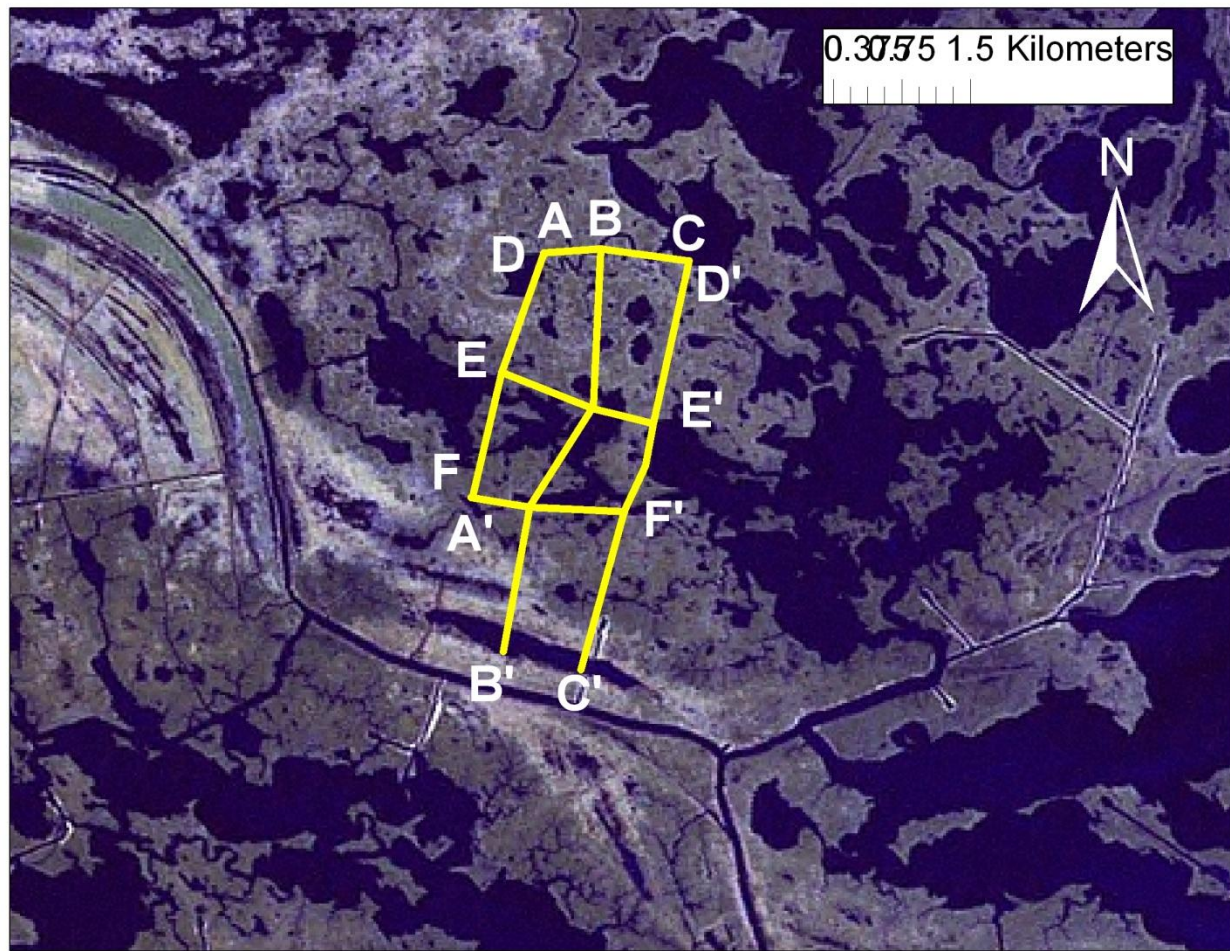


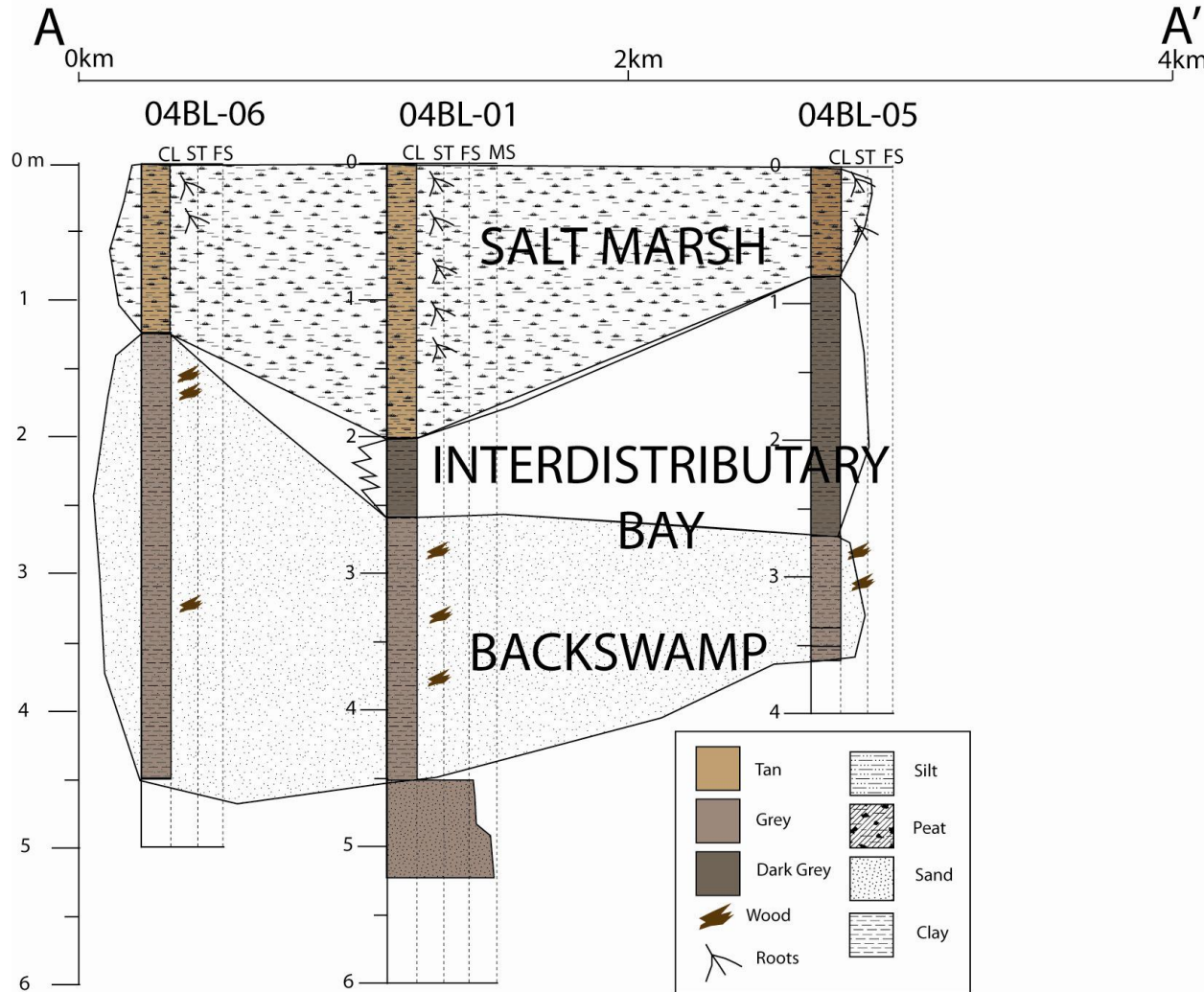
YS_B-B' is a cross-section that contains a high density of borings within a relatively short lateral length. The spacing of the borings accurately depicts the location and thickness of intradelta complex deposits. This cross-section follows a part of the Mississippi River Gulf Outlet channel. The cross-section shows the familiar stratigraphic stacking pattern of prodelta overlain by interfingering interdistributary and intradelta complex deposits. However, like previous cross-sections, these borings reflect pre-construction conditions of the Mississippi River Gulf Outlet channel. Once this channel was constructed, dredging and the subsequent evolution of the channel over the last 50 years likely has erased the majority of the stratigraphy seen in this cross-section.



The cross-section YS_C-C' trends southwest to northeast and intersects YS_A-A' near the intersection of Bayou La Loutre and the Mississippi River Gulf Outlet. This cross-section has an exceptionally high density of borings (25 borings over ~5 km) that show a highly developed point bar system associated with Bayou La Loutre. In fact, the most dominant aspect of this cross-section is the extent of the point bar deposits around Bayou La Loutre.

Bayou La Loutre (BL)

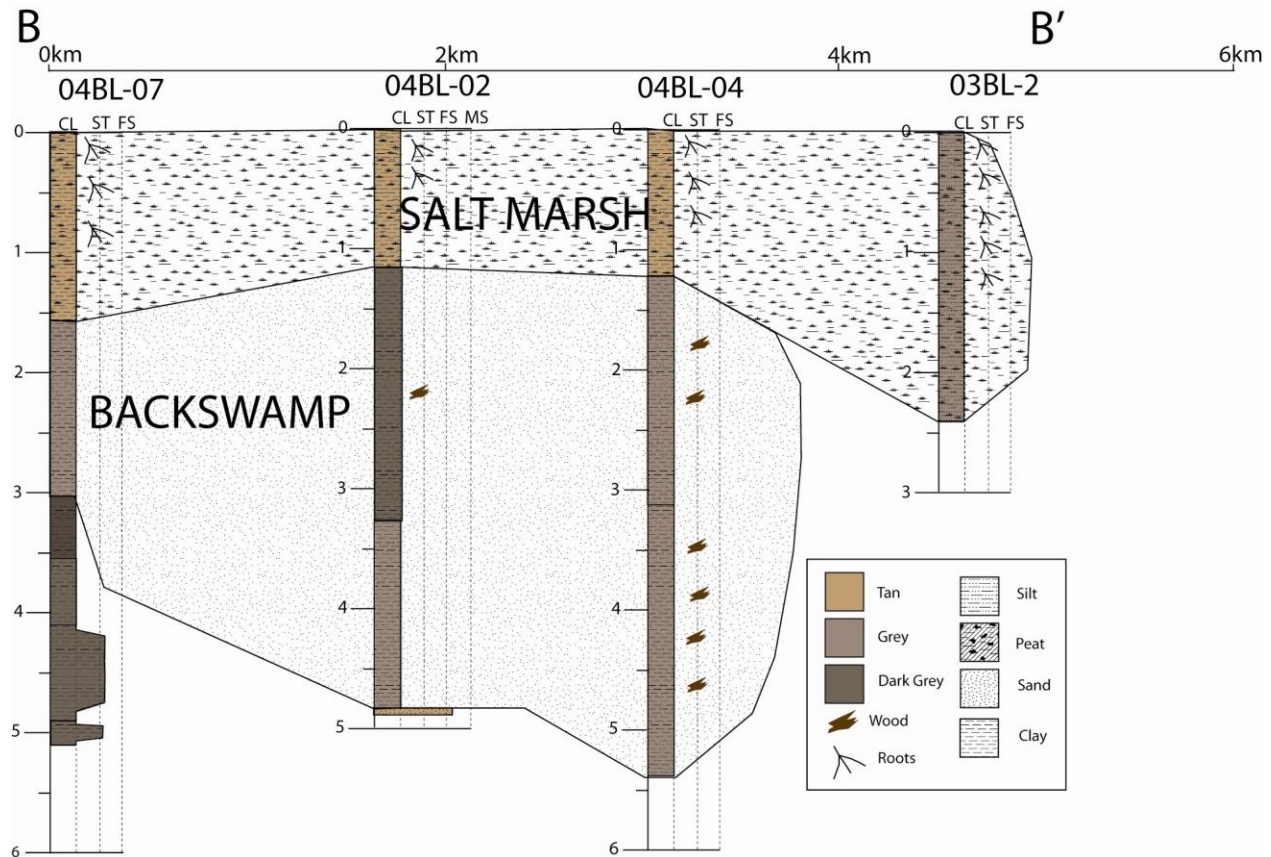




The cross-section A-A' contains three vibracores: 04BL-06, 04BL-01, and 04BL-05. 04BL-06 has two primary units: gray clay from the base of the core at 4.5m to 1.24m, with woody fragments at the top of this unit. The second unit is light-tan clay from 1.24m to the surface with numerous root fragments near the surface, likely associated with modern marsh. The base of 04BL-01 is light-gray, medium sand from 5.22 to 4.51m. Overlying this is a gray clay unit from 2.58m to 4.51m with wood fragments. From 2.00m to 2.58m is a unit of black to dark gray clay. The surface unit from 2.00m is tan clay with rooting near the surface. From 3.61 to 3.50m in 04BL-05 is a gray clay unit. Overlying this from 3.38m to 3.50m is a unit of medium gray to black clay. A gray clay unit with wood fragments exists from 2.70m to 3.38m. Above this from 0.80m to 2.70m is gray clay. The top unit in this core from the surface to 0.80m is organic-rich clay with abundant rooting.

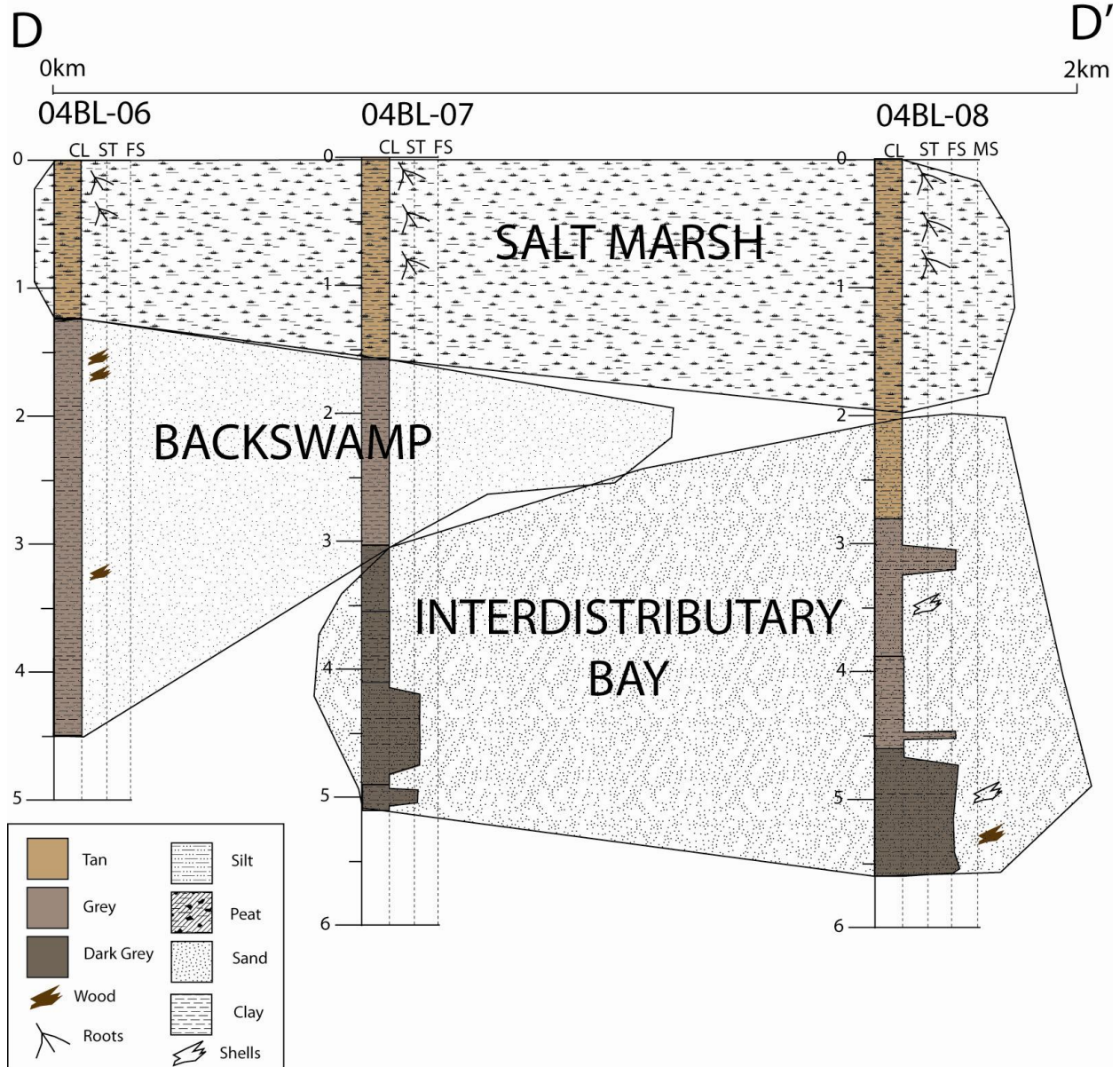
The cross-section A-A' contains three major environments of deposition: backswamp, interdistributary bay, and salt marsh. The backswamp environment is characterized by gray clay with wood fragments, present in all cores in the cross-section at depths greater than 1.25 meters. Above this in two of the cores lies a unit featuring darker gray clay and an absence of wood fragments. This environment is like a transitional environment from a backswamp to a salt marsh and thus is called an interdistributary bay. The topmost unit on this cross-section, the salt marsh,

is composed of organic rich clay, peat, and root material consistent with the modern marsh environment.



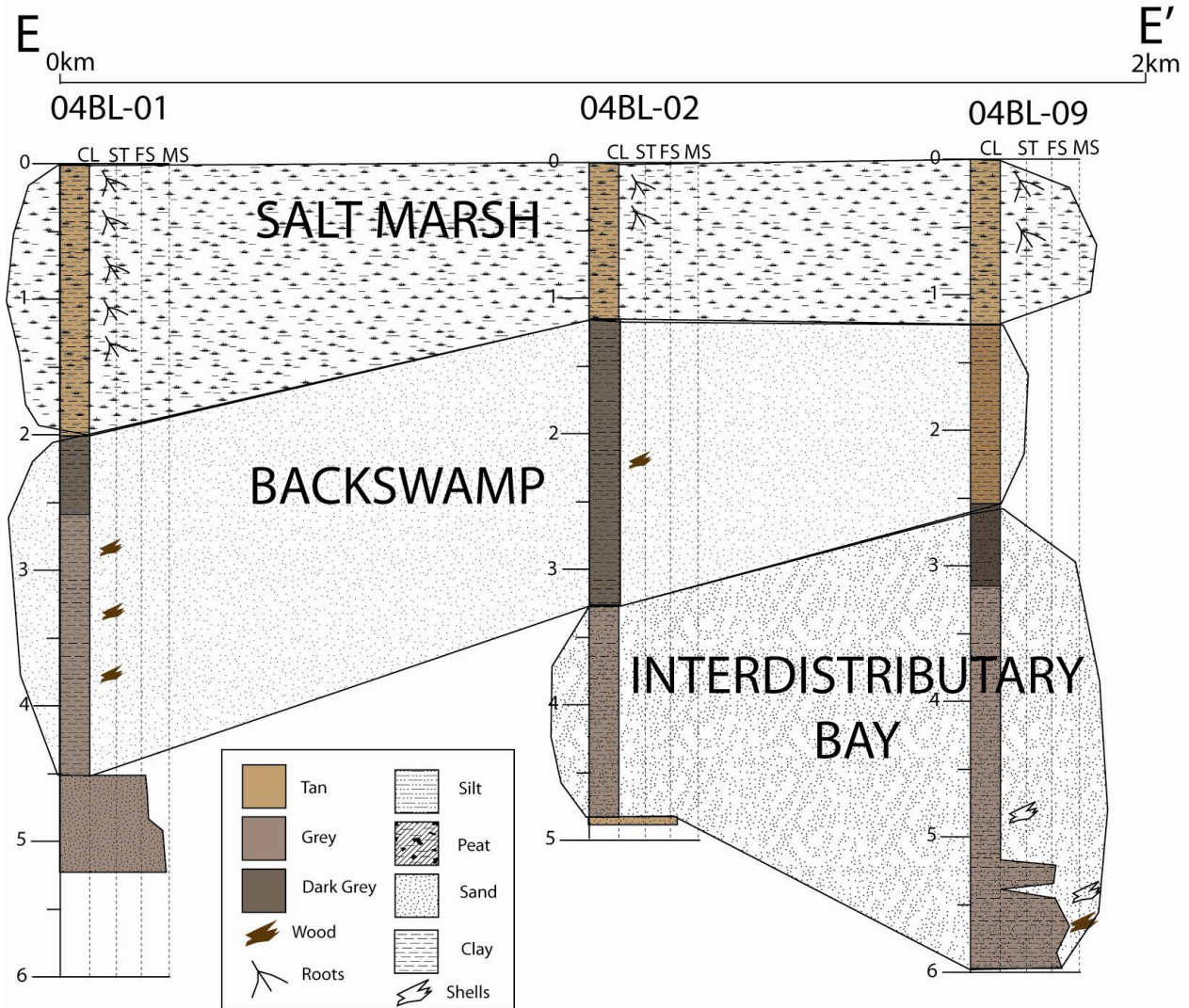
B-B' contains four vibracores: 04BL-07, 04BL-02, 04BL-04, and 03BL-2. 04BL-07 contains four units: the base begins at 5.10m to 3.55m and is gray sandy clay. Overlying this unit from 3.55 to 3.02m is a dark gray to black clay. From 3.02m to 1.55m is brown-gray clay. The top of this core to 1.55m is dark brown to black clay with rooting and organics throughout. There are three units in 04BL-02: brown-gray clay from 4.88m to 3.27m, dark gray from 3.27 to 1.15, and tan clay with rooting from 1.15m to the surface. The bottom unit in 04BL-04 from 5.39m to 3.12m is gray clay. Overlying this unit is gray clay from 1.21m to 3.12m with wood fragments and organics. At the surface of this core to 1.21m is tan clay with roots and organics. 03BL-2 contains gray sandy clays for the entirety of the core.

There are two depositional units in B-B': backswamp and salt marsh. Backswamp is present in three of the four cores in this cross-section and is characterized by gray clay, often with wood fragments present. The unit described as salt marsh contains tan or gray clay with organic material, peat, and rooting. Unlike the previous cross-section, B-B' does not have a unit of interdistributary bay suggesting that the bay was laterally confined, or perhaps that the unit is missing from B-B'. The former seems more likely because any significant erosion that would have removed this unit would have likely created open water that is unable to be colonized by modern salt marsh.



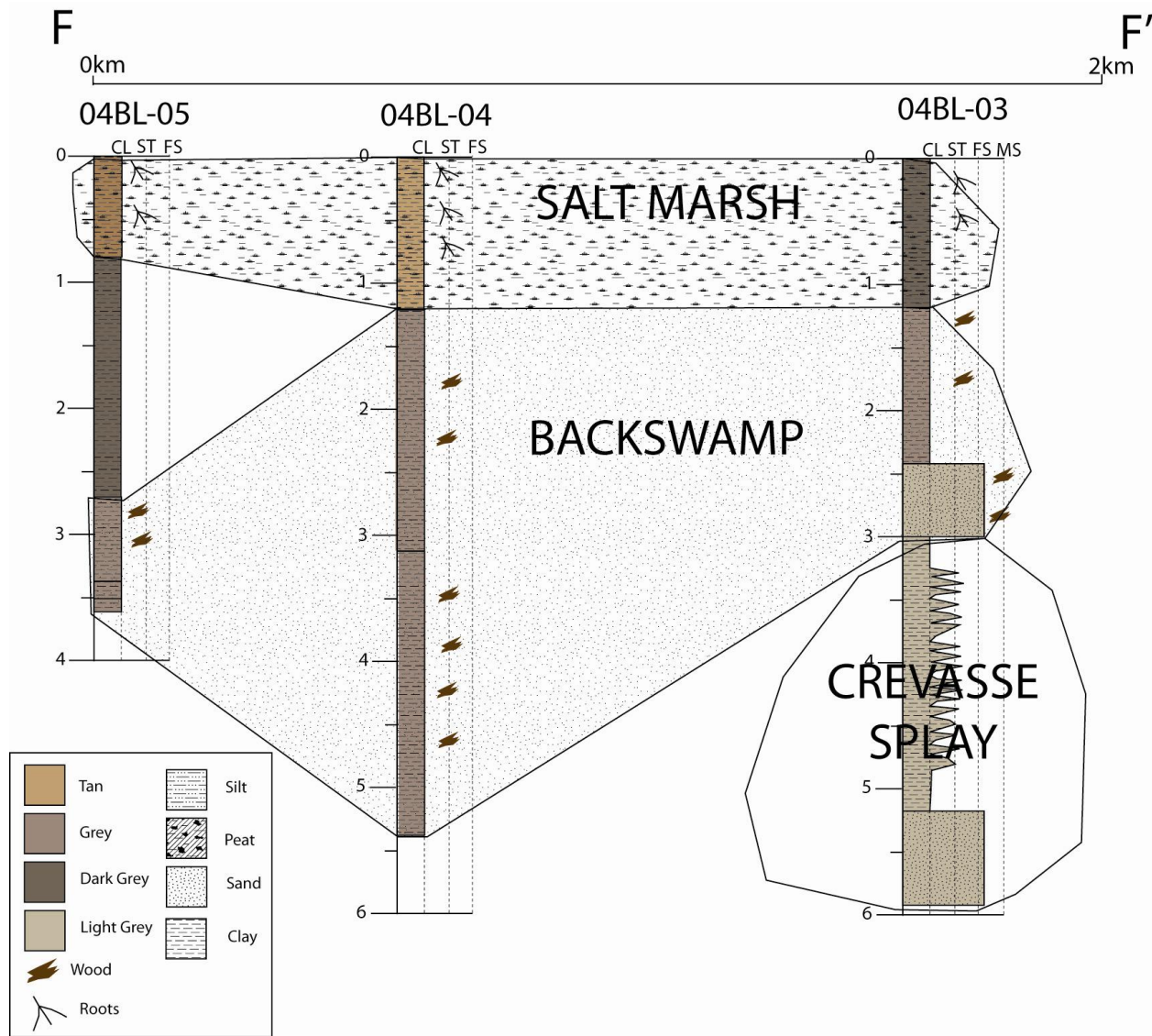
04BL-06, 04BL-07, and 04BL-08 are cores in the cross-section BL_D-D'. 04BL_06 was previously described in BL_A-A'. 04BL_07 was previously described in cross-section BL_B-B'. 04BL-08 was previously described in BL_C-C'.

There are three depositional units in D-D': interdistributary bay, backswamp, and salt marsh. The interdistributary bay is characterized by gray clay with shell material. Backswamp deposits contain wood material, but may also be gray clay similar to the interdistributary bay deposits. In this cross-section, it is not clear where the boundary between an interdistributary bay and backswamp occurs mainly because the lack of organic material (i.e. shells, wood fragments) in the middle core, 04BL-07. The salt marsh deposits are characterized by tan clay with organic rich material, peat, and roots.



The cross-section BL_E-E' consists of three vibracores: 04BL-01, 04BL-02, 04BL-09. 04BL-01 and 04BL-02 were previously described in BL_A-A' and BL_B-B', respectively. 04BL-09 was previously described in BL_C-C'.

Similar to D-D', the cross-section E-E' contains three depositional units: interdistributary bay, backswamp, and salt marsh. However, in this cross-section, the backswamp deposits are more laterally continuous whereas the interdistributary bay deposits are much more localized.

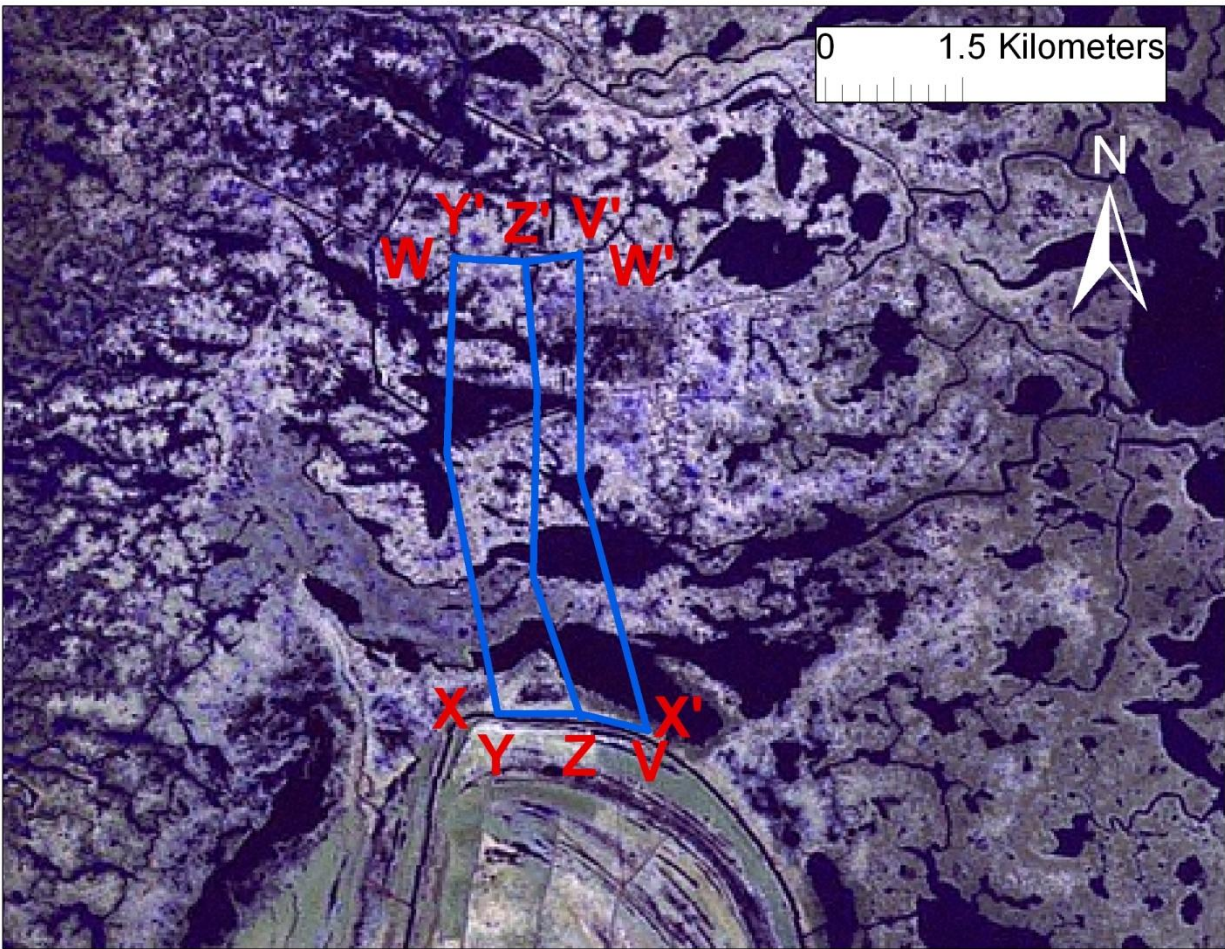


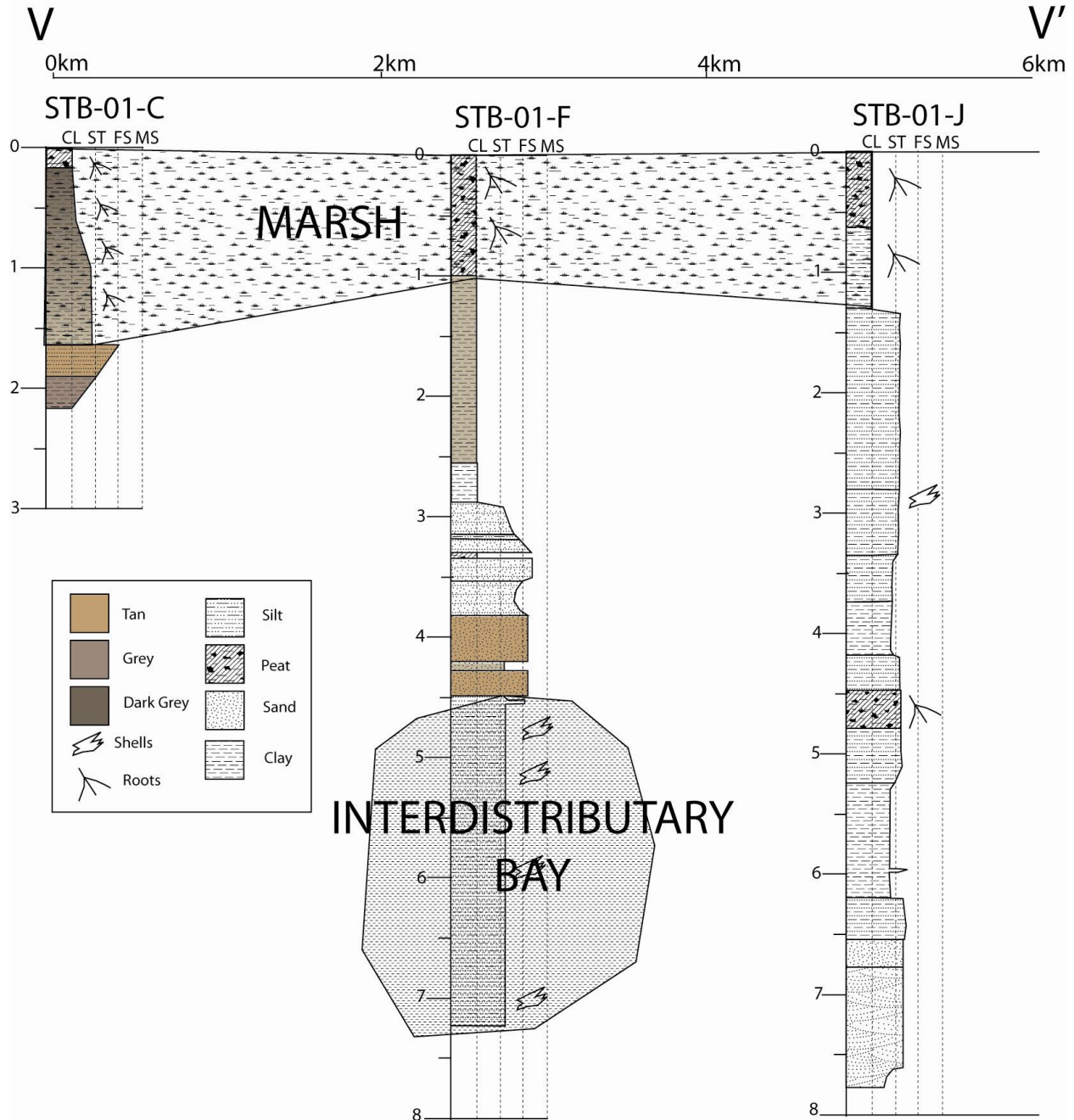
Three cores, 04BL-05, 04BL-04, and 04BL-03, make the cross-section BL_F-F'. 04BL-05 was previously described in BL_A-A'. 04BL-04 was previously described in BL_B-B'. 04BL-03 was previously described in BL_C-C'.

The cross-section F-F' contains three depositional environments: backswamp, salt marsh, and crevasse splay. This crevasse splay deposit is the same as seen in C-C'. Wood fragments are abundant in this cross-section, and help constrain the extent of backswamp deposits.

These cross-sections provide the opportunity to better understand not only vertical and lateral changes along Bayou La Loutre, but also collectively yield a three-dimensional framework of depositional environments. On the basis of these data, it appears that a crevasse splay exists in the southeastern extent of these cross-sections, and that this crevasse splay was likely deposited into an interdistributary bay. However, this bay was not widely extensive, and in some locations it occurs coevally with backswamp deposits. Essentially, what has been occurring in this location is a series of infilling events (both crevasse splays and bay infilling) that allowed marsh to colonize the modern surface.

St. Bernard Delta (STB)

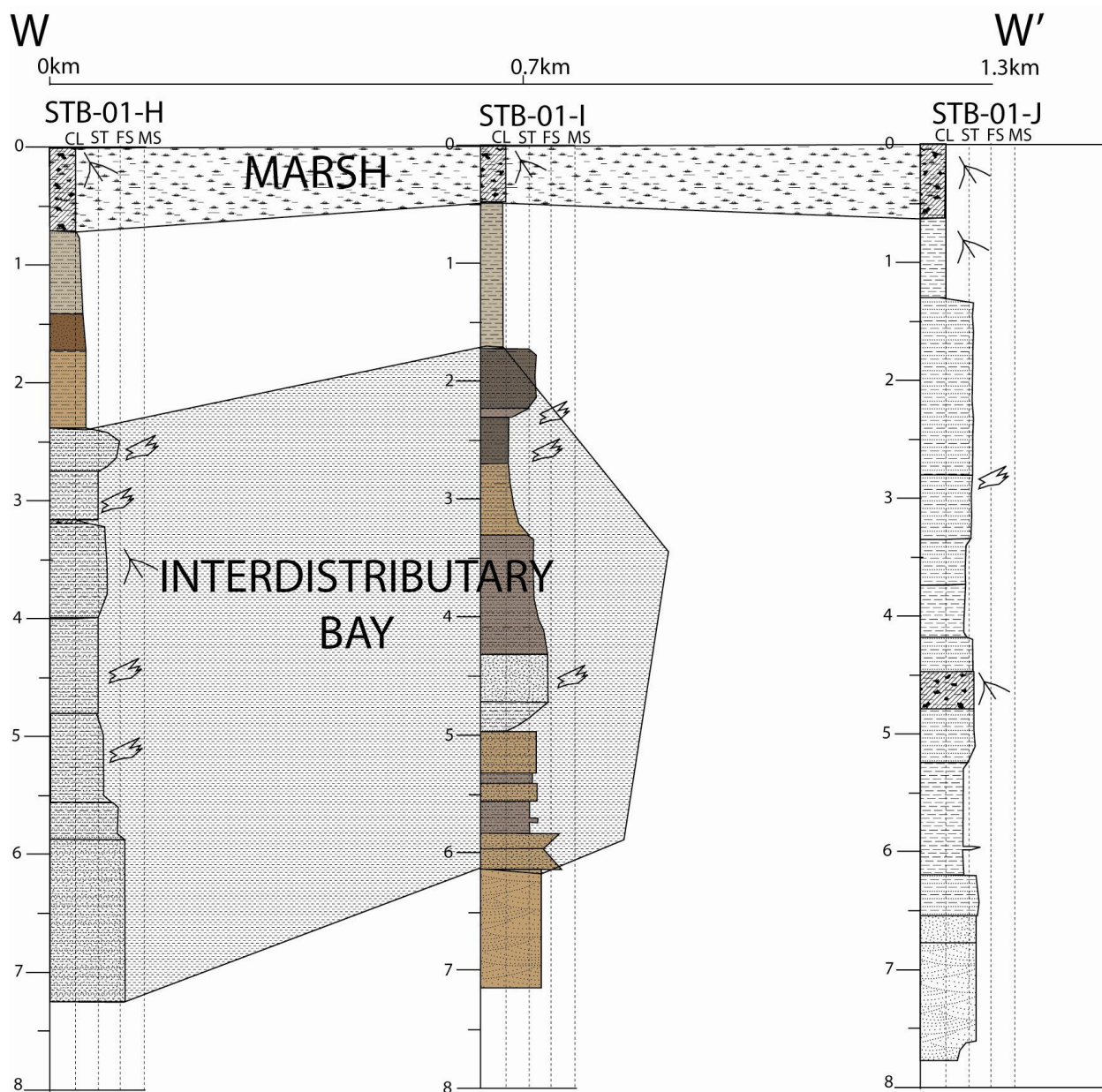




V-V' contains three cores: STB-01-c, STB-01-F, and STB-01-J. STB-01-C is a very short core, just over 2m in length. The bottommost unit coarsens from gray clay to gray silt. The unit above continues that coarsening upwards sequence from tan silt to tan fine sand. The unit above this is tan silt that fines upwards to an organic rich gray clay with rooting. The top unit is a 0.25m thick section of modern marsh deposits. STB-01-F has a total length of more than 7 meters. It begins in a silty unit with abundant shell material. Above this are interbedded units of sand and silt. From approximately 3m to 1m is a unit of tan clay. The topmost unit is modern marsh with high organic content and abundant roots. STB-01-J begins in a cross-bedded fine sand. The grain size in this core, in general, does not change dramatically until 1.25m. There are a few units in the core that contain roots (approximately 4.5m) and shell material (approximately

3 m). Like the other two cores in this cross-section, the top two units are tan clay overlain by modern marsh deposits.

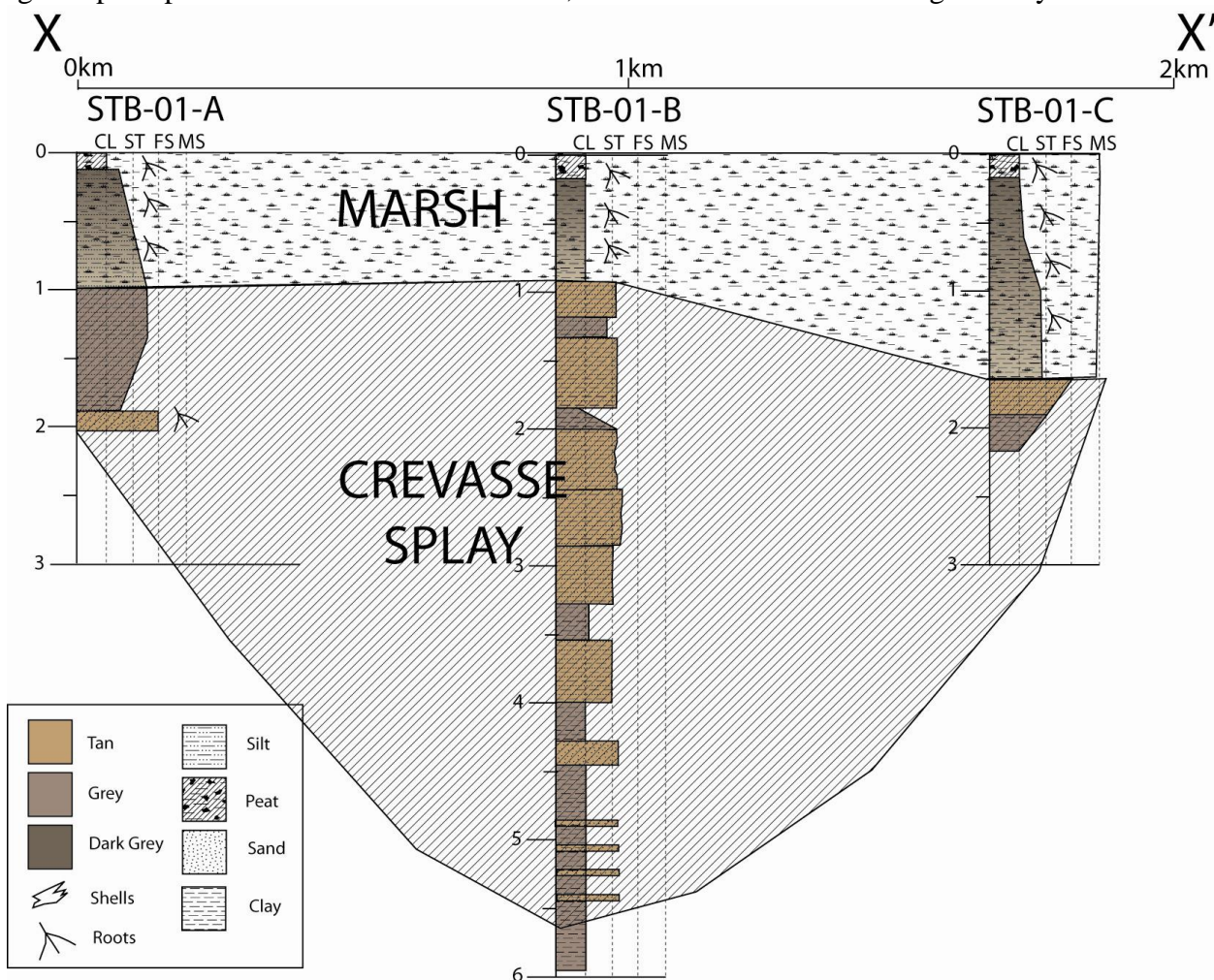
Only two environments of deposition have been identified in the cross-section V-V' primarily due to a lack of laterally continuous data. Only two cores in this cross-section penetrate further than 3 meters, and there is not a clear similarity between units in those cores to allow proper correlation. However, there are indicators, such as shell fragments and clay-rich sand, that the unit at the base of STB-01-F is an interdistributary bay. As usual, the surface deposits are modern salt marsh environments.



The cross-section W-W' consists of three cores, STB-01-H, STB-01-I and STB-01-J. STB-01-H extends to 7.25 m and begins in a thick (1m) bedded sand unit. Above this the units are fine to fine sand and silt with shell and some root content. Above this unit is tan and brown silty

clay. The topmost unit is the modern marsh surface with active rooting and high organic content. STB-01-I begins in a cross-bedded tan sand, overlain by a fining upwards sequence, which is then overlain by a coarsening upwards sequence. The units above this are alternating tan sand and gray silty sand. Above this at approximately 5m is a coarsening upwards sequence from silty clay to fine sand with shell content. There are two large fining upward units with shell contents. Similar to STB-01-H, STB-01-I has a unit of tan clay below a unit of modern marsh. STB-01-J was previously described in V-V'.

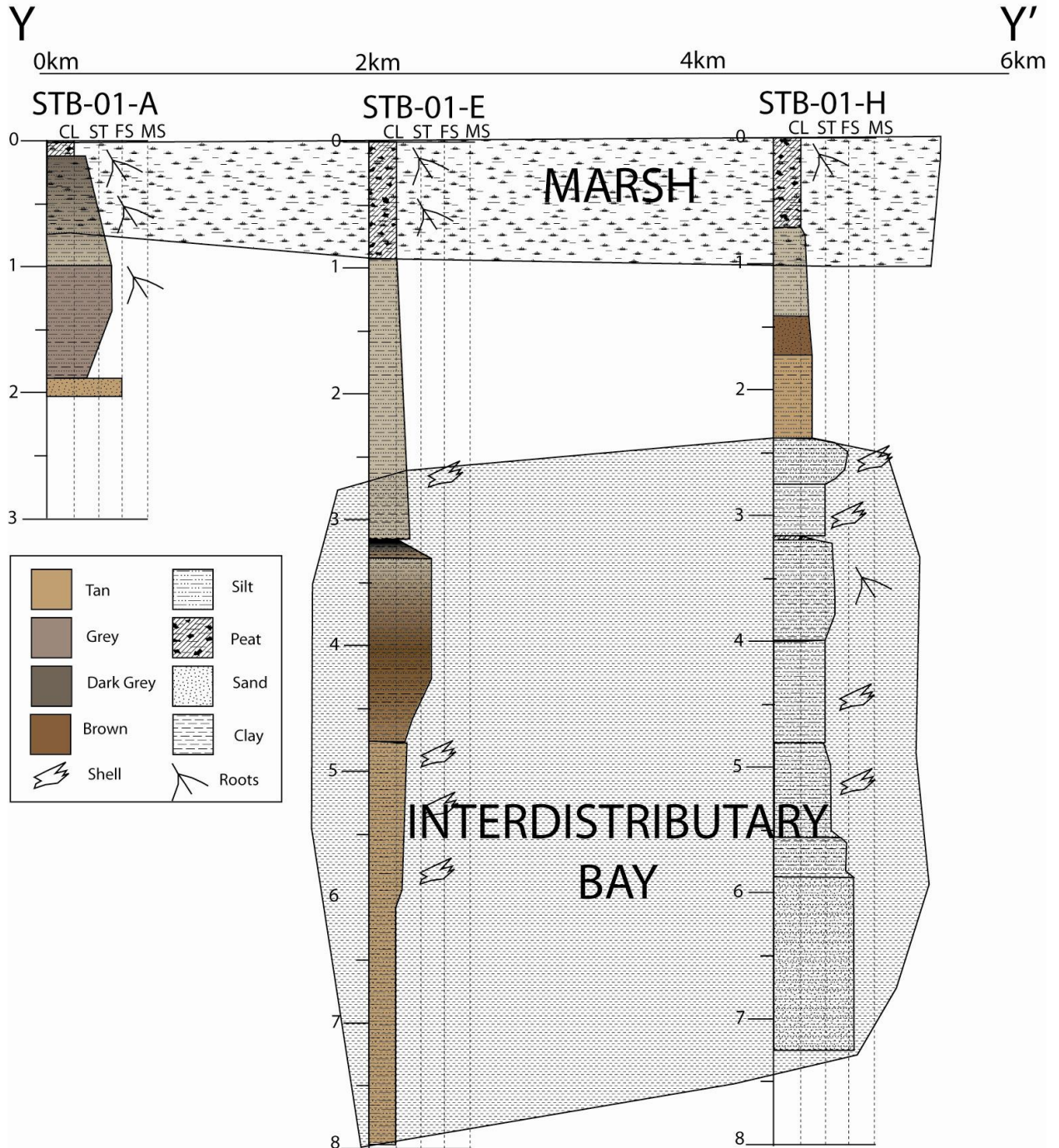
Like the previous cross-section, there are only two identifiable depositional environments in this cross-section due to a lack of laterally continuous data. However, the data that does exist indicates that the base of two cores, STB-01-H and STB-01-I are an interdistributary bay with abundant shell material and clayey sands. Interestingly, there is a unit containing root fragments, indicating that perhaps marsh colonized that location, or that there was a marsh edge nearby.



STB-01-A, STB-01-B, and STB-01-C are cores in the cross-section X-X'. STB-01-A begins in a sand unit with some rooting from 1.88m to 2.02m. Overlying this unit is silty sand that grades into silt and clay from 0.99m to 1.88m. From 0.11m to 0.99m is a massive bed of clay and silt. The topmost section of this core from 0.11m is organic-rich clay with rooting. In STB-01-B from 4.45m to 5.94m is a clay unit with sand lenses. Above this from 4.28m to 4.45m is sand interbedded with organic material. From 4.00m to 4.28m is another massive clay unit. The interval from 3.52m to 4.00m is fine sand or silt. Above this from 3.37m to 3.52m is another

clay unit. Another silt and fine sand unit exists from 2.84m to 3.37m. From 2.44m to 2.84m is an interbedded clay and fine sand unit. Another silt and fine sand bed occurs at 2.00m to 2.44m. Overlying this is a clay unit that grades upwards into silt and fine sand from 1.84 to 2.00m. Another silt and fine sand unit occurs at the interval from 1.36m to 1.84m. From 1.17m to 1.36m is a unit of clay and silt and directly overlying this from 0.92m to 1.17m is a massive bed of silt and fine sand. Above this is a unit of clay with some rooting from 0.15m to 0.92m. The top of this core from 0.15m is organic-rich clay with rooting. STB-01-C has a total length of 2.15m and begins in a clay unit from 1.90m to 2.15m. Above this is from 1.64m to 1.90m is an interbedded silt and fine sand interval. From 0.16m to 1.64m is a clay unit that grades upwards into clay and silt with rooting. The top 0.16m of this core contains abundant rooting and organic-rich clay.

The cross-section X-X' (Fig) has only one core that penetrates deeper than 3m. This core, STB-01-B, shows interbedded sand, silt, and clay, with the presence of sand and silt becoming more prevalent towards the top of the section. This coarsening upward sequence is consistent with overbank deposits, such as crevasse splays. The top of this cross-section is capped with an approximately 1m thick marsh deposit, and often this deposit is fining upward, suggesting incorporation of the coarser material below into the marsh above.

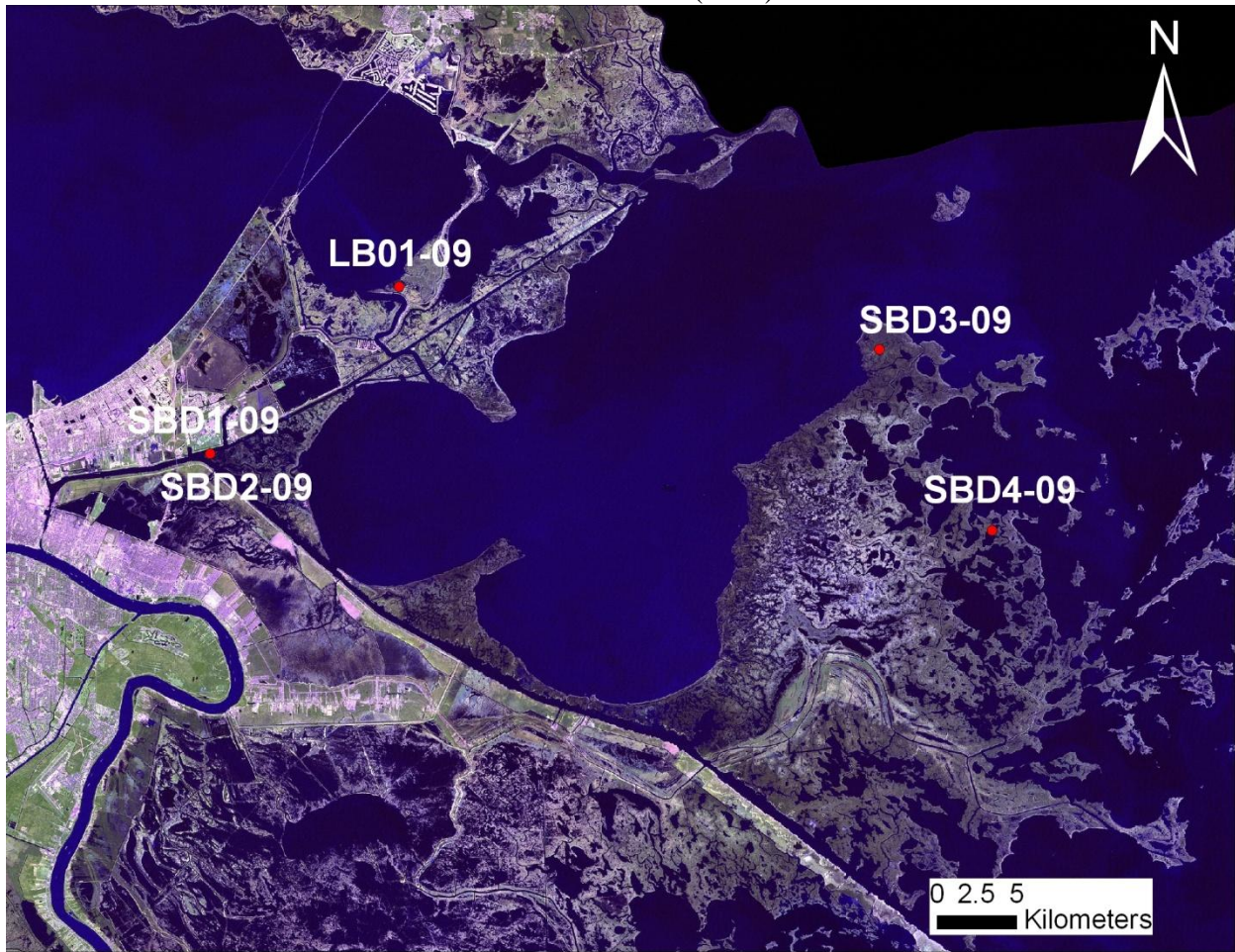


There are three cores in the cross-section Y-Y': STB-01-H, STB-01-F, and STB-01-A. STB-01-A was previously described in X-X'. The vibracore STB-01-H begins at 7.26m in an interval of medium sand that extends to 5.88m. Above this from 5.55m to 5.88m is an interval of interbedded clay, silt, and fine sand. From 4.80m to 5.55m is a fine sand unit with some shell fragments. Silt with small fine sand lenses and shell fragments occurs from 4.00m to 4.80m. Overlying this unit from 3.19m to 4.00m is another unit of interbedded silt, clay, and fine sand. The interval from 3.16m to 3.19m contains organic-rich clay. From 2.73m to 3.16m is a unit of silt with shell fragments. Above this from 2.37m to 2.73m is a unit of interbedded silt and sand with shell fragments. From 2.37m to 1.72m is a massive bed of clay and silt. A unit of fine sand

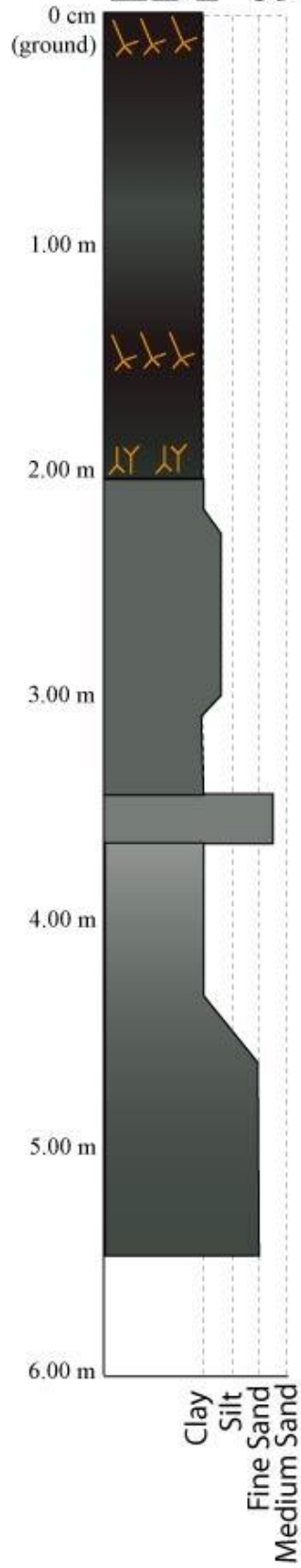
occurs from 1.42m to 1.72m. Above this from 0.70m to 1.42m is a unit of clay and silt with plant material. The top to 0.70 of this core is peat and organic-rich clay. The core STB-01-F has a total length of 7.22m and the first unit in the core is from 4.49m to 7.22m and is composed of silt and fine sand with shell fragments. Above this from 4.27m to 4.49m is a massive bed of medium sand. Fine sand occurs above the previous interval from 4.19m to 4.27m. Another massive bed of medium sand occurs in the interval 3.81m to 4.19m. Overlying this unit is a fine sand bed from 3.52m to 3.81m. From 3.36m to 3.52m is a unit of medium sand with horizontal laminations. Above this from 3.30m to 3.36m is a unit of roots. The next interval from 3.16m to 3.30m contains medium sand with horizontal laminations. Overlying this from 3.13m to 3.16m is an interval of interbedded silt and fine sand. From 2.88m to 3.13m is a bed of fine sand with horizontal laminations. Above this from 2.54m to 2.88m is organic clay that grades into silt. A massive clay bed exists in the interval between 1.00m and 2.54m. The top section of this core from 1.m is organic clay and peat with abundant rooting.

Like most other cross-sections, Y-Y' contains two depositional environments: interdistributary bay and marsh.

St. Bernard Delta (SBD)



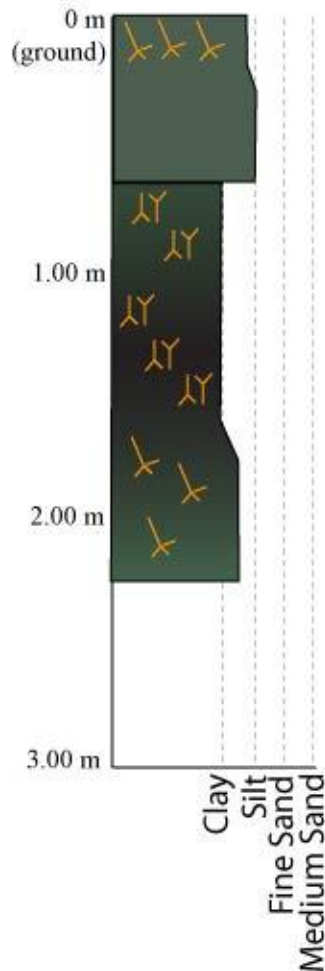
LB1-09



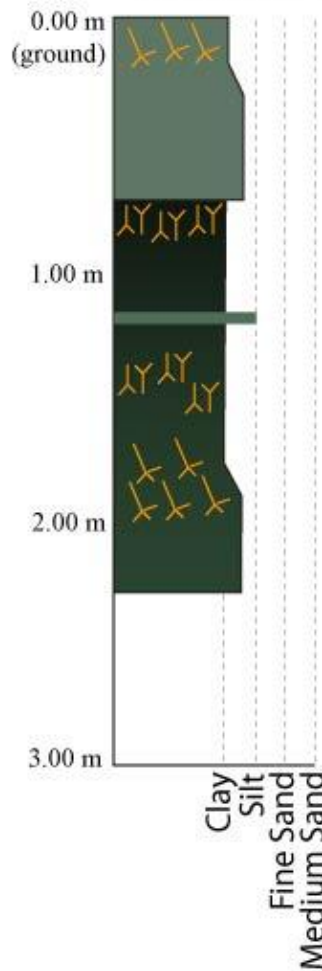
LB1 was taken at N 30.10030 and W 89.79174. The total length of this core is 5.49 m. The bottommost unit from 4.85 m to 5.49 m is dark gray fine sand with numerous shell fragments and one clay lens at 5.40 m. Above this unit from 4.85 m to 4.50 m is light gray fine sand with large shell fragments and a gradual bottom contact. Light olive gray clay with alternating layers of sand with increasing thickness of sand layers at the bottom overlies the previous unit from 3.93 m to 4.50 m. From 3.62 to 3.93 m is light olive gray clay with some silt to fine sand layers and a gradual bottom contact. Above this unit from 3.42 to 3.62 m is fine to medium light gray sand with several clay laminations and a sharp bottom contact. Overlying this from 3.03 to 3.42 m is light olive gray clay with one silt layer and a sharp bottom contact. Light olive gray clayey silt with dark organic lenses overlies the previous unit from 3.03 m to 2.21 m with a sharp bottom contact. From 2.05 m to 2.21 m is light olive gray clay with a gradual bottom contact. Overlying this unit from 2.05 m to 1.89 m is olive gray clay with few organics and a sharp bottom contact. Above this unit from 1.89 m to 1.17 m is dark brown to black organic rich clay that is almost entirely organic with some small intact roots and a gradual bottom contact. Medium olive gray clay overlies this organic-rich unit from 1.17 m to 0.7 m. From 0.70 m to the top is dark brownish black organic rich clay with heavy rooting above 14 cm.

LB1 is an interesting core due to the relatively greater distribution of sand at depth. This sand has been casually attributed to reworked Pine Island barrier island sand (Michael Miner, personal communication). The medium sand unit at 3.42 m was likely reworked during progradation of the St. Bernard Delta over the Pine Island barrier island and represents the back barrier environment. This medium sand deposited in a back barrier environment may have been due to a tropical cyclone and represents overwash deposits from that event. The sharp contacts around this unit represent an abrupt change in environment followed by a resumed environment, likely prodelta. Above this sand unit are large units of clay with sharp contacts at 2.05 m and 3.03 m. These contacts may represent erosional surfaces due to tidal channels, as it is unlikely that these contacts are connected with distributary networks. However, the change from prodelta clays to tidal channels implies that a silty or sandy distributary network either bypassed the area or was eroded. The top of this core is very similar to SBD3 despite the distance between them and represents a robust marsh environment with multiple organic units.

SBD1-09



SBD2-09

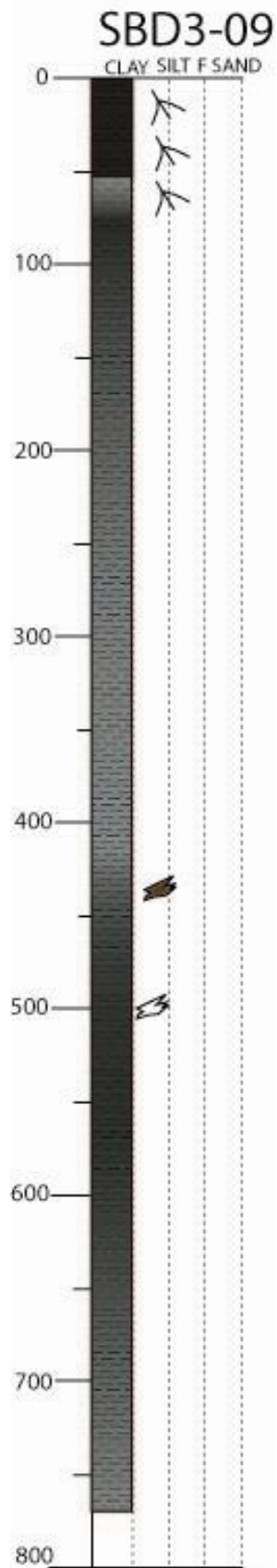


SBD1 and SBD2 were taken at N 30°00'32.3, W 89°55'01.5". The total length of SBD1 is 2.24m. The bottommost section from 1.71m to the bottom contains light, olive-gray silty clay with some rooting, and no apparent bedding. Above this layer, from 1.58-1.71m, is a gradual transition to olive black organic-rich clay with visible rooting. Overlying the organic-rich clay, from 1.06-1.58m is a gradational contact with an olive black organic layer with visible rooting and no visible bedding. Above this layer, from 0.64-1.06m is another organic rich olive black clay that grades upwards into nearly pure organics near 0.72m. There are two light olive gray clayey silt layers at 0.92-0.97m. Overlying this layer, from 0.26-0.64m, is olive gray silty sand to silty clay that varies between sandy and non-sandy layers. This section was deformed during the coring process and organic debris is present throughout the unit. The topmost section of SBD1 is light olive gray silty clay that fines upward.

The total length of SBD2 is 2.29m. The bottommost section of SBD2 begins at 1.86m and contains olive-gray, silty clay with some rooting above 2.05m. There is a heavily rooted section between 1.95-1.98 m and also above 1.90m. Some horizontal bedding occurs throughout. The overall color of the sediment darkens upwards from 2.05 and becomes olive-black around 1.98m. Overlying this section is a layer from 1.36-1.86m of olive-black organics with massive rooting. The contact between these two layers is gradational. Above the organic layer, to 0.85cm

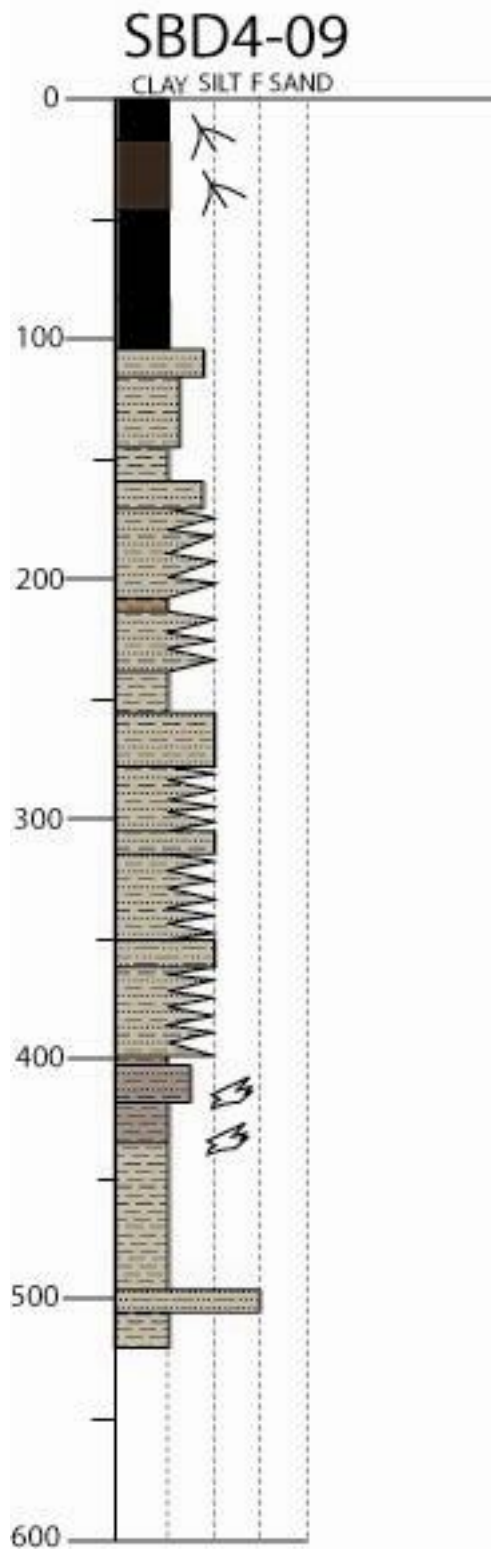
is an organic-rich olive black clay. A silty, light-olive gray layer is present between 1.18-1.22m. This contact is also gradual. Between 0.72-0.85 cm is another olive black organic layer with abundant rooting. The bottom contact with the underlying organic-rich clay is sharp. Overlying the organic layer is a sharp contact to light olive gray silty sand to sandy silt between 0.26-.072m. This layer varies between sand and non-sand layers and contains heavy dewatering deformation. The topmost layer contains light olive gray silty clay with no visible bedding, but heavy deformation. Above 0.08m, roots are abundant. The contact with the underlying layer is gradational.

SBD1 and SBD2 were taken at the intersection of the Mississippi River Gulf Outlet and the Gulf Intercoastal Waterway. Thus, the cores represent a change in environment likely due to the construction of the Mississippi River Gulf Outlet. The sharp contacts around 0.70 m to 0.60 m indicate a change from a quiet marsh environment seen in the sediments below to a higher energy environment. However, the tops of both of these cores have thick (0.26 m) units of modern marsh that have recovered since the formation of the Mississippi River Gulf Outlet.



SBD3 was taken at N 30°3'25.03", W 89°28'52.86". The total length of the core is 7.71 m. The bottommost unit from 6 m to bottom is a gray clay with numerous silt laminations. Above this unit, from 5.4 to 6 m is dark gray clay with no silt laminations. Overlying this, from 4.8 to 5.4 m is dark gray clay with some silt laminations and lenses along with a few shell fragments. From 4.8 m to 3.4 m is a dark gray clay with some shells and a large pocket of organics that appears to be rip up material. Above this unit from 3.4 m to 2.3 m is light gray clay. The bottom contact on this unit is gradual. Overlying this unit from 2.3 m to 1.55 m is a similar light gray clay with organic lenses and a gradual bottom contact. From 1.55 m to 1.17 m is a dark gray mottled clay. Above this unit to 0.55 m is a brown organic rich clay with massive rooting and silty lenses. A light gray clay lies above this unit from 0.47 m to 0.55 m. The top of this core is a dark brown-black organic rich clay with heavy modern rooting above 0.27 with a sharp bottom contact.

SBD3 contains mostly clay with very small variations in grain size for the entirety of the 7.71 m. However, the clay with silt laminations seen in the lower 5 m of the core indicate a prodelta environment with the silt laminations indicating flooding events. Above those units are similar clays with large shell fragments that were likely transported, possibly in a bay environment, and represent the progradation of the St. Bernard Delta lobe into paleo-Lake Borgne. Farther above these units, from approximately 1.5 m to the top represent a healthy marsh environment with multiple layers of organics.



SBD4 was taken at N 29°57'10.36", W 89°24'42.5". The total length of the core is 5.20m. The bottommost unit from 5.04m to the bottom is light gray clay with a small tan lens at 5.16m. Above this unit, from 4.94m to 5.04m is a light gray very fine sand. Overlying this from 4.34m

to 4.94m is a light gray clay with mottled black laminations. There is an interval of shell fragments from 4.31m to 4.34m. Above this interval from 4.17m to 4.31m is a dark gray clay. Overlying this unit from 4.14m to 4.17m is another unit of shell fragments in clay. From 4.02m to 4.14m is dark gray clay with some silt content. Above this from 3.99m to 4.02m is reddish gray clay. Overlying this from 3.62m to 3.99m is silt with interbedded clay; both are light gray and heavily bioturbated. From 3.50m to 3.62m is a light gray silt. Above this unit from 3.16m to 3.50m is light gray silt with interbedded clay. Overlying this unit from 3.04m to 3.16m is a light gray sandy clay with very high water content which potentially indicates deformation while coring. From 2.77m to 3.04m is light gray, interbedded clay and silt. Above this from 2.54m to 2.77m is another area of high water content in light gray sandy clay. This unit is gradational on both contacts. From 2.38m to 2.54m is light gray clay. Above this from 2.12m to 2.38m is light gray interbedded clay and silt. Overlying this from 2.09m to 2.12m is reddish-brown to gray clay with an erosional bottom contact. From 1.71m to 2.09m is interbedded clay and silt with bioturbation and a sharp bottom contact. Above this from 1.59m to 1.71m is light gray clayey silt. Overlying this from 1.44m to 1.59m is light gray clay with some reddish-brown mottling. From 1.15m to 1.44m is light gray silty clay. Above this from 1.04m to 1.15m is light gray bioturbated clayey silt. From 0.82m to 1.04m is black clay with large shell pieces and root fragments. This unit has some complete shells and a sharp bottom contact. From 0.45m to 0.82m is black organic-rich material, called "coffee grounds" colloquially. Overlying this from 0.15m to 0.45m is brownish black organic clay with root fragments. The topmost unit from 0.15m is black organic clay, heavily rooted with some live roots.

SBD4 is located near a mapped distributary network (Kolb and van Lopik, 1958a), and this proximity explains the abundance of sand in this core. The base of this core is fine clay with some shell material, which indicates a bay environment. This unit coarsens into interfingering silt and clay, which is indicative of bay-infilling or perhaps a crevasse splay, and this unit is continuous for the majority of the length of the core. The topmost unit is organic-rich clay indicative of modern marsh environments, particularly due to the abundance of roots and root fragments.

Vita

Mary Ellison was born in Millwood, Virginia on June 22. She spent time on Virginia's Atlantic coast, as well as many summers in Downeast Maine. She graduated from Wakefield School in June 2004 and received her Bachelor of Arts in Earth Science from Boston University in 2008. After obtaining her Bachelor's degree, Mary studied coastal environments in Queensland, Australia. Mary began her Master's Degree at the University of New Orleans in January of 2009.